National Library
of Canada

Acquisitions and
Bibliographic Services Branch

395 Wellington Street
Ottawa, Ontario
K1A 0N4

Bibliothèque nationale
du Canada

Direction des acquisitions et
des services bibliographiques

395, rue Wellington
Ottawa (Ontario)
K1A 0N4

Your file Votre référence

Our file Notre référence

NOTICE

The quality of this microform is heavily dependent upon the quality of the original thesis submitted for microfilming. Every effort has been made to ensure the highest quality of reproduction possible.

If pages are missing, contact the university which granted the degree.

Some pages may have indistinct print especially if the original pages were typed with a poor typewriter ribbon or if the university sent us an inferior photocopy.

Reproduction in full or in part of this microform is governed by the Canadian Copyright Act, R.S.C. 1970, c. C-30, and subsequent amendments.

AVIS

La qualité de cette microforme dépend grandement de la qualité de la thèse soumise au microfilmage. Nous avons tout fait pour assurer une qualité supérieure de reproduction.

S'il manque des pages, veuillez communiquer avec l'université qui a conféré le grade.

La qualité d'impression de certaines pages peut laisser à désirer, surtout si les pages originales ont été dactylographiées à l'aide d'un ruban usé ou si l'université nous a fait parvenir une photocopie de qualité inférieure.

La reproduction, même partielle, de cette microforme est soumise à la Loi canadienne sur le droit d'auteur, SRC 1970, c. C-30, et ses amendements subséquents.

Canada

UNIVERSITY OF ALBERTA

DEVELOPMENT OF MOMENT CONNECTIONS IN GLUED-LAMINATED ALBERTA SPRUCE AND PINE TIMBER

BY

CLIFF PETER HATTAR

A thesis submitted to the Faculty of Graduate Studies and Research in partial fulfillment of the requirements for the degree of **MASTER OF SCIENCE**.

IN

CIVIL ENGINEERING

DEPARTMENT OF **CIVIL ENGINEERING**

EDMONTON, ALBERTA

FALL 1994

National Library
of Canada

Acquisitions and
Bibliographic Services Branch

395 Wellington Street
Ottawa, Ontario
K1A 0N4

Bibliothèque nationale
du Canada

Direction des acquisitions et
des services bibliographiques

395, rue Wellington
Ottawa (Ontario)
K1A 0N4

Your file Votre référence

Our file Notre référence

The author has granted an irrevocable non-exclusive licence allowing the National Library of Canada to reproduce, loan, distribute or sell copies of his/her thesis by any means and in any form or format, making this thesis available to interested persons.

L'auteur a accordé une licence irrévocable et non exclusive permettant à la Bibliothèque nationale du Canada de reproduire, prêter, distribuer ou vendre des copies de sa thèse de quelque manière et sous quelque forme que ce soit pour mettre des exemplaires de cette thèse à la disposition des personnes intéressées.

The author retains ownership of the copyright in his/her thesis. Neither the thesis nor substantial extracts from it may be printed or otherwise reproduced without his/her permission.

L'auteur conserve la propriété du droit d'auteur qui protège sa thèse. Ni la thèse ni des extraits substantiels de celle-ci ne doivent être imprimés ou autrement reproduits sans son autorisation.

ISBN 0-315-95042-0

Canada

Name CLIFF HATTAR

Dissertation Abstracts International is arranged by broad, general subject categories. Please select the one subject which most nearly describes the content of your dissertation. Enter the corresponding four-digit code in the spaces provided.

CIVIL ENGINEERING — SUBJECT TERM

0543 — SUBJECT CODE

U·M·I

Subject Categories

THE HUMANITIES AND SOCIAL SCIENCES

COMMUNICATIONS AND THE ARTS
- Architecture 0729
- Art History 0377
- Cinema 0900
- Dance 0378
- Fine Arts 0357
- Information Science 0723
- Journalism 0391
- Library Science 0399
- Mass Communications 0708
- Music 0413
- Speech Communication 0459
- Theater 0465

EDUCATION
- General 0515
- Administration 0514
- Adult and Continuing 0516
- Agricultural 0517
- Art 0273
- Bilingual and Multicultural 0282
- Business 0688
- Community College 0275
- Curriculum and Instruction 0727
- Early Childhood 0518
- Elementary 0524
- Finance 0277
- Guidance and Counseling 0519
- Health 0680
- Higher 0745
- History of 0520
- Home Economics 0278
- Industrial 0521
- Language and Literature 0279
- Mathematics 0280
- Music 0522
- Philosophy of 0998
- Physical 0523
- Psychology 0525
- Reading 0535
- Religious 0527
- Sciences 0714
- Secondary 0533
- Social Sciences 0534
- Sociology of 0340
- Special 0529
- Teacher Training 0530
- Technology 0710
- Tests and Measurements 0288
- Vocational 0747

LANGUAGE, LITERATURE AND LINGUISTICS
- Language
  - General 0679
  - Ancient 0289
  - Linguistics 0290
  - Modern 0291
- Literature
  - General 0401
  - Classical 0294
  - Comparative 0295
  - Medieval 0297
  - Modern 0298
  - African 0316
  - American 0591
  - Asian 0305
  - Canadian (English) 0352
  - Canadian (French) 0355
  - English 0593
  - Germanic 0311
  - Latin American 0312
  - Middle Eastern 0315
  - Romance 0313
  - Slavic and East European 0314

PHILOSOPHY, RELIGION AND THEOLOGY
- Philosophy 0422
- Religion
  - General 0318
  - Biblical Studies 0321
  - Clergy 0319
  - History of 0320
  - Philosophy of 0322
- Theology 0469

SOCIAL SCIENCES
- American Studies 0323
- Anthropology
  - Archaeology 0324
  - Cultural 0326
  - Physical 0327
- Business Administration
  - General 0310
  - Accounting 0272
  - Banking 0770
  - Management 0454
  - Marketing 0338
- Canadian Studies 0385
- Economics
  - General 0501
  - Agricultural 0503
  - Commerce-Business 0505
  - Finance 0508
  - History 0509
  - Labor 0510
  - Theory 0511
- Folklore 0358
- Geography 0366
- Gerontology 0351
- History
  - General 0578
  - Ancient 0579
  - Medieval 0581
  - Modern 0582
  - Black 0328
  - African 0331
  - Asia, Australia and Oceania 0332
  - Canadian 0334
  - European 0335
  - Latin American 0336
  - Middle Eastern 0333
  - United States 0337
- History of Science 0585
- Law 0398
- Political Science
  - General 0615
  - International Law and Relations 0616
  - Public Administration 0617
- Recreation 0814
- Social Work 0452
- Sociology
  - General 0626
  - Criminology and Penology 0627
  - Demography 0938
  - Ethnic and Racial Studies 0631
  - Individual and Family Studies 0628
  - Industrial and Labor Relations 0629
  - Public and Social Welfare 0630
  - Social Structure and Development 0700
  - Theory and Methods 0344
- Transportation 0709
- Urban and Regional Planning 0999
- Women's Studies 0453

THE SCIENCES AND ENGINEERING

BIOLOGICAL SCIENCES
- Agriculture
  - General 0473
  - Agronomy 0285
  - Animal Culture and Nutrition 0475
  - Animal Pathology 0476
  - Food Science and Technology 0359
  - Forestry and Wildlife 0478
  - Plant Culture 0479
  - Plant Pathology 0480
  - Plant Physiology 0817
  - Range Management 0777
  - Wood Technology 0746
- Biology
  - General 0306
  - Anatomy 0287
  - Biostatistics 0308
  - Botany 0309
  - Cell 0379
  - Ecology 0329
  - Entomology 0353
  - Genetics 0369
  - Limnology 0793
  - Microbiology 0410
  - Molecular 0307
  - Neuroscience 0317
  - Oceanography 0416
  - Physiology 0433
  - Radiation 0821
  - Veterinary Science 0778
  - Zoology 0472
- Biophysics
  - General 0786
  - Medical 0760

EARTH SCIENCES
- Biogeochemistry 0425
- Geochemistry 0996
- Geodesy 0370
- Geology 0372
- Geophysics 0373
- Hydrology 0388
- Mineralogy 0411
- Paleobotany 0345
- Paleoecology 0426
- Paleontology 0418
- Paleozoology 0985
- Palynology 0427
- Physical Geography 0368
- Physical Oceanography 0415

HEALTH AND ENVIRONMENTAL SCIENCES
- Environmental Sciences 0768
- Health Sciences
  - General 0566
  - Audiology 0300
  - Chemotherapy 0992
  - Dentistry 0567
  - Education 0350
  - Hospital Management 0769
  - Human Development 0758
  - Immunology 0982
  - Medicine and Surgery 0564
  - Mental Health 0347
  - Nursing 0569
  - Nutrition 0570
  - Obstetrics and Gynecology 0380
  - Occupational Health and Therapy 0354
  - Ophthalmology 0381
  - Pathology 0571
  - Pharmacology 0419
  - Pharmacy 0572
  - Physical Therapy 0382
  - Public Health 0573
  - Radiology 0574
  - Recreation 0575
  - Speech Pathology 0460
  - Toxicology 0383
- Home Economics 0386

PHYSICAL SCIENCES

Pure Sciences
- Chemistry
  - General 0485
  - Agricultural 0749
  - Analytical 0486
  - Biochemistry 0487
  - Inorganic 0488
  - Nuclear 0738
  - Organic 0490
  - Pharmaceutical 0491
  - Physical 0494
  - Polymer 0495
  - Radiation 0754
- Mathematics 0405
- Physics
  - General 0605
  - Acoustics 0986
  - Astronomy and Astrophysics 0606
  - Atmospheric Science 0608
  - Atomic 0748
  - Electronics and Electricity 0607
  - Elementary Particles and High Energy 0798
  - Fluid and Plasma 0759
  - Molecular 0609
  - Nuclear 0610
  - Optics 0752
  - Radiation 0756
  - Solid State 0611
- Statistics 0463

Applied Sciences
- Applied Mechanics 0346
- Computer Science 0984
- Engineering
  - General 0537
  - Aerospace 0538
  - Agricultural 0539
  - Automotive 0540
  - Biomedical 0541
  - Chemical 0542
  - Civil 0543
  - Electronics and Electrical 0544
  - Heat and Thermodynamics 0348
  - Hydraulic 0545
  - Industrial 0546
  - Marine 0547
  - Materials Science 0794
  - Mechanical 0548
  - Metallurgy 0743
  - Mining 0551
  - Nuclear 0552
  - Packaging 0549
  - Petroleum 0765
  - Sanitary and Municipal 0554
  - System Science 0790
- Geotechnology 0428
- Operations Research 0796
- Plastics Technology 0795
- Textile Technology 0994

PSYCHOLOGY
- General 0621
- Behavioral 0384
- Clinical 0622
- Developmental 0620
- Experimental 0623
- Industrial 0624
- Personality 0625
- Physiological 0989
- Psychobiology 0349
- Psychometrics 0632
- Social 0451

UNIVERSITY OF ALBERTA

RELEASE FORM

NAME OF AUTHOR: **Cliff Peter Hattar**

TITLE OF THESIS: **Development of Moment Connections in Glued-Laminated Alberta Spruce and Pine Timber**

DEGREE: **Master of Science in Civil Engineering**

YEAR THIS DEGREE GRANTED: **Fall of 1994**

Permission is hereby granted to the University of Alberta Library to reproduce single copies of this thesis and to lend or sell such copies for private, scholarly or scientific research purposes only.

The author reserves all other publication and other rights in association with the copyright in the thesis, and except as hereinbefore provided neither the thesis nor any substantial portion thereof may be printed or otherwise reproduced in any material form whatever without the author's prior written permission.

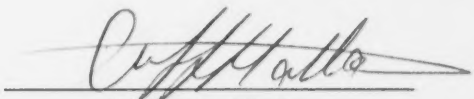

Cliff Peter Hattar
27 Tanglewood Drive
Longmeadow, Mass.
01106 USA

Date: 14/September/1994

UNIVERSITY OF ALBERTA

FACULTY OF GRADUATE STUDIES AND RESEARCH

The undersigned certify that they have read, and recommended to the Faculty of Graduate Studies and Research for acceptance, a thesis entitled **DEVELOPMENT OF MOMENT CONNECTIONS IN GLUED-LAMINATED ALBERTA SPRUCE AND PINE TIMBER** submitted by **CLIFF PETER HATTAR** in partial fulfillment of the requirements for the degree of **MASTER OF SCIENCE** in **CIVIL ENGINEERING**.

Dr. J.J. Roger Cheng (Supervisor)

Dr. S. H. Simmonds

Dr. L. Bach

Date: 9 **/September/1994**

To my Parents, Nweiser and Najwa

ABSTRACT

The use of right angle beam-column moment connections in rigid portal frames in glued-laminated timber construction is not common practice. It is customary to design the connections in wood structure as simple connections. This results in the need for more wood and a lateral force bracing system. To increase the competitiveness of wood in non-residential construction, it is necessary to develop an economical and reliable moment connection for wood construction. The objective of this study, therefore, is to develop a moment connection and method for its design to be used in glued-laminated timber. The glulam timber manufactured from Alberta spruce and pine is used in this study.

Two test phases are considered in this program. The first series of tests employs six specimens with different connection patterns. Three glulam rivet plate connections and three shear-plate bolted connections are used. The results of this phase are used to determine the best connector configuration to be further investigated and developed in the second phase of the program. In the second phase, one bolted connection is to determine the location of the instantaneous center of the butt joint. Another four riveted connections are tested to study the behaviour and methods to improve the performance, both strength and stiffness of the connection.

Moment rotation characteristic curves are developed for each connection tested. The beam-line concept was used to evaluate the viability of the connections in moment resistant frames. The use of the connections as semi-rigid joints are discussed. In addition, the behaviour of the specimens during the test, modes of failure and strain distribution are observed and recorded throughout the tests.

All specimens in the first phase failed in wood splitting perpendicular to the end grain. The riveted connections appear to be the most promising ones, although they still exhibit low rigidity and strength ratios with respect to rigid connections. Hence in the second phase, local strengthening for the riveted specimens to improve their performance is applied.

A design model and procedure are recommended for the design of the moment connections in glued-laminated timber. Predictions from this model are compared with the test results. Finally, methods for further improvement of the strength and stiffness of such joints are recommended and discussed.

ACKNOWLEDGMENT

Financial support was provided by the Canada-Alberta Partnership Agreement in Forestry. A special thanks extended to Western Archrib for their financial and technical support.

A special gratitude of thanks goes to the Project Officer, Mr. Russel Bohning, for his guidance.

The assistance of the technical staff of the I.F. Morrison Structural Laboratory at the University of Alberta is acknowledged.

A personal gratitude goes to my supervisor, Dr. J.J. Cheng, for his effective and enduring supervision during the course of this project.

TABLE OF CONTENTS

Chapter	Page
1.0 INTRODUCTION	1
1.1 General	1
1.2 Objectives and Scope	1
2.0 LITERATURE REVIEW	3
2.1 Research on Moment Connections	3
2.1.1 Bolted Joints	3
2.1.2 Glued and Epoxy Injected Connections	4
2.1.3 Nailed Gusset Plates Connections	5
2.2 Research on Timber Fasteners and Timber Joints	7
2.2.1 Nailed Connections	7
2.2.2 Glulam Rivet Connections	8
2.2.3 Shear Plates, Split Rings and Bolts in Timber Joints	10
3.0 EXPERIMENTAL PROGRAM	14
3.1 Introduction	14
3.2 Geometry and Material Specification	14
3.2.1 Specimens and Connections Patterns	14
3.2.2 Specimen Size, Preparation and Specified Strengths	16
3.3 Test Setup	17
3.4 Instrumentation	18
3.5 Test Procedure	19
3.6 Material and Embedment Tests	20
4.0 EXPERIMENTAL RESULTS	39
4.1 Introduction	39
4.2 Material Properties	39

4.3 Test Results 40
4.3.1 Phase 1 - Preliminary Investigation 40
4.3.1.1 General 40
4.3.1.2 The Riveted Connections 41
4.3.1.3 The Bolted Connections 42
4.3.2 Phase 2 - Further Studies on Riveted Moment Joints 44
4.3.2.1 General 44
4.3.2.2 Specimen C1 44
4.3.2.3 Specimen C2 and Specimen C3 45
4.3.2.4 Specimen C4 48
4.3.3 Location of the Instantaneous Center 49
5.0 DISCUSSION OF THE TEST RESULTS 74
5.1 Location of the Instantaneous Center 74
5.2 Design and Evaluation 76
5.2.1 Design Model and Calculation of Design Values 76
5.2.2 Evaluation of Specimen Performance 77
5.2.2.1 Phase 1 77
5.2.2.1.1 The Riveted Connections 77
5.2.2.1.2 The Bolted Connections 79
5.2.2.2 Phase 2 80
5.3 Effect of Rivet Distribution Pattern 82
5.4 General Comparison and Implication of the Test Results 83
5.5 Advantage of Semi-Rigid Joint Application 85
6.0 SUMMARY AND CONCLUSIONS 90
6.1 General 90
6.2 Recommendations 91

REFERENCES 94

APPENDIX A - Sample Calculations of Moment Connections' Resistance 97

LIST OF TABLES

Table		Page
3.1	Specified Strengths and Modulus of Elasticity of Specimens	21
3.2	Specified Properties of Glulam Rivets	21
4.1	Material Properties for Top Steel Brackets	51
4.2	Fastener Embedment Strengths	52
4.3	Summary of Test Results	52
5.1	Summary of Test Results	87
5.2	Evaluation of Specimen Performance	87

LIST OF FIGURES

Figure		Page
2.1	Glulam Timber Reinforcement System (Gardner, 1989)	12
2.2	Typical Portal Knee developed by Gardner (Gardner, 1989)	12
2.3	Direction of Forces on Bolts	13
2.4	Load Slip Schematic	13
2.5	The Glulam Rivet (McGowan, 1966)	13
3.1	Specimen A1 (7x10) Pattern	22
3.2	Specimen A2 (10x10) Pattern	22
3.3	Specimen A3 (10x7 Pattern)	23
3.4	10x7 Rivet Pattern	23
3.5	Specimen A4 and B1 (4x2)	24
3.6	Butt Joint Bolted Connection	24
3.7	Joint Comparison	25
3.8	Specimen A5 and A6 (Circular)	25
3.9	Circular Bolted Pattern	26
3.10	Bottom Bracket (Series C)	27
3.11	Specimen C2 and C3	27
3.12	Specimen C3	28
3.13	Top Bracket (Specimen C2&C3)	28
3.14	Schematic Test Setup	29
3.15	Photographic Test Setup	30
3.16	Manual Hydraulic Ram	31
3.17	Reaction Frame	31
3.18	Rotation Gauges and Cable Transducer Boxes	32
3.19	Gauge Layout on Specimen B1	33

3.20	Gauge Layout on Specimen B1	33
3.21	Strain Gauge Layout on Side Plate for Specimen C1, C2, C3	34
3.22	Strain Gauge Layout on Side Plate for Specimen C1, C2, C3	34
3.23	Strain Gauge Layout on Side Plate for Specimen C4	35
3.24	Strain Gauge Layout on Top Bracket	35
3.25	Strain Gauge Layout on Top Bracket	36
3.26	Photographic Test Setup for the 5x4 Rivet Plate Loaded Parallel to the Grain	37
3.27	Photographic Test Setup for the 4x4 Rivet Plate Loaded Perpendicular to the Grain	38
4.1	Typical Stress vs. Strain Plot for Steel Coupons	53
4.2	Plot of Load vs. Deformation for Embedded Fasteners Loaded Parallel to the Grain	53
4.3	Plot of Load vs. Deformation for Embedded Fasteners Loaded Perpendicular to the Grain	54
4.4	Moment Rotation Curve for Specimen A2 Demonstrating the Secant Stiffness	54
4.5	Moment Rotation Curves for Phase 1	55
4.6	Moment Rotation Curves for Phase 2	55
4.7	Cracks in End Grain for Specimen A1	56
4.8	Split Crack in Specimen A2	57
4.9	Dislocation of Shear Plates in Specimen A4	57
4.10	Large Cracks in End Grain for Specimen A4	58
4.11	Splitting in the Middle Member (Specimen A5)	59
4.12	Splitting in the End Grain (Specimen A5)	60
4.13	Cracks in the End Grain (Specimen A6)	61

4.14	Cracks in the End Grain (Specimen C1)	62
4.15	Strain Gauge Readings for Top Part of Side Plate (Specimen C1)	62
4.16	Strain Gauge Readings for Bottom Part of Side Plate (Specimen C1)	63
4.17	Wood Splitting and Bracket Bending (Specimen C2)	63
4.18	Brittle Fracture through Member (Specimen C2)	64
4.19	Strain Gauge Readings for Top Part of Side Plate (Specimen C2,C3)	65
4.20	Strain Gauge Readings for Bottom Part of Side Plate (Specimen C2,C3)	65
4.21	Strain Gauge Readings for Top Bracket (Specimen C2,C3)	66
4.22	Failure in Bearing Plate and Top Bracket (Specimen C4)	67
4.23	Rivet Withdrawal and Wood Crack in Top Grain (Specimen C4)	68
4.24	Strain Gauge Readings for Top Part of Side Plate (Specimen C4)	69
4.25	Strain Gauge Readings for Bottom Part of Side Plate (Specimen C4)	69
4.26	Strain Gauge Readings for Top Bracket (Specimen C4)	70
4.27	Cracks in the Side Grain (Specimen B1)	70
4.28	Strain Readings Ga#1-Ga#2 (Specimen B1)	71
4.29	Strain Readings Ga#3-Ga#5 (Specimen B1)	71
4.30	Strain Readings Ga#6-Ga#8 (Specimen B1)	72
4.31	Strain Readings Ga#9-Ga#11 (Specimen B1)	72
4.32	Strain Readings Ga#12-Ga#14 (Specimen B1)	73
5.1	Principle Force Directions on Bolts in Specimen B1	88
5.2	Axes of Longitudinal Strain Gauges in a Rosette Gauge	88
5.3	Beam Line Applied on Moment Rotation Curves	89
5.4	Bending Moment Diagrams for Various Boundary Conditions	89

LIST OF SYMBOLS

Symbols

a = curve fitting constant

f_b+ = specified stength in bending, positive moment (MPa)

f_b- = specified stength in bending, negative moment (MPa)

f_c = specified stength in compression parallel to grain (MPa)

f_{cb} = specified stength in compression parallel to, combined with bending (MPa)

f_{cp} = specified stength in compression perpendicular to grain (MPa)

f_{tn} = specified stength in tension parallel to grain at net section (MPa)

f_{cg} = specified stength in tension parallel to grain at gross section (MPa)

f_{tp} = specified stength in tension perpendicular to grain (MPa)

f_v = specified stength in shear (MPa)

Ga = strain gauge

I.C. = instantaneous center

L = span length (m)

M = applied moment (kN.m)

M.C. = Moisture Content (%)

M_d = design moment value based on materials' strength specified on CAN/CSA-O86.1 M89 (kN.m)

M.O.E. = Modulus of Elasticity (MPa)

Mp = Predicted moment value based on materials' tests' results (kN.m)

M_u = ultimate moment resistance (kN.m)

N_r = resistance of embedded fastener loaded at an angle ϕ to the grain (kN)

P_r = embedded fastener resistance parallel to the grain (kN)

P_u = ultimate load resistance (kN)

Q_r = embedded fastener resistance perpendicular to the grain (kN)

r_i = radius from instantaneous center (m)

S = measured slip (m)

Sp = spacing between rivets in both directions to grain (mm)

T_i = force component in a direction normal to r_i (kN)

ε_x and ε_y = longitudinal strains in x and y axes directions respectively (microstrain)

ϕ = angle between wood grain direction and individual fastener load direction (degree)

ϕp = principle strain directions in the steel plates (degree)

γ_{xy} = shear strain about x and y axes (microstrain)

$\mu\epsilon$ = microstrain

Θ = relative rotation of joint members (radians)

θ = rotational angle change between two connected members (degree)

θu = ultimate rotational angle change (degree)

1.0 INTRODUCTION

1.1 GENERAL

Moment resistant rigid portal frames have been widely used in steel and concrete structures. This practice has lead to the efficient and economical use of materials in steel and concrete construction. In wood construction, it is customary to design the connections as simple connections, i.e. no moment resisting capability for the connections. This causes not only the use of more wood, but also the need for a bracing system, thus reduces the competitiveness of wood in construction, especially in non-residential construction. There are very few studies on the design and/or behaviour of moment connections for wood structures and, in particular, moment joints for glued-laminated timber.

Of the few researches and applications where moment resistant joints exist, are portal frames with nailed plywood gussets (Batchelar, 1982). However, they are only used in light structures. Chapter 2 discusses this application further and the few research studies conducted on moment joints in glued-laminated timber.

1.2 OBJECTIVES AND SCOPE

It is the intention of this study to develop practical moment connections to be used in wooden frames; hence, a more economical design can be achieved. Glued-laminated timber manufactured from Alberta spruce and pine is used in this study.

This study includes the two series of the experimental program aiming at studying the behaviour and performance of various types of moment connections under monotonic

loading. The results from the first series were used to further develop and improve certain configurations of glulam rivet joints.

The testing of the first phase was conducted on a total of six specimens: three glulam rivet moment joints that varied with respect to the rivet layout pattern, and three shear-plate bolted moment joints, (one butt joint type of connection with steel cover plates and two lap joints with circular bolted patterns, one with plywood cover plates and another with steel cover plates). The moment capacity results from the tests were compared with those predicted from theory.

The location of the instantaneous center (I.C.) for the butt type joints is determined in the second phase where a rectangular shear-plate bolted joint similar to that of the first phase is tested with the appropriate instrumentation. Four glulam rivet moment joints similar to the first phase were tested with additional improvements. The connections were reinforced with steel brackets and/or steel bearing plates to improve their performance.

A design model and procedure were developed for the moment connections in glued-laminated timber. Further improvement of the strength and stiffness of such joints were also discussed.

2.0 LITERATURE REVIEW

2.1 RESEARCH ON MOMENT CONNECTIONS

There is very little research on moment connections in timber construction. Crews (1990) investigates work in this area throughout the world.

2.1.1 Bolted Joints

Crews (1990) states that in Europe, the use of circular bolted patterns has become widely accepted as a means of connection design for moment resisting connections, particularly between columns and rafters in large free-spanning timber structures.

Work conducted by Rodd (1973) on circular connectors and split rings at Brighton Polytechnic has formed the basis of ongoing work to construct moment resistant joints for glued-laminated timber portal frames, which can be readily fabricated on site. His observations demonstrated circular pattern joints made with circular dowels that had high circumferential friction with the timber, increased the strength of the joints. Hence, by filling the tolerance of the bolt holes with resin, strength is increased and all fasteners can be assumed to take up the load instantaneously, leading to stiffer joints. However, the ultimate strength capacity of the joint is governed by the tension strength perpendicular to the grain of lumber. Several conclusions were discussed such as the shift in the center of rotation away from the centroid of the bolt group resulted in significant differences in the loads per bolt. The higher forces tended to occur in bolts closest to the corners of the connections. It was also concluded that gluing a 3 mm thick plywood to the sides of the laminates limits the splitting and increases the ductility of the joint, but not significantly the strength (maximum of 20%).

In truss structures, work by Gehri (1982) has focused upon the development of high capacity end plate connections utilizing dowels. The theory for design is based on Johansen's theory (1949) which assumes that both the fastener and the timber are ideal rigid-plastic materials. His equations predicted bearing failure of the timber member or simultaneous development of plastic hinge formation in the fastener. Gehri's testing confirmed that a careful selection of fin plate interfaces and dowel size will result in a high strength ductile connection which has a "gentle" failure mode rather than a brittle and "catastrophic" timber failure mode.

2.1.2 Glued and Epoxy Injected Connections

Syme (1987) highlighted the use of glued bolt connections. His technique uses slightly undersized holes (1 mm to 2 mm), which are half filled with glue. A groove is needed along the length of the thread to allow the glue to mix around the embedded portion of the dowel as well as permitting relief of hydrostatic pressure from the epoxy in the timber. The disadvantages of this system are that splitting can easily occur within the timber member and quality control is difficult to monitor. It is also impossible to determine whether the glue has been evenly distributed across the interface between the dowel thread and the timber. A newer technique slightly different from the above was developed by Riberholt (1986). In this technique the rods were placed in oversized holes about 2 mm larger than the thread diameter and an epoxy glue is injected through a hole in the timber at the bottom of the embedment hole for the dowel rod. This tackles the disadvantages of the previous technique.

Crews (1990) indicates that epoxy injected connections have been used successfully in Denmark for over ten years and have resulted in moment resisting connections which have

a capacity of approximately 75% of that of a glue laminated beam. Similar work was investigated by Rodd et al. (1989).

Other applications include Gehri's work (1982) on the use of pre-stressed post-tensioned rods and cables ducting inside the laminates, couped with epoxy to cope with high shear and bearing stresses. Gardner's work (1989), however, focuses upon beam elements which have steel reinforcing deformed rods set in high strength epoxy and built into the outer top and bottom laminates of the beam, to form a "composite" beam section as shown in Figure 2.1. This system has been adapted for use in moment resistant connections as shown in Figure 2.2. Buchanan (1990) indicates that the failure mechanism for this type of connection is a combined tension parallel and perpendicular to the grain failure, and at the end of the tension dowels.

The analytical models used to predict the performance of the moment joints are normally based upon rivet/bolt group theory. Modifications to account for the injected resin frictional bond were made to the models by Rodd et al. (1989).

2.1.3 Nailed Gusset Plates Connections

Research on moment resistant joints in wood structures have been conducted on nailed plywood gusset joints for timber portal frames by Batchelar (1982). He developed a design procedure covering laminated beam connections formed with nailed plywood gussets. He modified his design from a mitred joint at the intersection of the glued-laminated leg and rafter members to a joint where the rafter rested on top of the leg member. This was accompanied by a change in the orientation of the plywood gusset. Further methods of analysis to determine nail loads and gusset stresses were described by

Walford (1988). He indicated that a method described by Mitchell (1979) was both simple and consistent over a wide range of joint shapes when compared to an "exact" analysis which allowed for non-linear load/slip behaviour of nails. He also recommended that a torsion tube analogy for nail load-slip analysis may be more appropriate in calculation of ultimate joint capacity.

A study by Perkins, et al. (1964) concluded that the torsion or rivet formula as in Eqn. 2.1 was found to be adequate for most nail patterns. The equation notations are shown schematically in Figure 2.3.

$$T_i = (M.r_i)/\Sigma r^2 \qquad \textbf{(Eqn. 2.1)}$$

where T_i is the force component in a direction normal to the distance r_i (radius from the centroid of the pattern) and M is the applied moment.

In their study, the relative rotation of the joint members as shown in Figure 2.4 was related to load-slip behaviour by Eqn. 2.2 and Eqn. 2.3.

$$\Theta = M/(a\,\Sigma r). \qquad \textbf{(Eqn. 2.2)}$$

$$S_i = \Theta r_i \qquad \textbf{(Eqn. 2.3)}$$

Where Θ is the angular rotation in radians, S_i is the measured slip and a is a fitting constant. This formula fitted his test curves quite sufficiently.

The torsional formula makes no provision for distortion in a joint and indicates that the portion of the entire load carried by the individual nails will be proportional to their respective distances from the instantaneous center; whereas the curvilinearity of the load-slip relationship dictates that once a nailed joint does slip there will be automatic lessening of the load on the extreme nail. This causes the other nails in the pattern to share the load in greater than linearly proportional amounts.

Finally, Kivell et al. (1981) produced hysteretic models of nailed gussets in moment-resistant timber joints where they later conducted research on cyclic loading on such joints (1982).

2.2 RESEARCH ON TIMBER FASTENERS AND TIMBER JOINTS

2.2.1 Nailed Connections

Through the mid 1970's, Foschi (1974) investigated the load-slip characteristics of nails, which is defined as a nonlinear relationship between a force applied to the head of a nail (which is already driven into the wood) and the head displacement, caused by a force applied in a normal direction to the nail shank.

Foschi's work led to the development of analytical models which are useful in predicting the yielding mechanism of the nail due to bending and the nonlinear bearing behaviour of the wood material due to the effects of the load.

Characteristic properties of nailed and bolted joints under short-term lateral loads were investigated by Smith et al. (1987). The short-term test observations suggest that bolted connections are more prone to brittle failure than nailed connections. Higher load factors relating working strength to ultimate strength might therefore be reasonably applied. In nailed joints, high load factors are used to reduce the ultimate load capacity to a level which will give a slip that is sufficiently low to ensure serviceable connections at the working load levels. Bolts are often used in connections where slip is less critical and where design loads can be assigned a higher proportion of the ultimate capacities than is appropriate for nailed connections. Rather than using tabulated data for design, Smith

suggested that the basic material property equations and the set of yield equations be presented instead. This would enable designers to calculate the appropriate ultimate load for any arrangement, and would identify the mode of failure to be expected.

2.2.2 Glulam Rivet Connections

In the late 1960's, Madsen developed a high strength nail (commonly called glulam rivet) to be used in conjunction with a steel plate and glued-laminated timber. The glulam rivet has geometric properties as shown in Figure 2.5, where the rectangular shaft is pushed through an undersized circular hole in a steel plate. The high stresses developed on the sides of the shaft holds the nail firmly in place. The cantilever action from the nails was used to resist the lateral load as shown schematically in Figure 2.5. Research by Aune and Patton-Mallory (1986) has indicated that for joints with an initial gap between the members, the effect of driving the nails flush to the surface is to increase the lateral load by about 30%. In practical structures nail heads may not be driven flush to the surface, and the timbers may not be in close contact after shrinkage movements have occurred, hence it is more appropriate to ignore this increase in design.

McGowan (1966) studied the glulam rivet plate connector's performance under different variables such as nail length, nail spacing, fixity of nailhead in plate, form of shank, and end and edge distances. Profound differences were realized. He concluded that where fastenings contained large numbers of nails, strength on a per nail basis was not constant, but was largely dependent on the number of nails aligned in the direction of the applied load. He also found that glulam rivet plate fastenings were superior in stiffness properties to bolted shear plate connectors.

In glulam rivet connections, a stress analysis for the cluster of rivets loaded parallel and perpendicular to the grain has been done by Foschi (1974). This analysis, together with a report on the maximum load-carrying capacity of a single rivet, allows a simple design procedure for this type of connection. The procedure is advantageous in that it permits taking into account all different parameters controlling the design of these connections such as rivet spacing in both directions, end and edge distances and the number of rows (parallel to the grain) and columns (perpendicular to the grain) of rivets in a joint. Foschi work was conducted on Douglas fir species of wood.

Further work by Foschi and Longworth (1975) investigated group behaviour of glulam rivets and the effects of loads distribution and nailing patterns. The conclusions were:

1) Nail spacing control the mode of failure of the connection, with wider spacing producing nail yielding modes.

2) Close nail spacing may produce brittle wood failures, usually by shearing around the groups of nails at loads less than the nail capacity.

3) For the same nail spacing a longer end distance increases the ultimate load based upon shear failure.

4) It is possible to estimate both nail yielding failure and wood bearing failure so that wood failures will not occur before nail yielding, thus optimizing nail utilization.

In order to extend the use of glulam rivets to other wood species, Karacabeyli and Fraser (1989) carried out tests using spruce glulam and solid timber. Buchanan and Lai (1993) found that glulam rivets in radiata pine have 70-90% of the strength of rivets in Douglas fir. He also found that the European yield theory (originally developed by Johansen (1949)) gave excellent predictions of rivet strength and failure mode in those conditions where wood tension failures were not expected. This theory predicts the ultimate lateral load of a nailed timber joint assuming plasticity in both the wood and the fastener.

2.2.3 Shear Plates, Split Rings and Bolts in Timber Joints

The investigation of Masse et al. (1988) on the lateral strength and stiffness of single and multiple bolts in glued-laminated timber loaded parallel to the grain was part of a study to determine if the analytical yield model based on Larsen (1973) could predict adequately the strength of single and multiple bolt connections. His study dealt only with the experimental determination of bolted connections with varied end distances, bolt spacing, number of rows, and columns of bolts.

Wilkinson (1993) later investigated the properties of bolted connections with steel side plates. He found that the European Yield Model predicted bolted connection yield load with acceptable accuracy, and that the yield load slightly increased with increased steel member thickness, except when the increased thickness caused the side member to bear on the bolt threads. He also found that connections loaded parallel to the grain by tension or compression loading gave the same results.

Lheude (1985) conducted studies where he found that the maximum tension load capacity of 102 mm diameter shear plates and split rings was approximately 50% of the

compression capacity, however the capacities were similar for the smaller diameter connectors. In addition, where connectors were fitted into grooves cut in the green condition and allowed to dry, splitting reduced the average green tension capacity by 20%. Lheude also found that an increase in end distance with the larger diameter shear plates improved the tension load capacity for two species tested.

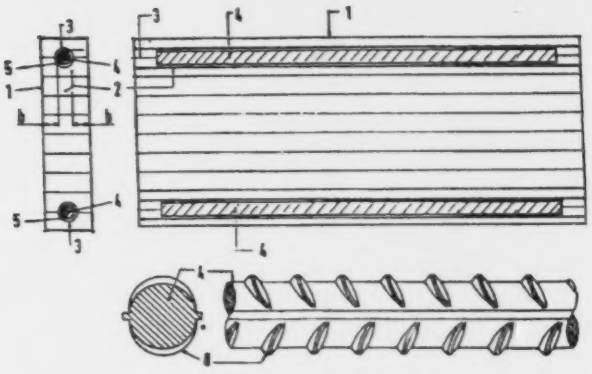

Figure 2.1 - Glulam Timber Reinforcement System (Gardner, 1989)

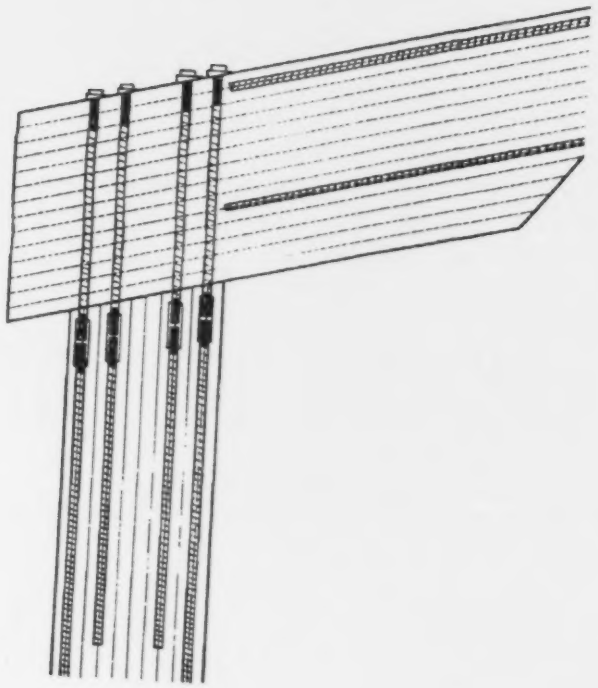

Figure 2.2 - Typical Portal Knee developed by Gardner (Gardner, 1989)

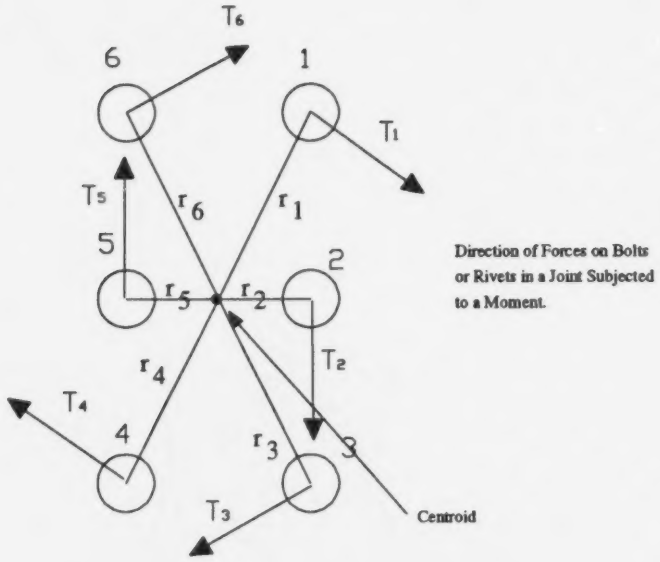

Figure 2.3 - Direction of Forces on Bolts

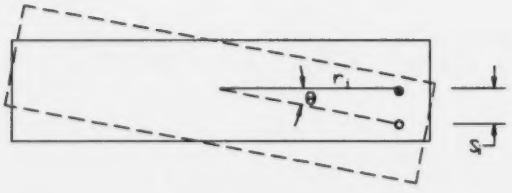

Figure 2.4 - Load-Slip Schematic

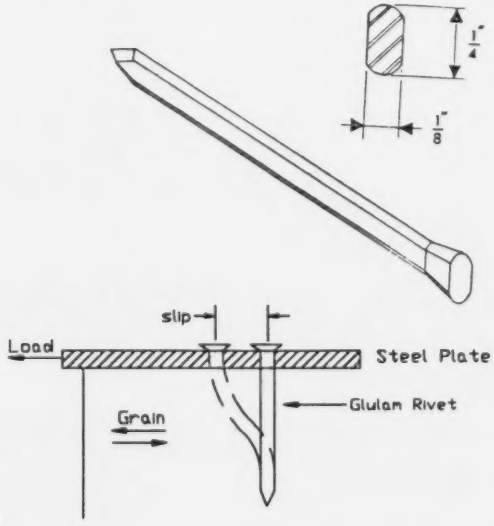

Figure 2.5 - The Glulam Rivet (McGowan, 1966)

3.0 EXPERIMENTAL PROGRAM

3.1 INTRODUCTION

The experimental program was conducted in two phases. The first was a preliminary investigation to establish a comparison between the different glued-laminated timber moment connections based on the type of mechanical fastener used to hold the joint. The joint with the best performance in this phase was further investigated and studied in the second phase where improvements were also made and evaluated.

3.2 GEOMETRY AND MATERIAL SPECIFICATION

3.2.1 Specimens and Connections Patterns

The first phase consisted of six specimens (A1 to A6): three steel rivet plate connections, and three bolted connections. The three riveted connections had rivet patterns of 7x10, 10x10 and 10x7 for specimens A1 to A3, respectively. Figures 3.1 and 3.2 show the 7x10 and 10x10 patterns, respectively. Figures 3.3 and 3.4 show the rivet plate used in Specimen A3 in which 10x7 signifies 10 rows of rivets multiplied by 7 columns of rivets. A row of rivets is a line of rivets parallel to the grain in the top member, whereas the column of rivets is a line of rivets in a direction perpendicular to the grain in the top member (See Figure 3.4). The opposite is true for the bottom member. The dashed line shows the boundary between the two connecting members. The same patterns were used on each of the two connecting members and on both sides. The specimens were designed to study the effects of the number of the rivets and their patterns on the behaviour of the

connections under the action of a moment. Specimen A4 had two steel side plates (size 270 mm x 600 mm) with a rectangular 4x2 bolt pattern as shown in Figures 3.5 and 3.6. These specimens where the two connecting members lie in the same plane are butt type joints. The differences between butt and lap type joints are shown in Figure 3.7. Two circular bolt patterns as shown in Figures 3.8 and 3.9, one with wooden side plates and another with steel side plates for Specimens A5 and A6, were tested using lap type joints. This phase aimed at studying the effect of various rivet and bolt patterns on the performance of moment connections. All bolted connections (Specimens A4, A5, A6 and B1) utilized 67 mm (2-5/8") shear plates on each side of every member in each joint.

The second phase consisted of 5 specimens. This phase was further divided into series B and C. Series B consisted of Specimen B1 which had a rectangular bolted connection as shown in Figure 3.5, similar to Specimen A4, but different with respect to the thickness of the members. This specimen was designed to study the force distribution among the bolts and locate the instantaneous center (I.C.) of the butt type of joints.

Series C consisted of 4 specimens. Specimen C1 was similar to Specimen A3 (i.e. 10x7 rivet pattern) with the addition of a 6.3 mm thick bottom steel bracket, as shown in Figure 3.10, fixed to the bottom corner of the joint with wood screws. Specimens C2 and C3 (Figures 3.11 and 3.12) were also similar to specimen A3 (i.e. 10x7 rivet pattern) with the addition of a bottom steel bracket and a rivet 6.3 mm thick top steel bracket as shown in Figure 3.13. Specimen C3 had a larger moment arm than Specimen C2. A steel bearing plate between the two connecting members was used in lieu of the bottom steel bracket in Specimen C4. Both the bearing plate and the top bracket had a thickness of 9.5 mm. In addition, a 5x4 rivet pattern was used in Specimen C4 instead of the 10x7 used in the other specimens tested in series C. Hence, the spacing between the rivets in both parallel

and perpendicular directions to the grain was increased from 25 mm in the 10x7 patterns to 40 mm in the 5x4 pattern.

3.2.2 Specimen Size, Preparation and Specified Strengths

Alberta spruce and pine glued-laminated timber manufactured by Western Archib in Edmonton, Alberta was used for the specimens. The cross section of the main member in the lap joints and both members in the butt joints were chosen to be 130 mm x 380 mm. That is 10 laminates of 130 mm x 38 mm timber sections. The smaller section, 80 mm x 380 mm (i.e. 10 laminates of 80 x 38 mm) was chosen for Specimen B1 and the side members in the lap joints (A5 and A6), since only one half of the applied force on the middle member is applied on each of the side members.

Specimen C3 had member lengths of 1500 mm and 1880 mm forming a moment lever arm of 980 mm. All the other specimens had member lengths of 1120 mm and 1500 mm providing a moment lever arm of 720 mm (see Figure 3.14). The length of all the members in the lap joints were 1500 mm giving a moment lever arm of 720 mm since the instantaneous center of the lap joints is in the center of the circular bolt pattern as opposed to the bottom corner in all the butt joints.

The timber used was spruce and pine of grade 20f-EX. Its specified strengths are presented in Table 3.1 (CAN/CSA-O86.1-M89, 1989). The bolts and rivets used conform to the requirements of CSA Standard CAN3-G40.21 (1989) and ASTM Standard A36 (1988). The bolts were 19 mm (3/4") diameter of type ASTM-A307 with a specified shear strength of 33.4 kN in single shear. The specified properties of the glulam rivets used (also called "griplam nails"), are shown in Table 3.2.

The rivets were driven through using a sledge hammer, positioned by aligning their longitudinal axis parallel to the wood grain of each member. The bolt holes, however, were made using a 21 mm (13/16") bit drill to fit the 19 mm (3/4") steel bolts, then a special grooving tool was attached to the drill to create the groove holes for the 67 mm (2-5/8") shear plates.

3.3 TEST SETUP

The test setup is shown in Fig. 3.14. The photographic setup is illustrated in Figure 3.15. A manual hydraulic ram (shown in Figure 3.16) with a capacity of 200 kN was used to apply the load. The specimen was mounted on rollers at the load point and on a stub beam bolted to the ground at the other end (Shown in Figure 3.17) using two steel brackets. The attachment was achieved using pins to allow rotation at the ends of the specimens. Friction from the pins was ignored since its effect on the moment applied was considered to be negligible. Bolt holes of 27 mm (1-1/16") in diameter were created in the brackets and the ends of each specimen, to attach the brackets to the specimen. To prevent out-of-plane side sway of the specimen during the test, a beam with attached angles was set on two columns and used to brace the specimens at the apex as shown in Figure 3.15.

3.4 INSTRUMENTATION

The instrumentation can be categorized based on the measurements taken: loads, displacements, slips measurements and strains. Figure 3.14 shows the location of the various instrumentation used.

The main characteristic to be found from this test is the load-rotation (moment-rotation) curve. A load cell was installed at the load point to measure the applied load. To measure the rotation, electronic rotational gauges were installed approximately on the quarter points of each member away from the joint. The influence of the beam bending and verification of rotational gauge data was of some concern, hence cable transducers were installed at the quarter points and half points of each member to measure the movement of each of the members at points of concern. The cable transducer boxes were fixed to a plywood board and on a timber column mounted on the board in the first series of tests; however, they were mounted on the member itself in the later series to reduce the measurement error (see Figure 3.18).

The movement of the point load (i.e. the stroke) was measured using a cable transducer. The slippage of the reaction frame (stub column) was also measured using a mechanical dial gauge mounted on a fixed point against the frame. Measurements of the movement of the cover (side) steel or wooden plates with respect to the timber were taken throughout the first series using the 50 mm spaced demec points at selected locations on both sides of each plate.

Strain gauges were used in the second phase of the experimental program. Rosette strain gauges were mounted on the steel plate at the far row of bolts in Specimen B1 as shown in

Figures 3.19 and 3.20 to locate the principal strains. In series C, longitudinal strain gauges were mounted on the side plate below certain rivets (see Figures 3.21 and 3.22) to measure the stress distribution between the rivets. Since Specimen C4 had a different rivet pattern on the side plates, the strain gauge layout varied as in Figure 3.23. Longitudinal strain gauges were also mounted on the top bracket as in Figures 3.24 and 3.25. Some of the gauges were mounted only on the outer surface to measure the stress distribution between the rivets. However, at four locations strain gauges were placed on both sides of the bracket to measure its total average cross-sectional strain.

3.5 TEST PROCEDURE

During the test, all data from the cable transducers, the load cell, the strain gauges, and the rotational gauges were gathered automatically by a computerized data acquisition system. This data was measured and collected continuously during the test every fourth scan on the computer system (i.e. about every 10 seconds). The reaction frame displacements and the demec measurements were gathered manually. The load, which was applied on the specimen manually, was stopped at load increments of 3 kN, and after allowing it to settle down for a short period of time, that is until the load cell reading stabilized, the manual readings were taken and the propagating cracks were marked. The sustained load increased as well as the propagation of the cracks until ultimate loading capacity was achieved, and a significant drop in the sustained load occurred. The experiments averaged a testing period of two hours, after which, photographs were taken for each failed specimen.

In Specimen B1, however, the loading process was different. The load was applied in four cycles. The highest load reached in each cycle was 5 kN, 9 kN, 11 kN and finally the ultimate load capacity of the specimen.

3.6 MATERIAL AND EMBEDMENT TESTS

Tests were conducted to determine the properties of the steel used in the top brackets of the specimens in series C, and the embedment strength of glulam rivets and shear plates in glued laminated timber used to construct the specimens.

Three steel tension coupons were fabricated from the top bracket of Specimen C3, and three from Specimen C4. A 50 mm gage length was used. All coupon tests were conducted in accordance with ASTM Standard A370-92 (1992). Embedment tests for the rivets and shear plates were conducted in accordance with ASTM Standard D1761-88 (1990).

Two distribution patterns of rivets were tested in the parallel to the grain direction. Two replications were tested in each pattern. A 5x4 pattern (similar to the side plate of Specimen C4) with a spacing (Sp) between rivets equal to 40 mm in both directions, and a 8x4 pattern (used in the top brackets of series C) with a spacing (Sp) between rivets equal to 25 mm in both directions. The test setup is shown in Figure 3.26, where only one plate of the tested pattern was attached to one end of the beam, and two heavily riveted plates were attached on the other end. This guaranteed that the failure would occur at the pattern to be tested. Concern of some eccentric loading was eliminated since the load deformation characteristics of both ends were not equal.

Shear plate embedment tests were conducted in a direction once parallel and once perpendicular to the grain, where a 67 mm (2-5/8") shear plate was embedded on both sides of the beam and loaded. A 4x4 rivet pattern with a spacing (Sp) between rivets of 25 mm was attached to both sides of the beam and loaded perpendicular to the grain as shown in Figure 3.27. A clear distance between supports greater than three times the transverse depth of the member was maintained as required in ASTM Standard D1761-88 (1990).

Table 3.1 - Specified Strengths and Modulus of Elasticity of Specimens (MPa)

f_b+	f_b-	f_v	f_c	f_{cb}	f_{cp}	f_{tn}	f_{tg}	f_{tp}	M.O.E.
25.6	25.6	1.75	15.3	17.2	5.3	17.0	12.7	0.51	10 300

Table 3.2 - Specified Properties of Glulam Rivets

Length (mm)	Hardness	Ult. Tensile Strength	Finish
65	Rockwell C32-39	1 000 MPa, minimum	Hot-dip galvanized

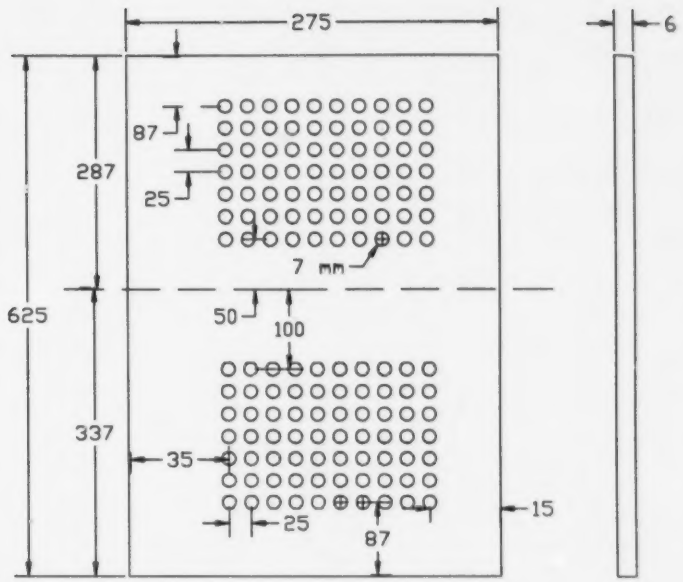

Figure 3.1 - Specimen A1 (7x10) Pattern

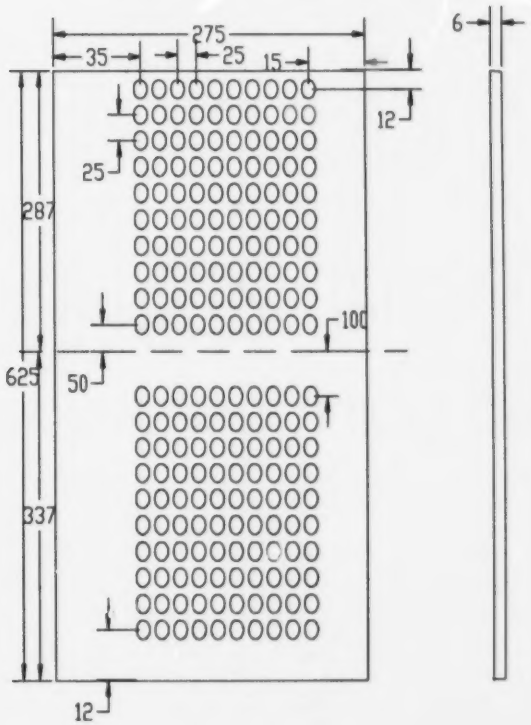

Figure 3.2 - Specimen A2 (10x10) Pattern

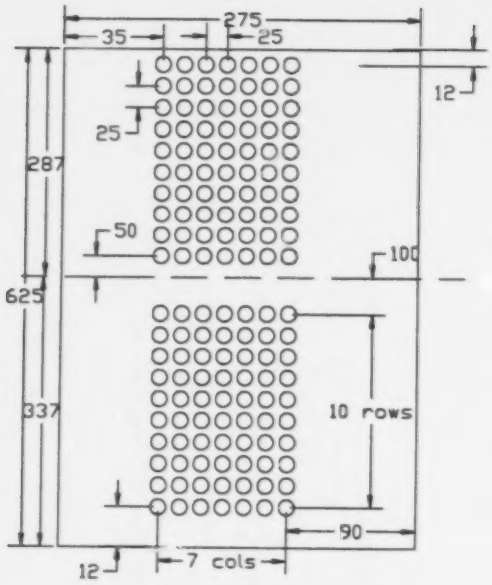

Figure 3.3 - Specimen A3 (10x7) Pattern

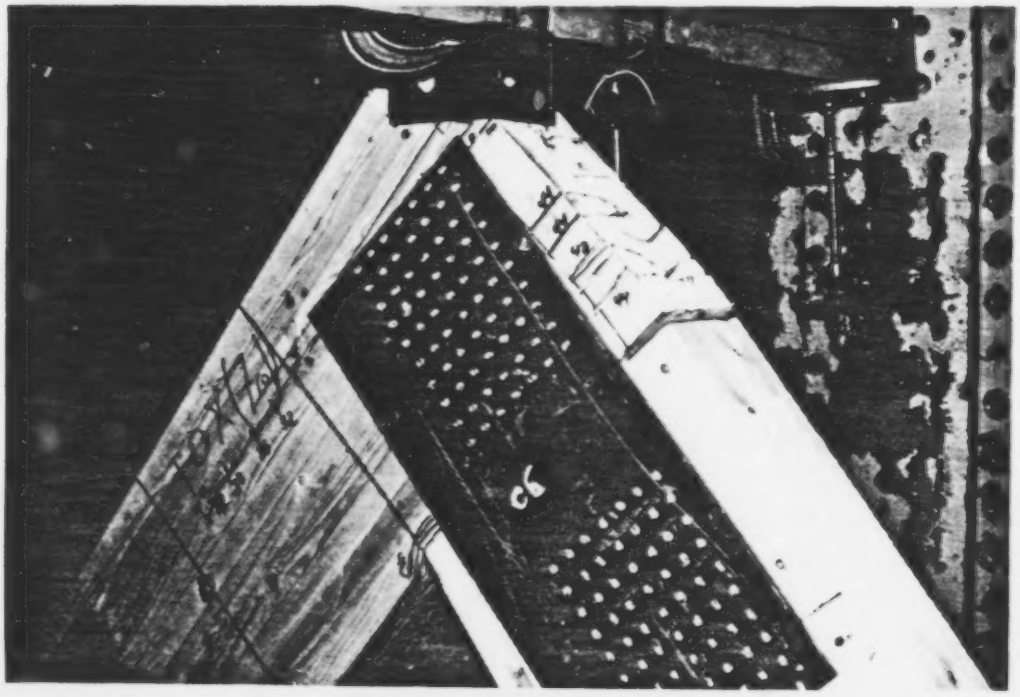

Figure 3.4 - 10x7 Rivet Pattern

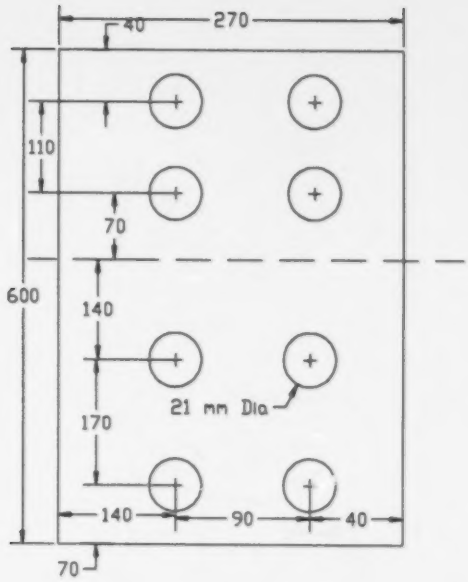

Figure 3.5 - Specimen A4 & B1 (4x2)

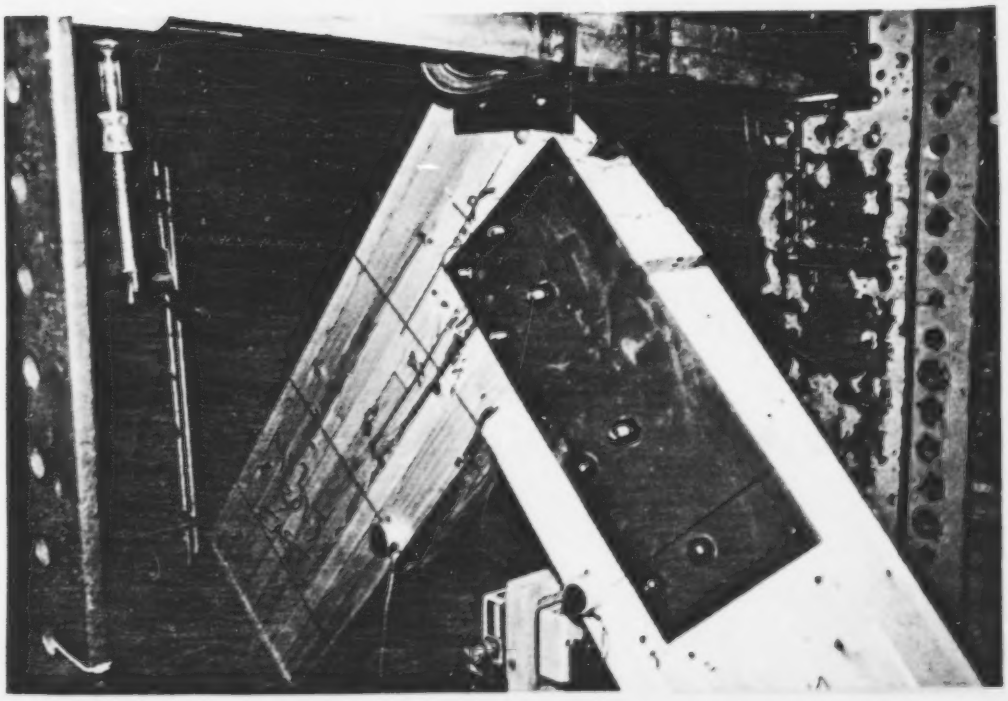

Figure 3.6 - Butt Joint Bolted Connection

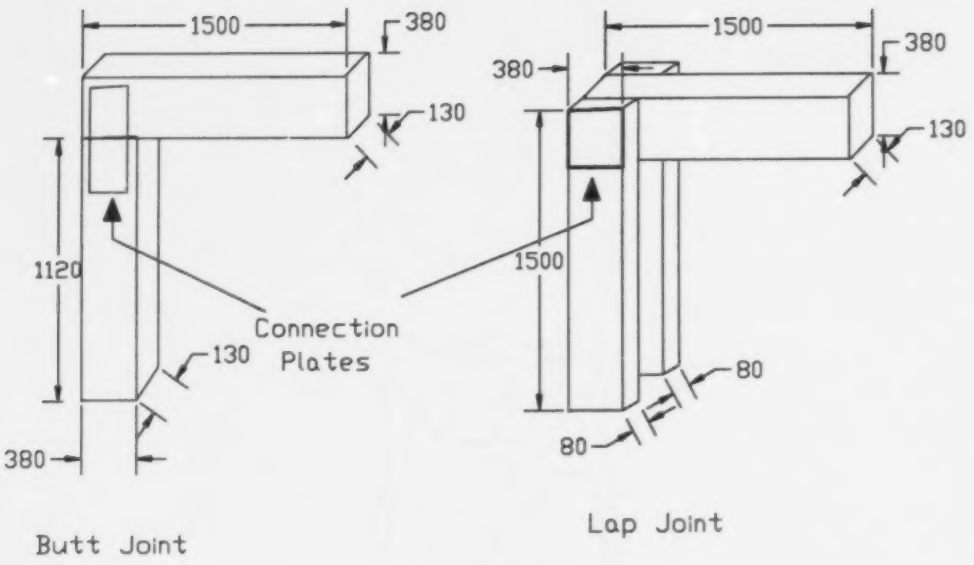

Figure 3.7 - Joint Comparison

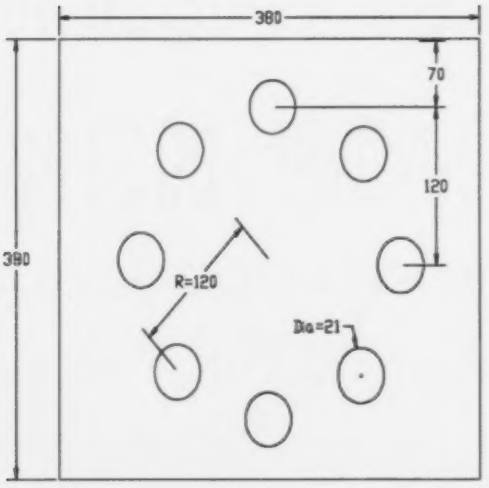

Figure 3.8 - Specimen A5 & A6 (Circular)

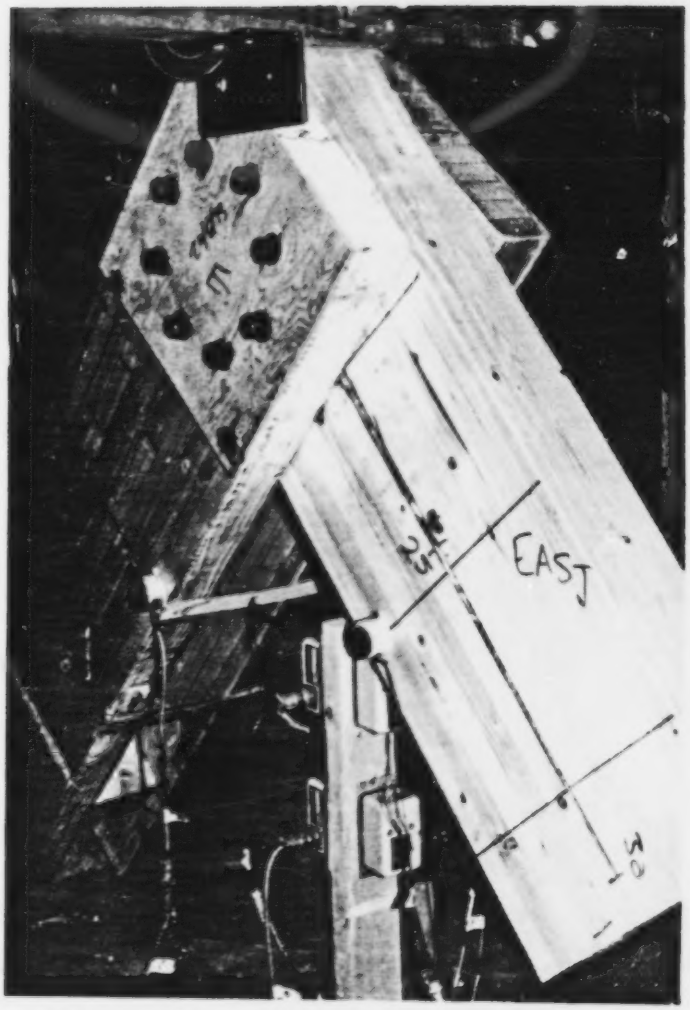

Figure 3.9 - Circular Bolted Pattern

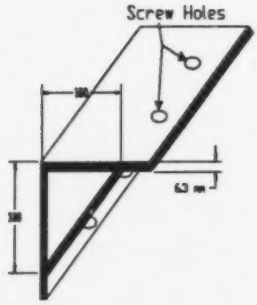

Figure 3.10 - Bottom Bracket (Series C)

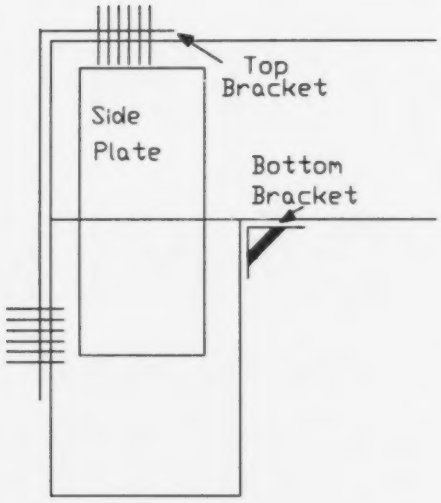

Figure 3.11 - Specimen C2 & C3

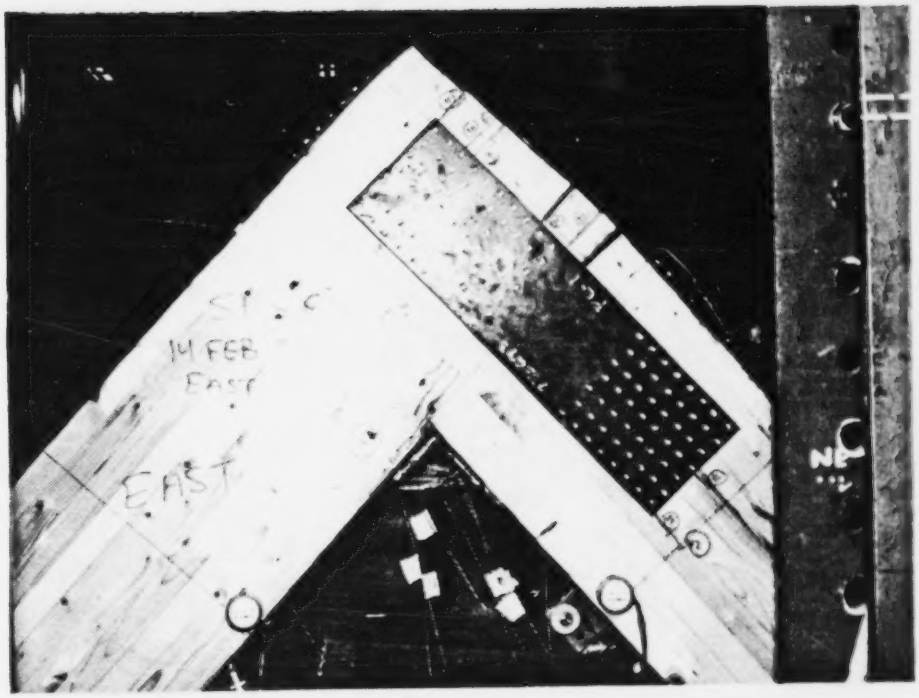

Figure 3.12 - Specimen C3

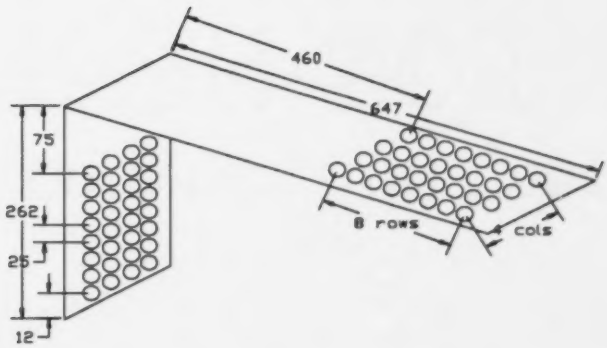

Figure 3.13 - Top Bracket (Specimen C2 & C3)

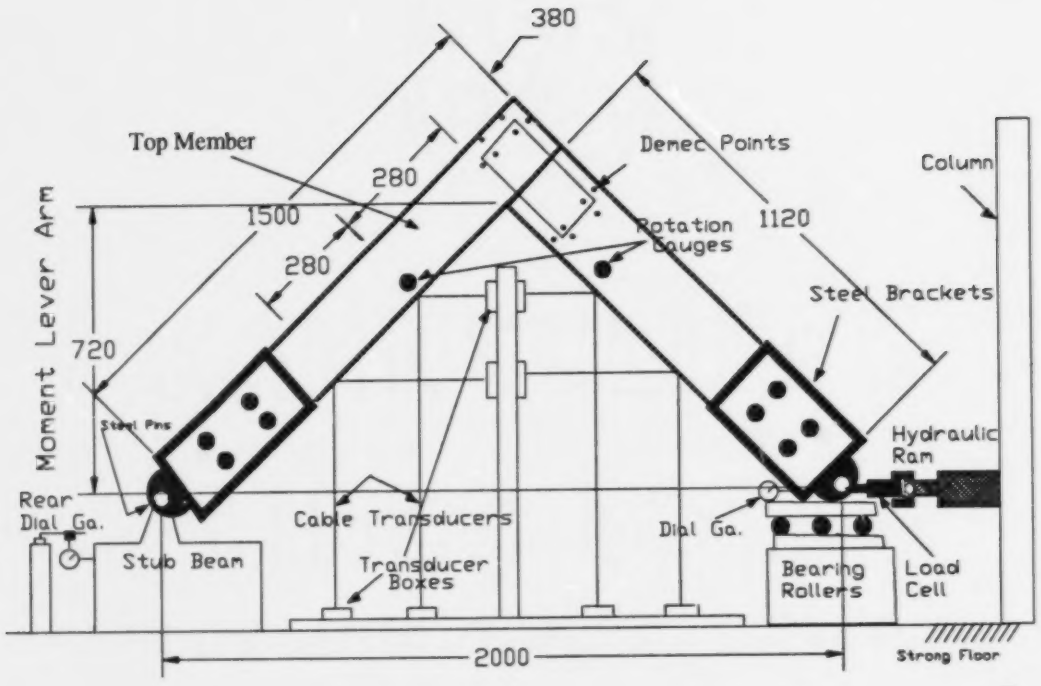

Figure 3.14 - Schematic Test Setup

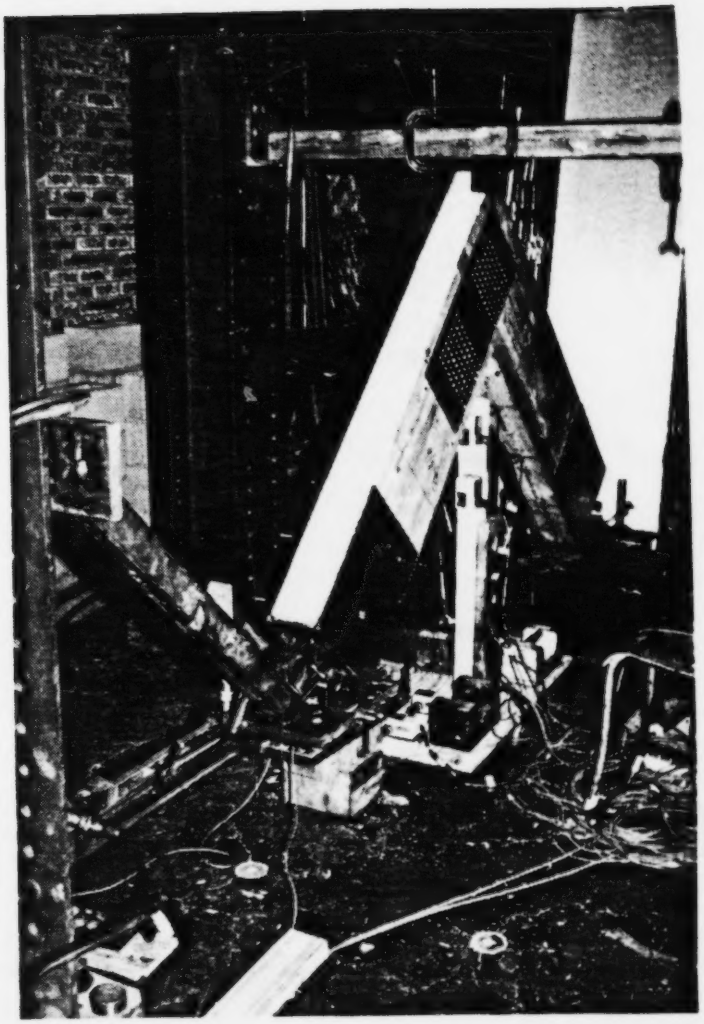

Figure 3.15 - Photographic Test Setup

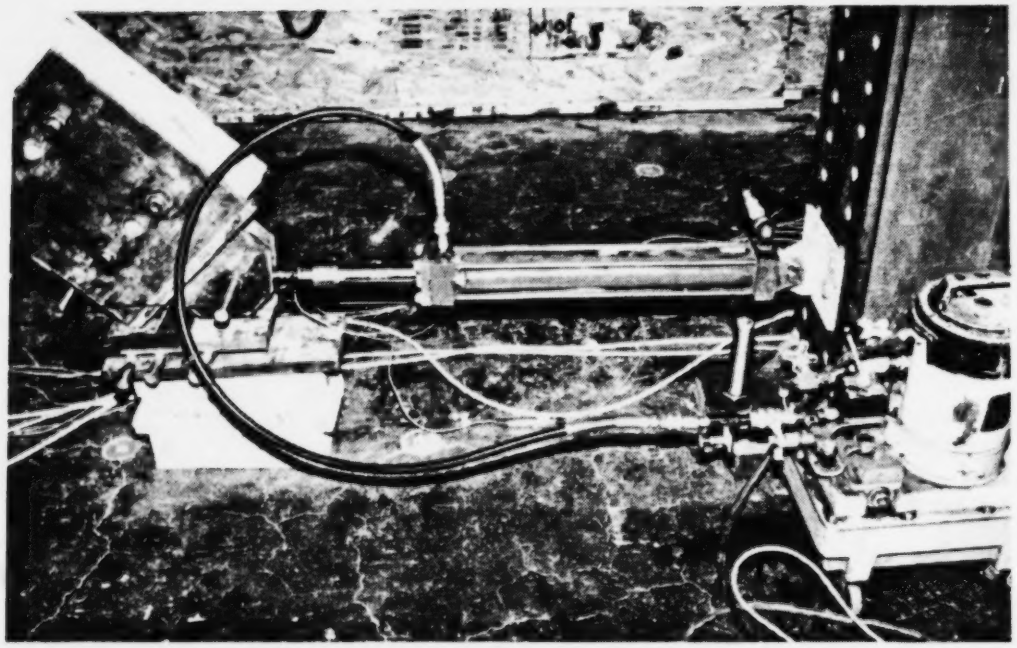

Figure 3.16 - Manual Hydraulic Ram

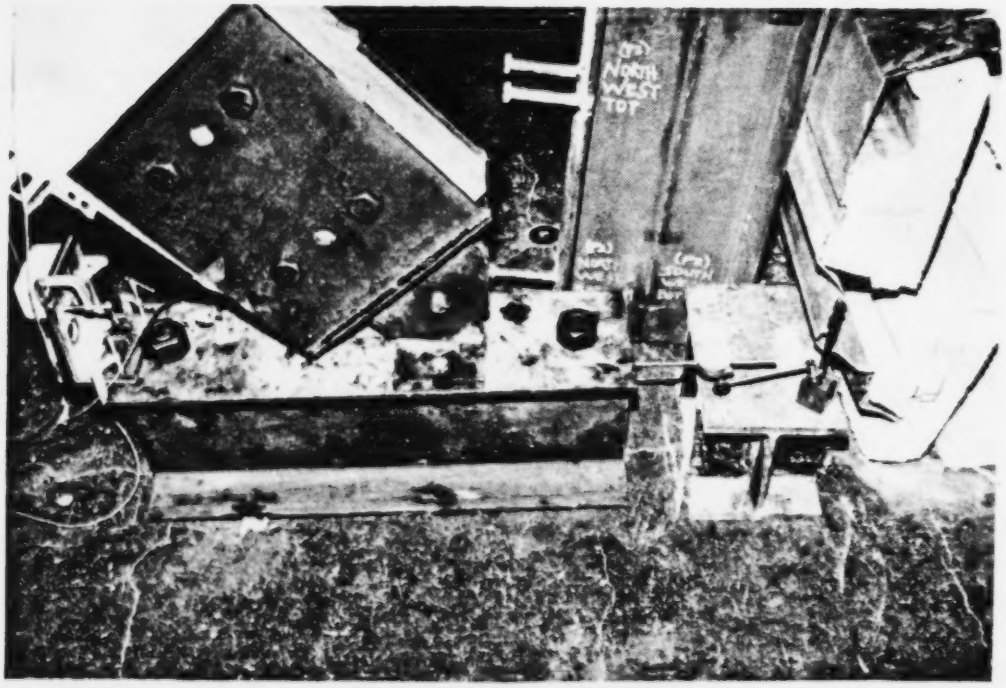

Figure 3.17 - Reaction Frame

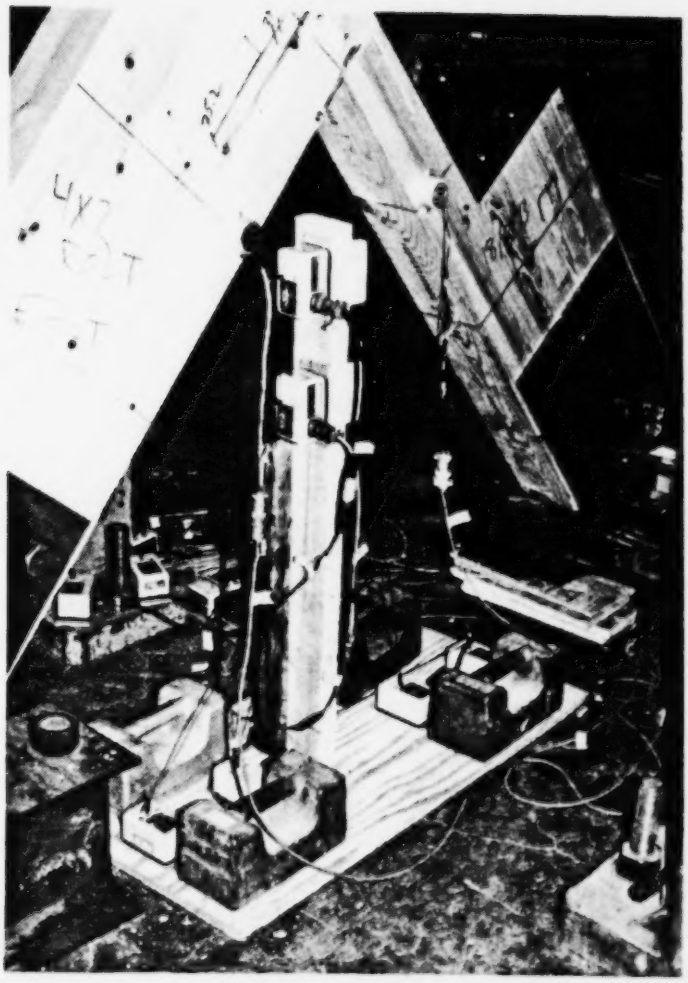

Figure 3.18 - Rotation Gauges and Cable Transducer Boxes

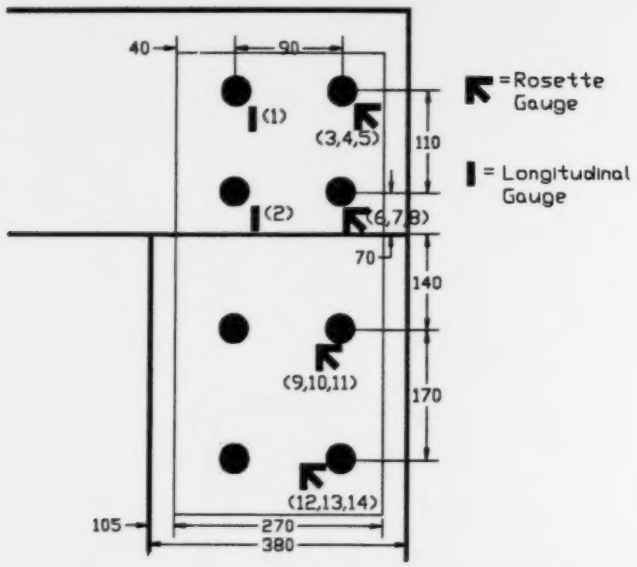

Figure 3.19- Gauge Layout on Specimen B1

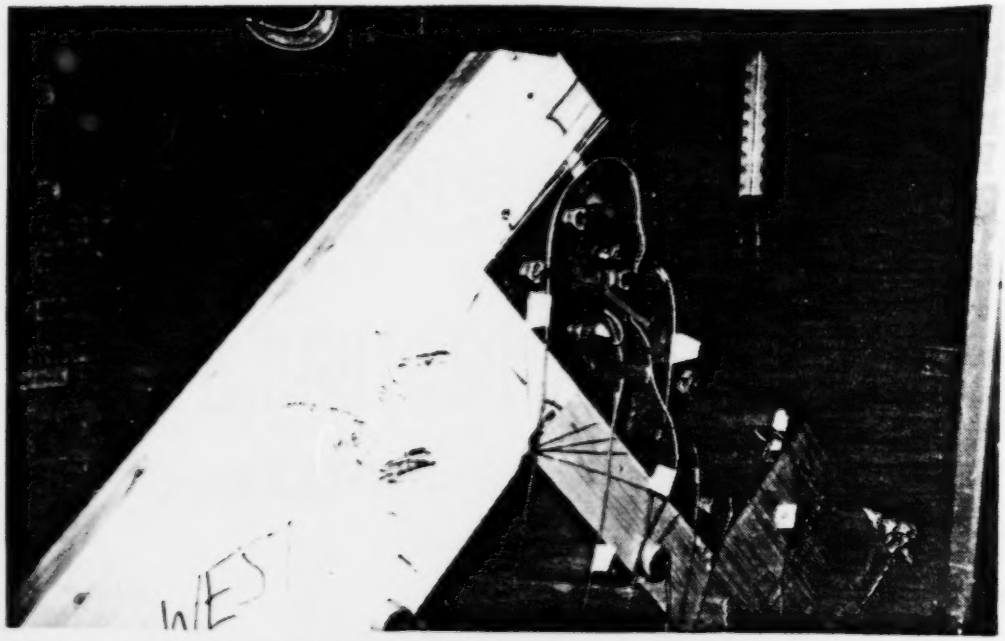

Figure 3.20 - Gauge Layout on Specimen B1

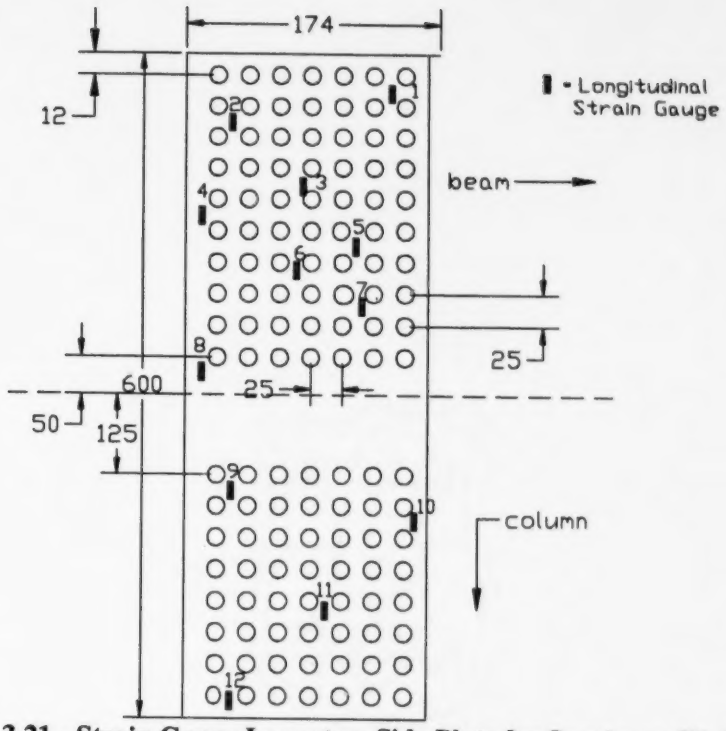

Figure 3.21 - Strain Gauge Layout on Side Plate for Specimen C1, C2, C3

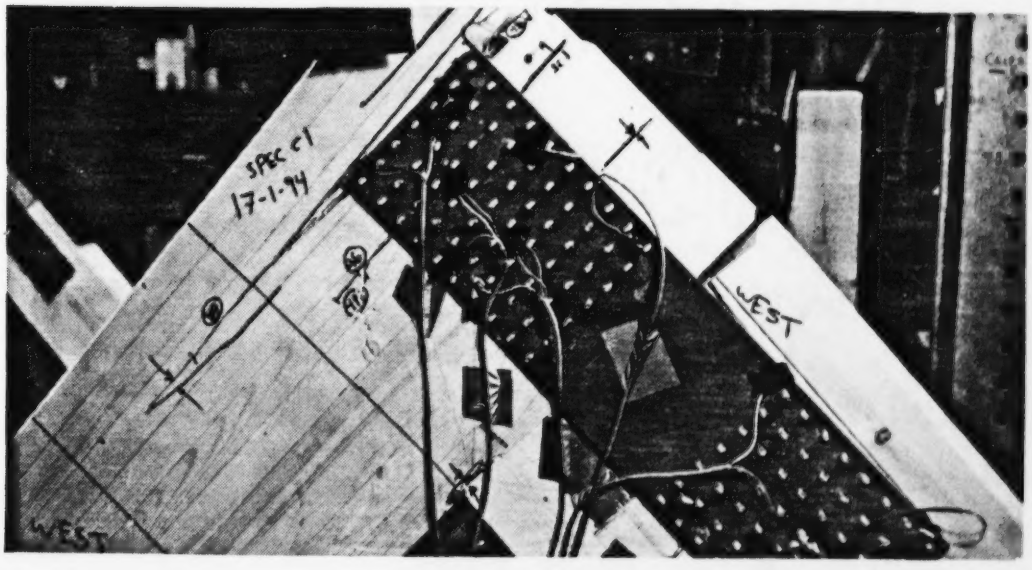

Figure 3.22 - Strain Gauge Layout on Side Plate for Specimen C1, C2, C3

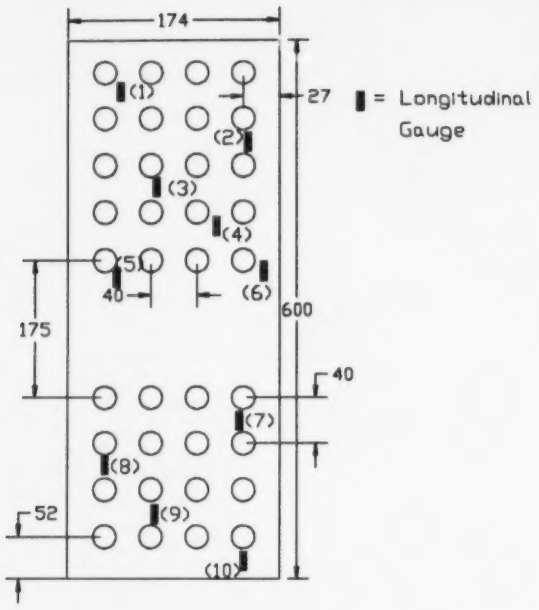

Figure 3.23 - Strain Gauge Layout on Side Plate for Specimen C4

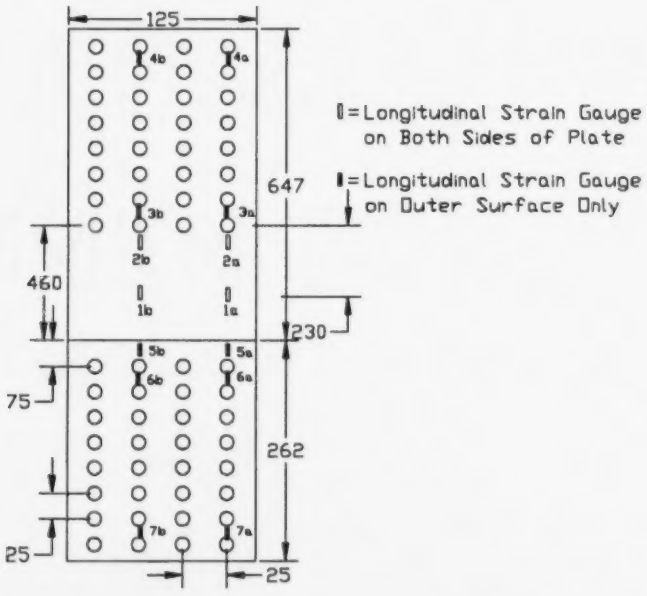

Figure 3.24 - Strain Gauge Layout on Top Bracket

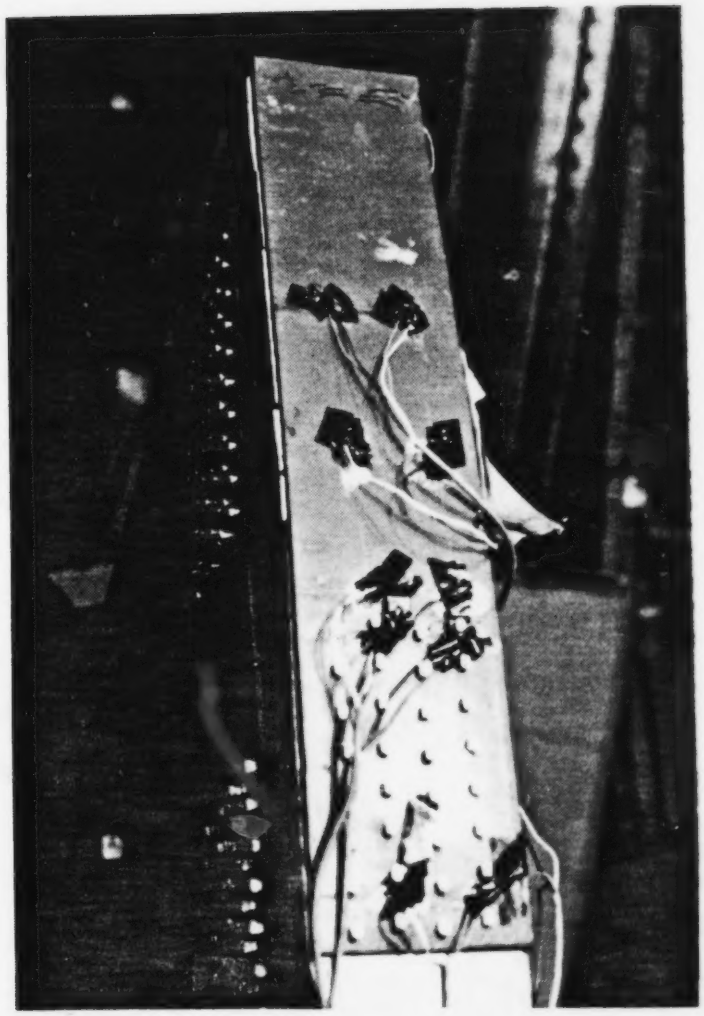

Figure 3.25 - Strain Gauge Layout on Top Bracket

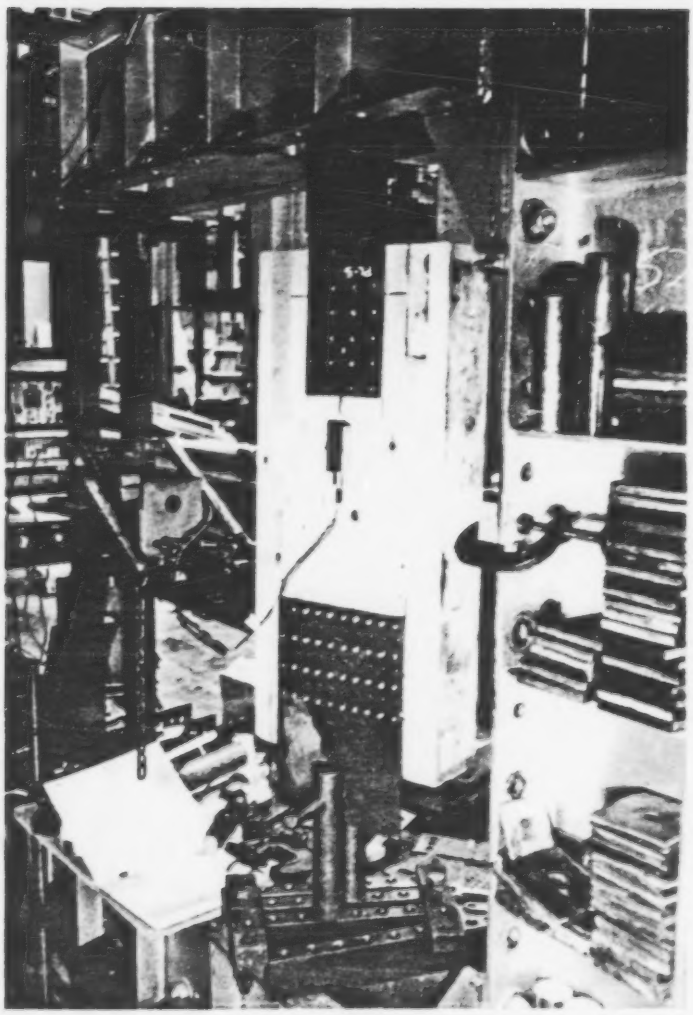

Figure 3.26 - Photographic Test Setup for the 5x4 Rivet Plate Loaded Parallel to the Grain

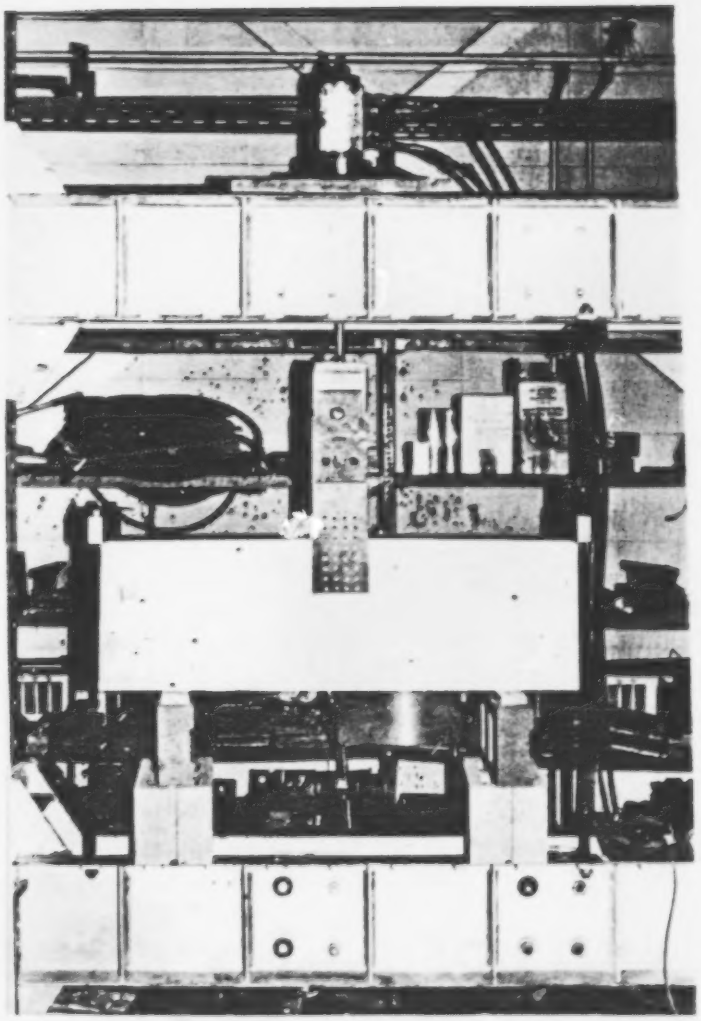

Figure 3.27 - Photographic Test Setup for the 4x4 Rivet Plate Loaded Perpendicular to the Grain

4.0 EXPERIMENTAL RESULTS

4.1 INTRODUCTION

The results of the two phases of the experimental program are presented in this chapter. The material properties of the test specimens are presented in Section 4.2. The full test behaviour of each specimen is presented in Section 4.3. This includes the physical behaviour of the specimens, the moment vs. rotation curves, and the strain distribution in the steel fastener plates.

4.2 MATERIAL PROPERTIES

Table 4.1 presents the results from the steel coupon tests. That includes the elastic modulus, the static yield, strength and the ultimate strength. Both the thin and thick sections provided lower than expected elastic moduli. The thick section had a higher average static yield strength than the thinner one but a lower average ultimate strength. A typical plot of stress vs. strain is shown in Figure 4.1.

The results of the fastener embedment tests are presented in Table 4.2. For the patterns where more than one test was performed, the average embedment strength is presented. The specified strength of each connection from CAN/CSA-O86.1-M89 (1989) is also listed. Both the specified and tested strengths were very similar for all but test #3 where the embedment strength of the 67 mm (2-5/8") shear plate loaded parallel to the grain was 50% higher than the specified value.

The embedment strength of the riveted plates was divided by the number of rivets, hence the average strength per rivet in both directions, can be used in the analysis to calculate the moment resistance of the moment connections. Typical plots of load vs. deformation for fasteners loaded in both parallel and perpendicular directions to the grain are shown in Figures 4.2 and 4.3. In addition, the moisture content (M.C.) for each specimen is presented in Table 4.3.

4.3 TEST RESULTS

The summary of the results from all series of experiments is presented in Table 4.3. The ultimate loads at which the connection failed are presented accompanied by the rotational angles. The rotation values represent the change in the 90 degree angle of the joint. The moment vs. rotation curves of all specimens are presented in Figures 4.5 and 4.6. The moment was calculated based on a lever arm as shown in Figure 3.14. The Secant Stiffness (The slope of the line that intersects the moment-rotation curve at 50% of the ultimate moment and at zero moment) for each specimen is also presented in Table 4.3. They are illustrated using the moment vs. rotation curve of Specimen A2 in Figure 4.4.

4.3.1 Phase 1 - Preliminary Investigation

4.3.1.1 General

This section provides a descriptive behaviour of the tested connections. Referring to Figure 4.5, Specimens A2 and A3, which have rivet patterns of 10x10 and 10x7, respectively, appeared to have performed similarly in terms of strength and stiffness; however, the latter exhibited a longer period of plastic rotation. Specimen A1, with 7x10

rivet, yielded less strength and stiffness than Specimens A2 and A3. Nevertheless, all three riveted connections performed better than the other three bolted specimens (A4 to A6).

Specimen A5 and A6, having circular bolt patterns, performed with higher strength and stiffness, than Specimen A4 with the rectangular bolt pattern. Specimen A6 with steel side plates performed slightly better than Specimen A5. Nevertheless, all three exhibited large rotations.

4.3.1.2 The Riveted Connections

The ultimate load at which Specimen A1 (7x10 rivet) failed was 31 kN corresponding to a moment of 22.3 kN.m. The specimen witnessed an ultimate rotational angle change of 3.9°. After this point, the load dropped dramatically (Figure 4.5). The specimen failed mainly in splitting along the side grain near the farthest rivet from the bottom corner of the connection. Cracks in the end grain started to develop at 8.6 kN.m and opened up as wide as 20 mm at the end of the test, as shown in Figure 4.7. These cracks opened up and spread throughout the top member. The highest cracks in the end grain occurred first and opened up the most since they were the ones closest to the most stressed rivet.

Another phenomenon of interest was the crushing of the wood at the bottom corner of the joint where the two members met. This was not a cause for failure, but the differential displacement between the bottom of the joint (where the crushing occurred) and the top (where the gap opened) contributed to the joint rotation hence reducing the joints stiffness.

Specimen A2 (10x10 rivet) had an ultimate loading capacity of 45 kN, corresponding to a moment of 32.4 kN.m. The ultimate rotational angle change achieved in this specimen was 3.55°. Similar to Specimen A1, Specimen A2 failed in splitting along the side grain. The pattern provided a large number of rivet columns perpendicular to the grain, hence one big crack occurred just above the highest row of rivets, as shown in Figure 4.8, leading to a brittle sudden failure. The crack spread throughout the specimen similar to Specimen A1. Crushing of the wood at the joint also occurred in the same manner. Before the test on Specimen A2 commenced, the gap between the two connecting members on the east side was smaller than that on the west side, so during the test, it was observed that the east side crack spread less through the member than on the west side.

Specimen A3 (10x7 rivet) failed ultimately at a load of 43 kN, corresponding to a moment of 31.0 kN.m. The ultimate rotational angle change achieved in this specimen was 5.5°. Similar to the two previous butt joint specimens, the mode of failure was the same. However, since less rivet columns perpendicular to the grain existed, more cracks were distributed along the side grain at the furthest column of rivets from the instantaneous center than the previous two specimens as shown in Figure 3.4.

4.3.1.3 The Bolted Connections

The ultimate load capacities of the bolted connections are smaller than the riveted connections. Specimen A4 (4x2 bolted pattern) failed at a load of 24.5 kN that corresponds to a moment of 17.6 kN.m. It witnessed an ultimate rotational angle change of 6.2°. The mode of failure was somewhat different from the riveted connections. Bearing failure occurred at the location of the shear plates where the top ones crushed through the wood, splitting it along the grain. Figure 4.9 shows the dislocation of the

shear plates from both sides of the specimen, whereas Figure 4.10 shows the splitting of the grain. Similar to the rivet connections, cracks developed and spread throughout the top member (where bolt forces occurred perpendicular to grain), and openings in the end grain as high as 40 mm were observed; however, no damage to the bolts or shear plates was found.

The connections in double shear exhibited higher strengths than Specimen A4. Specimen A5 (lap joint with wooden side plates) failed at an ultimate load of 30 kN, corresponding to a moment of 29.7 kN.m. The ultimate rotational angle change achieved in this specimen was 6.6°. This specimen failed in splitting along the grain mostly in the middle member as shown in Figures 4.11 and 4.12. The cracking started at moments about 15.3 kN.m in the middle member. Cracks in the outer members were developed in the end grain at moments around 20 kN.m. Throughout the test, cracks opened up and spread throughout the middle member as apparent in Figure 4.11, caused by the stress at the bolt closest to the outer edge.

Specimen A6 (lap joint with steel side plates) failed at a higher ultimate load of 36 kN (or a moment of 35.6 kN.m). Similarly, the ultimate rotational angle change achieved in this specimen was 6.5°. The mode of failure was similar to that of Specimen A5 where splitting along the side and end grain occurred as shown in Figure 4.13. The difference was that the cracks opened up at loads higher than those in Specimen A5.

4.3.2 Phase 2 - Further Studies on Riveted Moment Joints

4.3.2.1 General

The addition of various combinations of steel plates and steel brackets in series C increased the strength and stiffness of the rivet connected specimens. Specimens C2 and C3 performed very similar to one another since both had a bottom bracket and a top riveted bracket. Specimen C1, with a bottom bracket only, performed with less strength and stiffness than Specimens C2 and C3. The bottom bracket, substituted with a bearing plate in Specimen C4 which also had a top riveted bracket but less side rivets, performed with more ductility but less strength and stiffness than the previous three specimens.

4.3.2.2 Specimen C1

The strength and stiffness exhibited in this specimen were superior to that of Specimen A3 which had the same rivet pattern in the side plates as Specimen C1. The specimen achieved an ultimate load capacity of 50 kN corresponding to a moment of 36 kN.m. The ultimate rotational angle change obtained was 6.0°. The mode of failure was similar where end grain splitting of the wood occurred in the top member at the side rivets as in Figure 4.14. Crushing of the top member at the bottom corner of the joint was reduced due to the existence of the bottom bracket.

The longitudinal strain gauges (Ga#1 to Ga#12) mounted on the side plate as in Figures 3.21 and 3.22 provided strain readings throughout the loading of the specimen. Figure 4.15 shows the strain readings for the top portion of the side plate. Strain readings from Ga#1 increased linearly in compression until a reading of -700 microstrain ($\mu\epsilon$) was obtained at the ultimate applied moment of 36 kN.m. Ga#2, Ga#3, Ga#4, and Ga#6 all

had non-linear increasing tension readings until about 90% of the ultimate loading capacity when these strain readings descended and went through a sign change to exhibit compression behaviour up to a similar strain reading of -1000 $\mu\epsilon$. Throughout the loading, Ga#5 and Ga#7 witnessed low compression. Ga#8 however witnessed very high tension behaviour giving a reading of 1500 $\mu\epsilon$.

Figure 4.16 shows the strain readings for the bottom portion of the side plate. Strain reading from Ga#9 was significantly the highest compared with the other gauges in this portion. The strain reading was in tension and reached a high of 800 $\mu\epsilon$ at the ultimate load capacity after which it started to drop until a reading of 200 $\mu\epsilon$. Ga#10 exhibited negligible readings; however, Ga#11 exhibited an increasing tension strain until a reading of 200 $\mu\epsilon$ was obtained at an applied moment of 25 kN.m after which the tension began to decrease. Finally, the strain reading from Ga#12 increased linearly in compression with the load until -120 $\mu\epsilon$ was achieved at the ultimate applied load.

4.3.2.3 Specimen C2 and Specimen C3

Both specimens will be discussed together since their behaviour was almost identical. Specimens C2 and C3 performed with higher strength and stiffness than Specimen C1. The specimens achieved an ultimate moment capacity of 45 kN.m. This corresponded to a load of 61 kN in Specimen C2, which had a lever arm of 720 mm (similar to all previous specimens). However, this moment corresponded to a load of 45 kN in specimen C3, which had a lever arm of 980 mm. The ultimate rotational angle changes achieved in both specimens were 6.0° and 7.0°, respectively.

The mode of failure in these specimens was somewhat different. During the loading process, splitting along the side grain occurred at the furthest column of rivets from the bottom corner of the joint (see Figure 4.17). At the ultimate load, Specimens C2 and C3 witnessed local yielding at the apex of the joint in addition to further bending throughout the bracket. Crushing at the bottom corner of the joint was reduced due to the attachment of the bottom bracket. However, at the ultimate load, Specimen C2 (with a moment arm of 0.72 m) witnessed a sudden brittle fracture where the grain split wide open at the bracket bolts used to load the specimen as shown in Figure 4.18. It was believed that the ultimate moment resistance of the joint was achieved from the yield plateau on the specimen's moment-rotation curve (Figure 4.6). However, in order to verify such conclusion, a second test (Specimen C3) with a larger moment arm of 0.98 m was constructed and tested. Precaution was taken to prevent a similar type of sudden brittle failure in the form of rivet plates nailed at the bottom of the member (where the previous member failed). The ultimate moment resistance of Specimen C3 reached the same level as Specimen C2. Specimen C3, however, exhibited continuous splitting along the side grain, yielding at the apex, and crushing at the bottom corner until the ultimate load was reached. The magnitude of the stresses in the side plates was less than that in Specimen C1 because of the existence of the top bracket.

The longitudinal strain gauges (Ga#1 to Ga#12 and Ga#1a to Ga#7b) mounted on the side plate and top bracket respectively, as in Figures 3.21, 3.22, 3.24, and 3.25, provided strain readings throughout the loading of the specimens. Strain readings for both specimens were very similar. Therefore, the average strain readings of the two specimens were used in Figures 4.19 and 4.20.

Figure 4.19 shows the strain readings for the top portion of the side plate. Strain readings from Ga#2, Ga#3, and Ga#6 witnessed negligible linear increases up to a maximum of 300 $\mu\epsilon$ in tension, then decreased as the ultimate load approached. Ga#4 started in tension up to a strain reading of 50 $\mu\epsilon$ at a moment of 25 kN.m then decreased in tension and increased nonlinearly in compression up to a strain of -500 $\mu\epsilon$ at the ultimate load. Readings from Ga#1, Ga#5, and Ga#7 increased linearly in compression at a moment of 35 kN.m then increased nonlinearly up to -1000 $\mu\epsilon$ at the ultimate load. Ga#8, however, witnessed a continuous strain increase in tension up to a strain reading of 1500 $\mu\epsilon$ at the ultimate load.

In the bottom portion of the side plate, Ga#9 gave strain readings that increased linearly in tension up to around 400 $\mu\epsilon$ at 90% of the ultimate load then decreased to 100 $\mu\epsilon$ at the ultimate load. Strain readings from Ga#10 and Ga#11 increased linearly up to -200 $\mu\epsilon$ (compression) and 200 $\mu\epsilon$ (tension), respectively, at the ultimate load. Finally, Ga#12 gave negligible strain readings throughout the test. Strain readings for the bottom portion of the side plate are shown in Figure 4.20.

For the top bracket, every strain gauge gave readings very similar to the readings of the neighbouring gauge on the same line of the top bracket (i.e. Ga#4a and Ga#4b gave similar results). Therefore, averages of the two were presented in Figure 4.21. From Figure 4.21, there was negligible strain at both Ga#4 and Ga#7. Strain readings from Ga#3 and Ga#6 increased linearly in tension up to 1500 $\mu\epsilon$ and 2500 $\mu\epsilon$ respectively. There was no plate bending between the glulam rivets, hence such strain values for the top bracket could be used as the average cross-sectional strain from which the force through the plate could be calculated. However, there was considerable bending at the locations of Ga#1, Ga#2, and Ga#5. Nevertheless, strain readings from Ga#2 (on the outside surface

of the bracket) increased linearly in tension until 90% of the ultimate load then inelasticaly up to a strain of 1500 $\mu\epsilon$. Ga#1 (on the outside surface of the bracket) gave a negligible strain gauge reading until the applied moment was 37 kN.m then it increased in tension up to 600 $\mu\epsilon$ at the ultimate load. The strain reading from Ga#5 (on the outside surface of the bracket) increased linearly in tension up to 2000 $\mu\epsilon$ at 90% of the ultimate load, then it increased inelasticaly up to 4500 $\mu\epsilon$ at the ultimate load.

4.3.2.4 Specimen C4

This specimen performed with less strength and stiffness but with more ductility than the other specimens in series C. Specimen C4 achieved an ultimate load capacity of 47 kN corresponding to a moment of 34 kN.m. The ultimate rotational angle change that the specimen witnessed was 9.5°.

The mode of failure for this specimen was somewhat different from the other specimens. There was little splitting along the side grain at the furthest column of rivets from the bottom corner of the joint. The bearing plate between the two connected members did not significantly reduce the crushing at the bottom corner of the butt joint, in addition to the fact that the plate bent quite significantly as shown in Figure 4.22. Another mode of failure feature is shown in Figure 4.23 where the rivets of the top bracket in the top member withdrew completely in addition to the wood split type of failure in the top grain. However, similar to Specimens C2 and C3, local yielding at the apex in the top bracket was noticed in addition to severe bending throughout the rest of the bracket as shown in Figure 4.22.

The strain gauges mounted on the side plate are shown in Figure 3.23. The strain gauge readings for the side plate and top bracket are shown in Figures 4.24 to 4.26. On the upper side (Figure 4.24), only Ga#6 gave a significant strain gauge reading, which increased linearly in tension up to 700 $\mu\epsilon$ at the ultimate load. Ga#1 to Ga#5 gave negligible strain readings ranging from -100 $\mu\epsilon$ in compression (Ga#5) to 100 $\mu\epsilon$ in tension at Ga#4. On the lower side (Figure 4.25), Ga#7 provided a strain reading of 50 $\mu\epsilon$ at 90% of the ultimate load, then decreased and changed to -150 $\mu\epsilon$ at the ultimate load. Ga#8 and Ga#10 output readings that increased up to 100 $\mu\epsilon$ in tension at the ultimate load. The reading from Ga#9 increased linearly up to 200 $\mu\epsilon$ in tension at the ultimate load.

Figure 4.26 shows the strain readings of the top bracket. Only Ga#1, Ga#2 and Ga#5 were mounted on both sides of the top bracket dissimilar to that of Specimens C2 and C3 (see Figure 3.21). Readings from Ga#2 increased linearly on both sides up to 1500 $\mu\epsilon$ in tension on the outside and -500 $\mu\epsilon$ in compression on the inside at the ultimate load. Ga#1 output low readings until a moment of 28 kN.m when the inside gauge reading increased to -500 $\mu\epsilon$ in compression and the outside gauge reading increased up to 1000 $\mu\epsilon$ in tension at the ultimate load. The largest readings were provided by Ga#5, where the inside gauge reading increased linearly up to -2500 $\mu\epsilon$ in compression at the ultimate load, and similarly the outside gauge reading increased linearly up to 2500 $\mu\epsilon$ in tension at the ultimate load.

4.3.3 Location of the Instantaneous Center (I.C.)

To locate the I.C., Specimen B1 was tested. Similar to Specimen A4, it failed with a low strength and stiffness. The ultimate load capacity was 18 kN corresponding to a moment

of 14.3 kN.m. The ultimate rotational angle change witnessed was 3.7°. The specimen failed after large cracks occurred along the side grain and in the end grain as in shown Figure 4.27, in addition to plug shear failure in the wood by the shear plates.

Behaviour of the specimen and the stress distribution in the connecting plate was to be determined from the strain gauges mounted as shown in Figure 3.19. The strain readings of Ga#1 and Ga#2 are shown in Figure 4.28. Four sets of rosette gauge readings are shown in Figures 4.29 to 4.32. The strain readings from Ga#1 increased linearly up to 180 $\mu\epsilon$ in tension at the ultimate load. Readings from Ga#2 were in compression at a load of 8 kN in cycle 1, then a slip occurred (friction between shear plate and steel cover plate diminished). Hence, strain readings increased to 50 $\mu\epsilon$ in tension, then in applying the load cycle 3, the strain changed to compression again up to -100 $\mu\epsilon$ at the ultimate load.

For the rosette gauge, (Figure 4.29) that contained Ga#3, Ga#4, and Ga#5, strain readings were mainly in tension. Ga#4 and Ga#5 had readings that increased linearly until the load equaled 13 kN then continued nonlinearly up to 250 $\mu\epsilon$ at the ultimate load. Ga#3 witnessed a change when the load equaled 7 kN, nevertheless, it provided a negligible strain reading up to 40 $\mu\epsilon$.

From Figure 4.30, the readings from Ga#6 increased in compression up to -100 $\mu\epsilon$ at the ultimate load. The readings were in the tension zone for a brief period in load cycle 3 after the load equaled 7 kN. A change in the strain path occurred when the load equaled 13 kN. The strain readings from Ga#7 and Ga#8 increased linearly in tension, then diverted and increased inelasticaly up to a strain of 200 $\mu\epsilon$ at the ultimate load.

The readings from Ga#9 to Ga#11 are shown in Figure 4.31. The readings from Ga#9 increased in the compression zone up to -140 με at the ultimate load. A path diversion was noticed at a load of 10 kN. The readings from Ga#10 and Ga#11 were negligible until a load of 13 kN when readings from Ga#11 increased in tension up to 60 με at the ultimate load.

In Figure 4.32, the readings from Ga#12 were negligible and increased in compression only after a load of 13 kN, up to -30 με at the ultimate load. The strain readings from Ga#13 were negligible also and alternated between tension and compression readings during the first three load cycles. In load cycle 4, it increased after a load of 13 kN up to -60 με at the ultimate load. Finally, the strain readings from Ga#14 increased in compression up to -40 με at a load of 7 kN, then decreased to zero and increased in tension after a load of 14 kN, up to 20 με at the ultimate load.

Table 4.1 - Material Properties for Top Steel Brackets

Specimen	Cross-Sectional Area (mm^2)	Elastic Modulus (MPa)	Yield Static Strength (MPa)	Ultimate Strength (MPa)
Coup 1	78.94	188501	338	475
Coup 2	77.75	182815	327	475
Coup 3	78.19	200000	338	477
Average 1-3	78.29	190439	334.3	475.7
Coup 4	116.84	197195	363	456
Coup 5	117.35	188877	366	454
Coup 6	117.65	202448	369	454
Average 4-6	117.28	196173	366	454.7

Table 4.2 - Fastener Embedment Strengths

Test #	Fastener/ Pattern	Direction to Grain	# of Tests	Embed. Strength (kN)	Strength wrt Code (kN.m)	Avg. Embed. Strgth./Riv (kN)
1	5x4 Rivet Sp*= 40 mm	Parallel	2	62	70	3.5
2	8x4 Rivet Sp*= 25 mm	Parallel	2	97	96	3.0
3	2x 67 mm Shear Plts.	Parallel	1	65	46	32.0
4	2x 67 mm Shear Plts.	Perpend.	1	35	34	17.5
5	2x (4x4 Riv) Sp*= 25 mm	Perpend.	1	29	23	0.9

Note: Sp^* = spacing between rivets in both directions.

Table 4.3 - Summary of Test Results

Spec.	Conn. Config.	M.C. (%)	Ult. Load P_u (kN)	Ult. Mom. M_u (kN.m)	Ult. Rot. Ang. θ_u (Deg)	Secant Stiffness (kN.m/Deg)
A1	7x10	11	31	22.3	3.9	9.3
A2	10x10	10	45	32.4	3.55	13.5
A3	10x7	12	43	30.9	5.5	17.1
A4	4x2	12	24.5	17.6	6.2	3.6
A5	8circw	11	30	29.7	6.6	6.9
A6	8cirst	11	36	35.6	6.5	7.9
B1	4x2	11	18	14.3	3.7	3.6
C1	10x7b	12	50	36	6	14.4
C2	10x7bt	11	61	44	6	20.0
C3	10x7bt	11	45	45	7	20.0
C4	5x4tbr	12	47	34	9.5	15.5

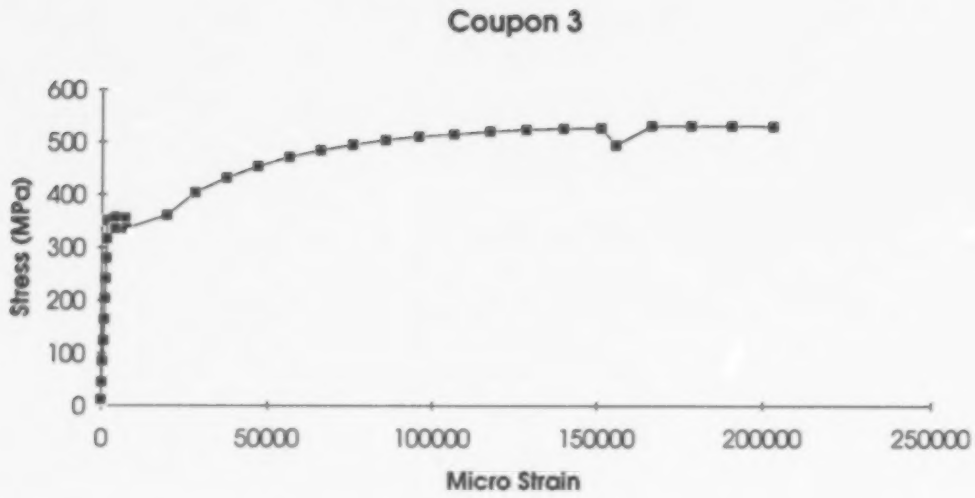

Figure 4.1 - Typical Stress vs. Strain Plot for Steel Coupons

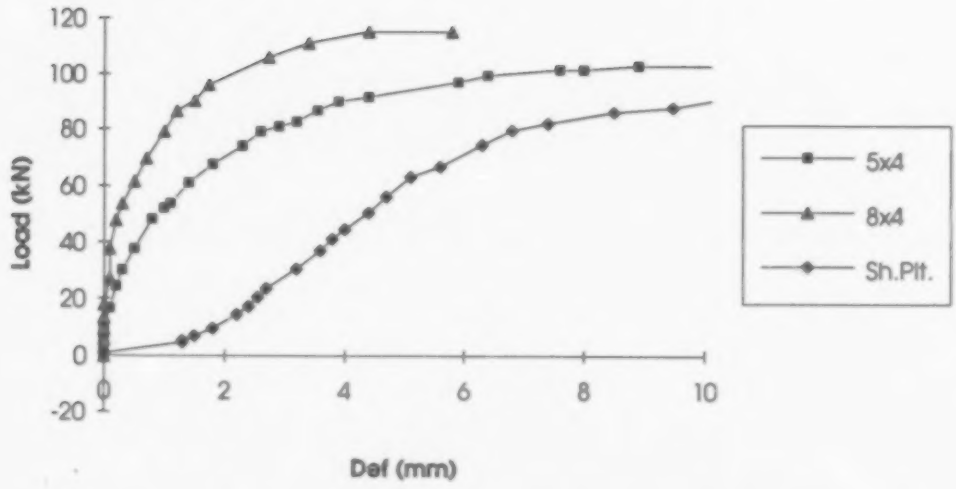

Figure 4.2 - Plot of Load vs. Deformation for Embedded Fasteners Loaded Parallel to Grain

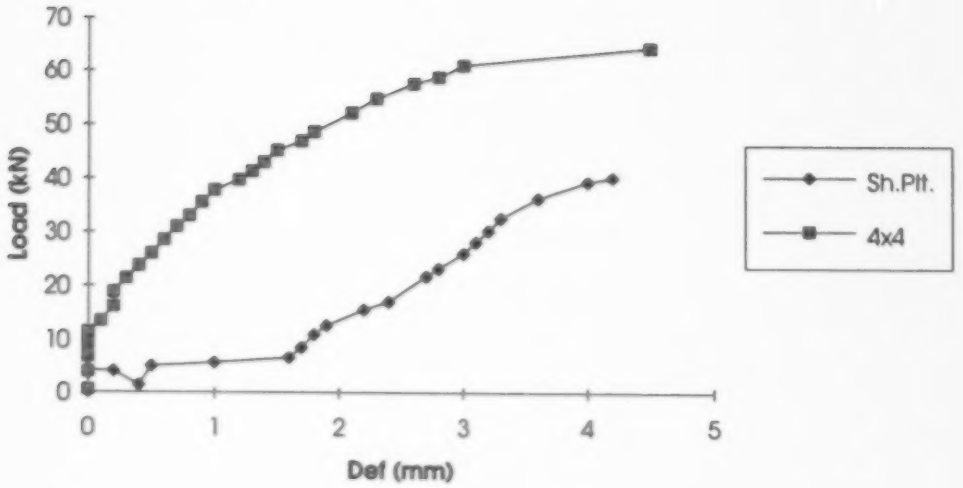

Figure 4.3 - Plot of Load vs. Deformation for Embedded Fasteners Loaded Perpendicular to Grain

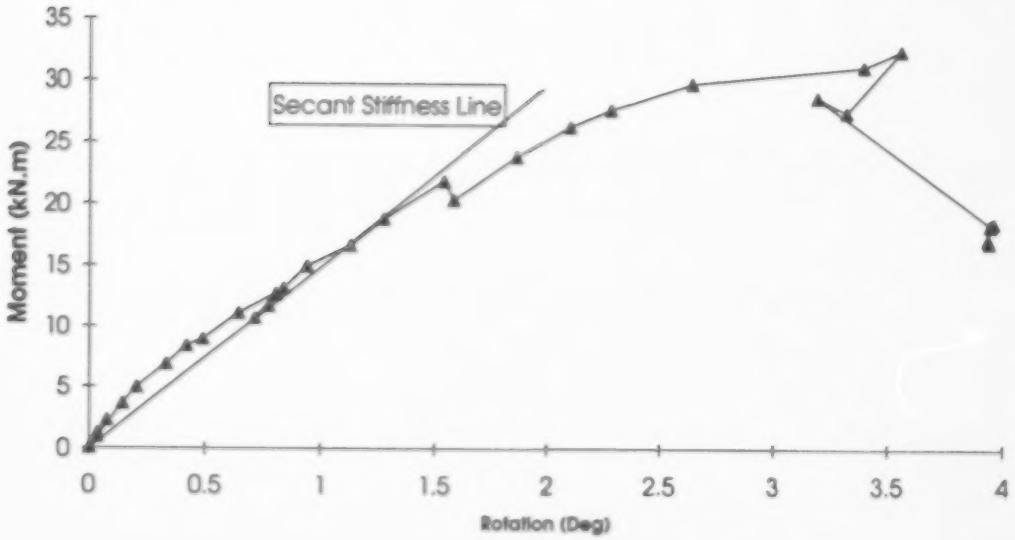

Figure 4.4 - Moment Rotation Curve for Specimen A2 Demostrating the Secant Stiffness

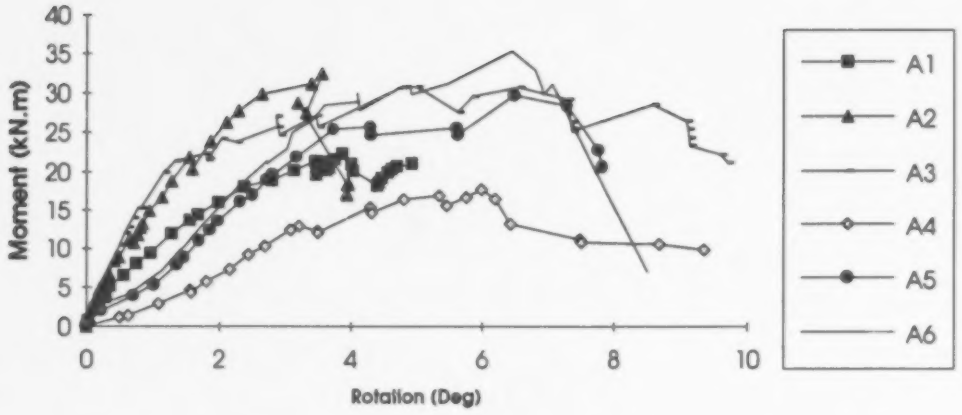

Figure 4.5 - Moment Rotation Curves for Phase 1

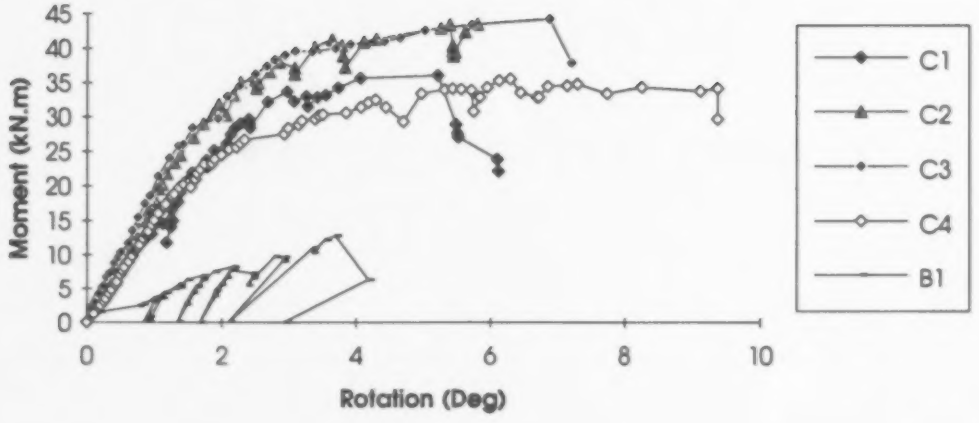

Figure 4.6 - Moment Rotation Curves for Phase 2

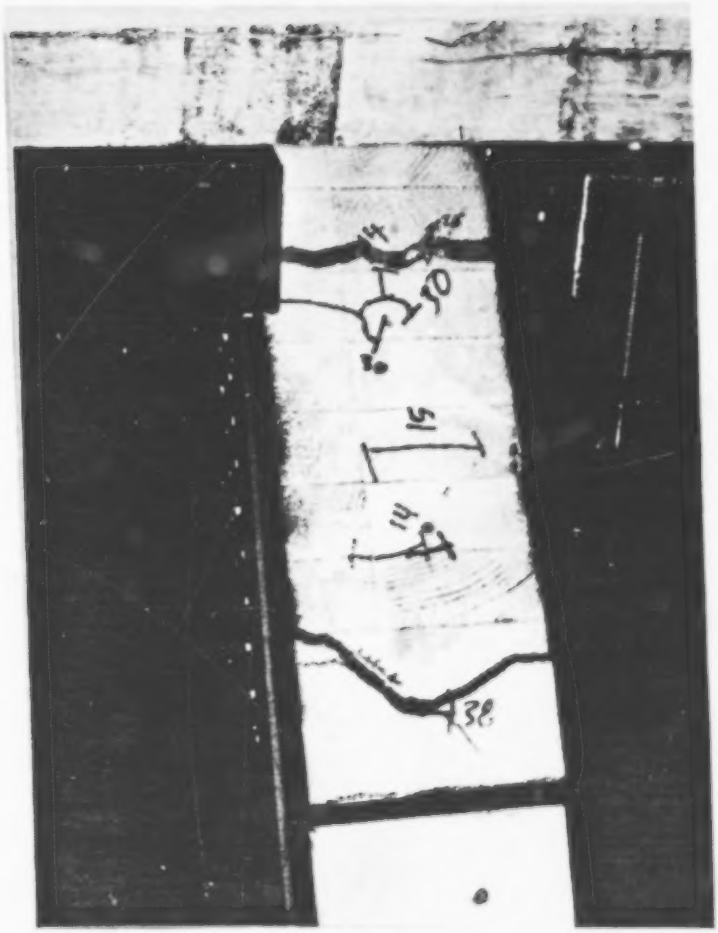

Figure 4.7 - Cracks in the End Grain for Specimen A1

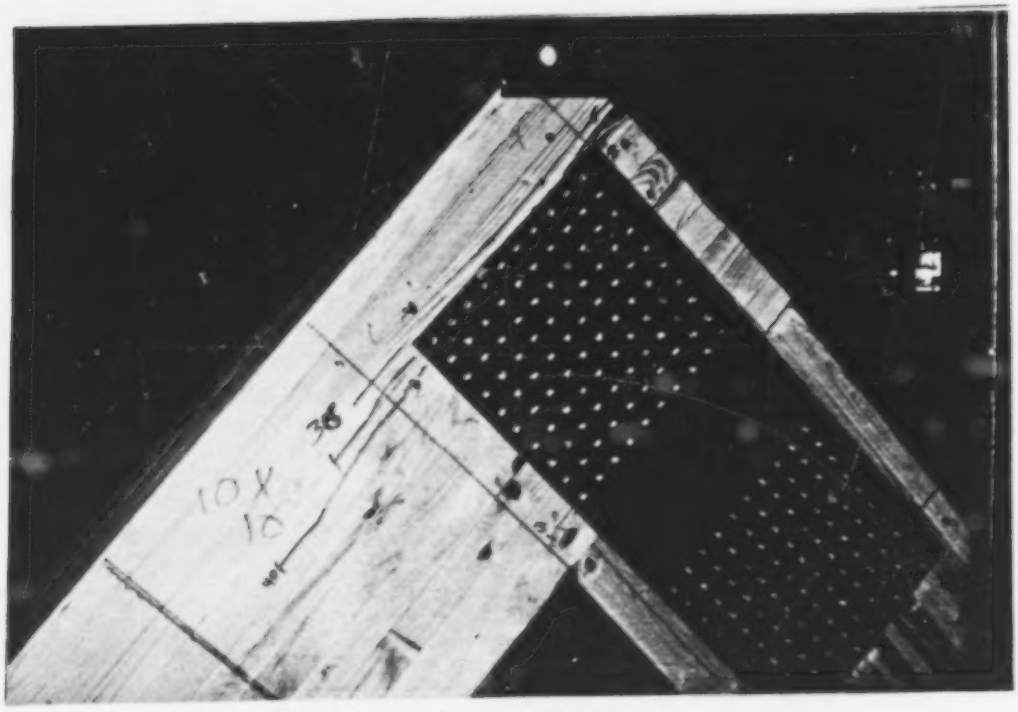

Figure 4.8 - Split Crack in Specimen A2

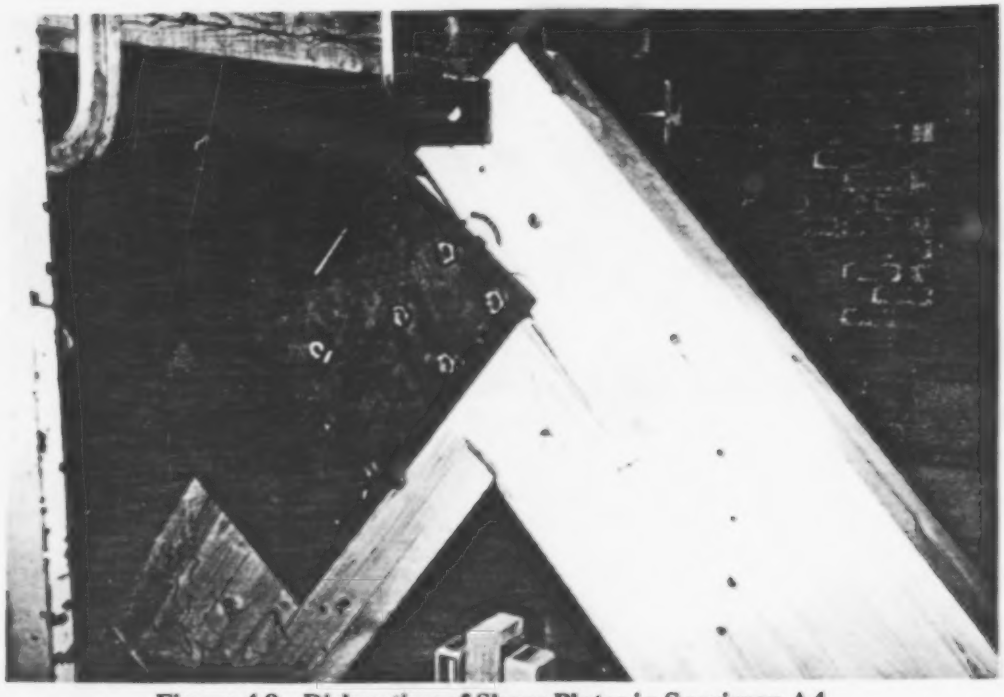

Figure 4.9 - Dislocation of Shear Plates in Specimen A4

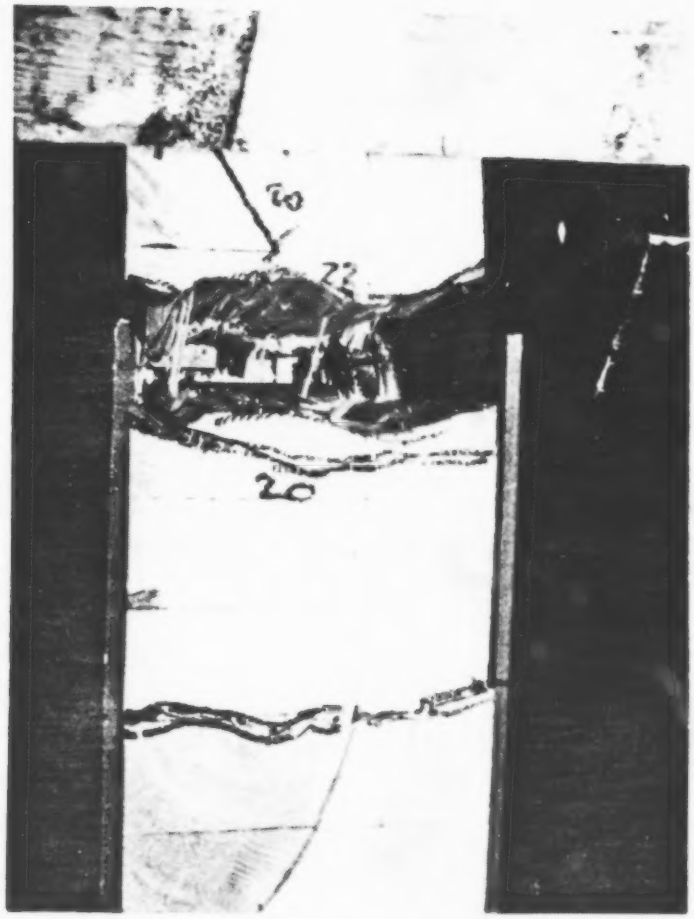

Figure 4.10- Large Cracks In End Grain for Specimen A4

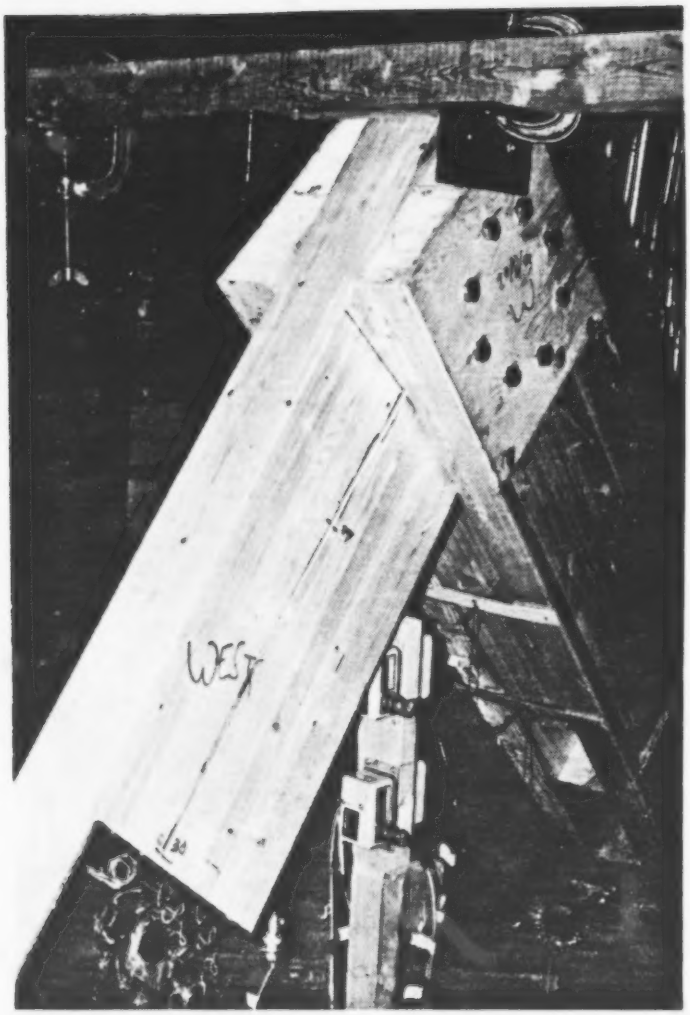

Figure 4.11 - Splitting in the Middle Member (Specimen A5)

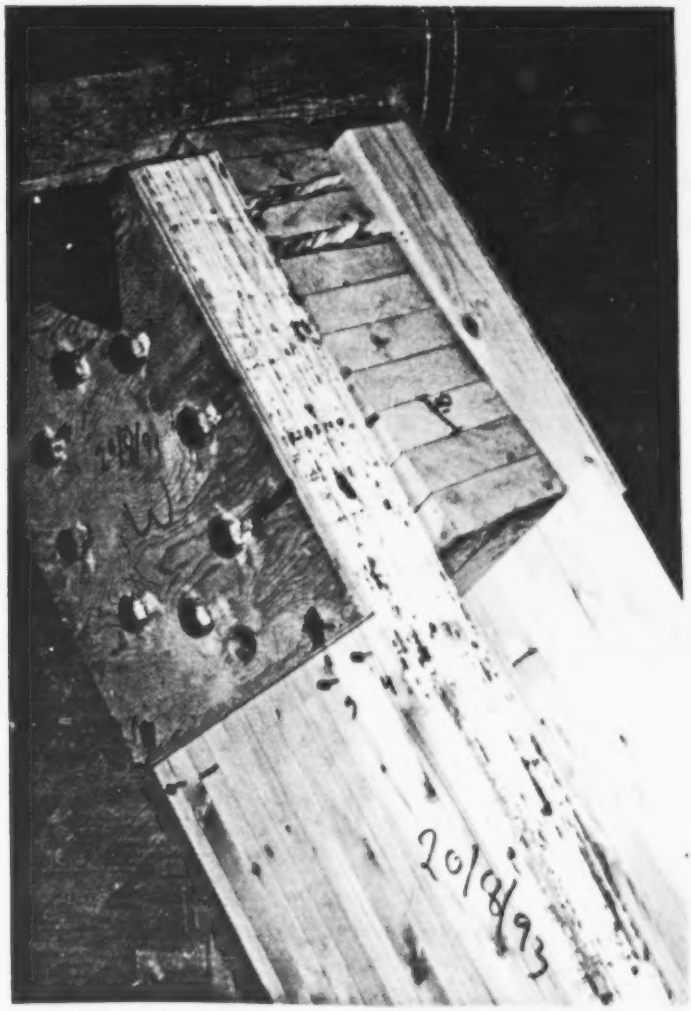

Figure 4.12 - Splitting in the End Grain (Specimen A5)

Figure 4.13 - Cracks in the End Grain (Specimen A6)

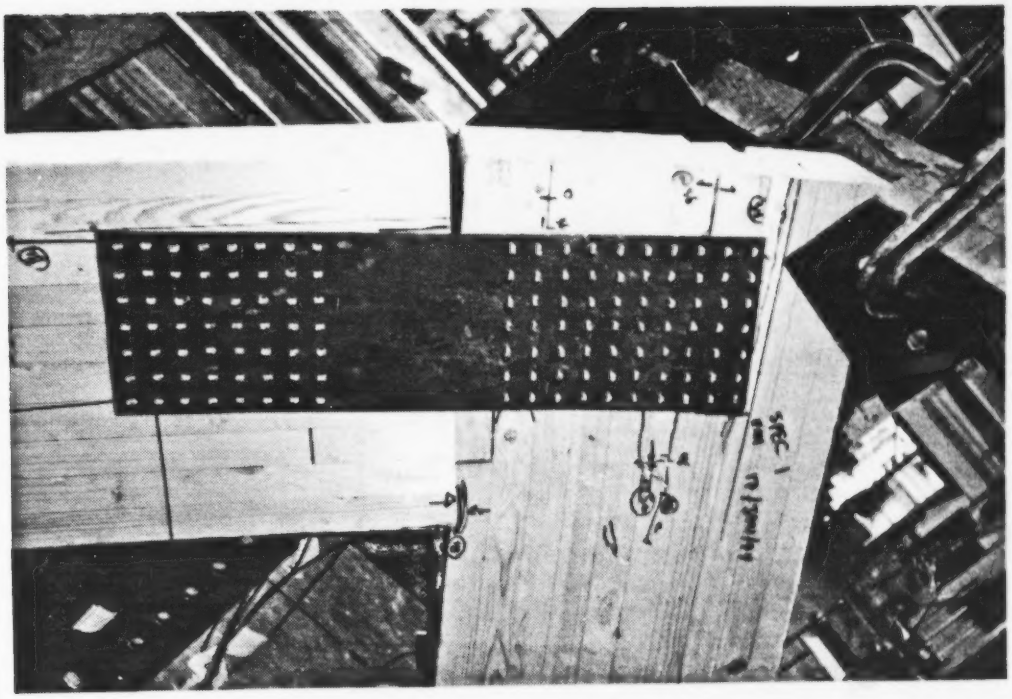

Figure 4.14 - Cracks in the End Grain (Specimen C1)

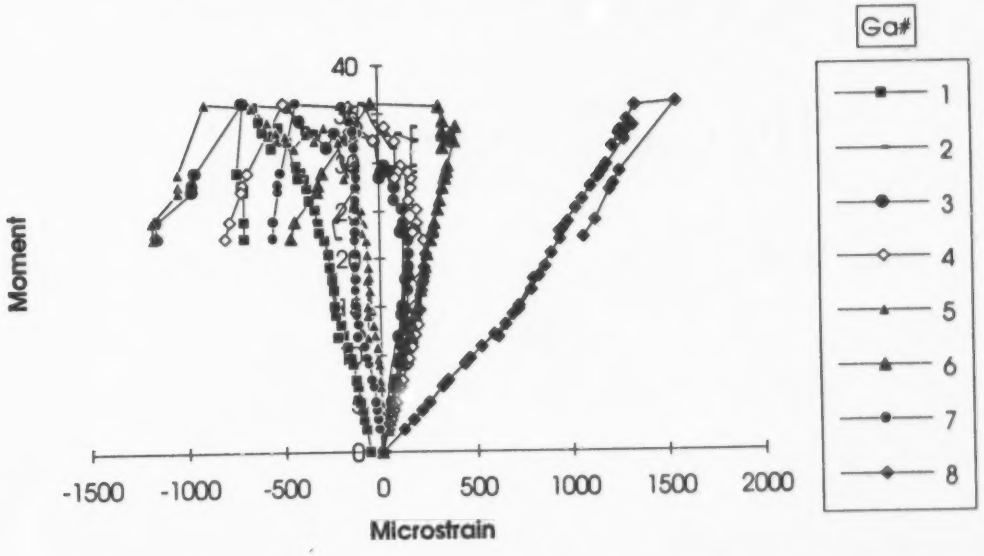

Figure 4.15 - Strain Gauge Readings for Top Part of Side Plate (Specimen C1)

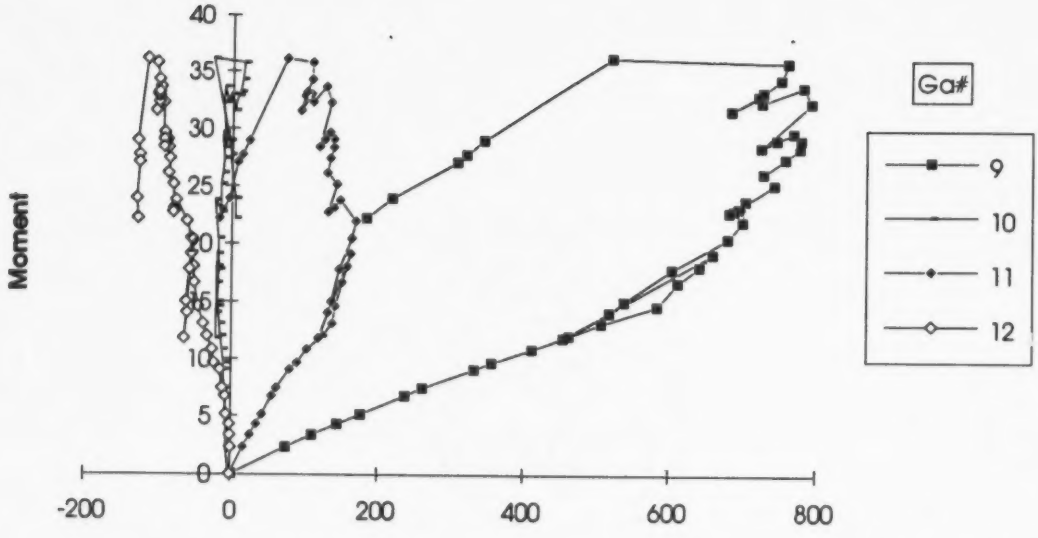

Figure 4.16 - Strain Gauge Readings for Bottom Part of Side Plate (Specimen C1)

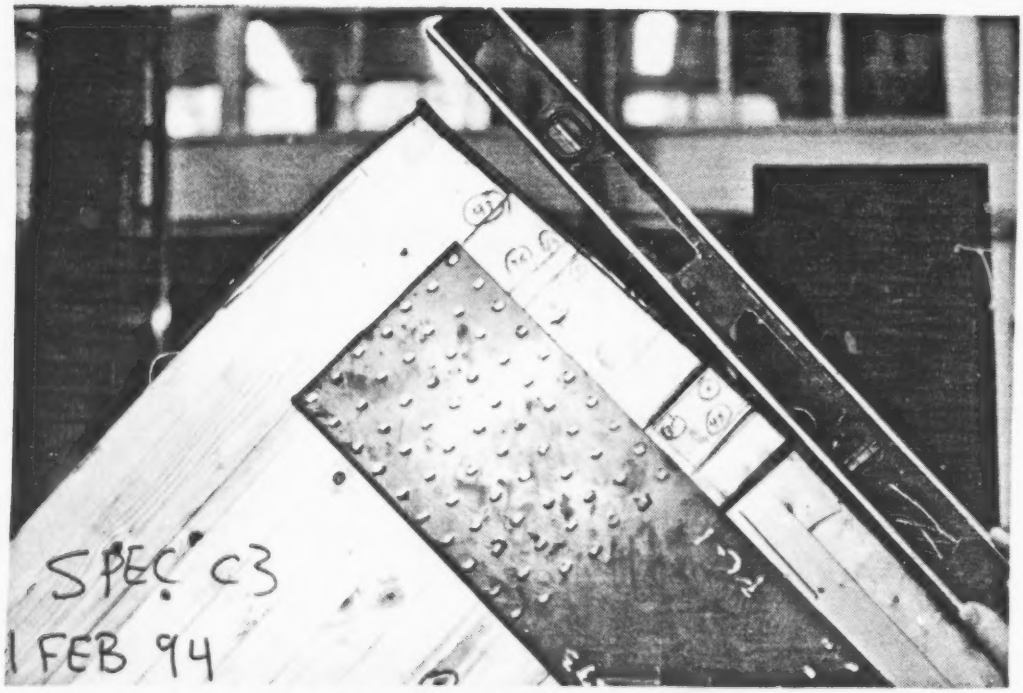

Figure 4.17 - Wood Splitting and Bracket Bending (Specimen C2)

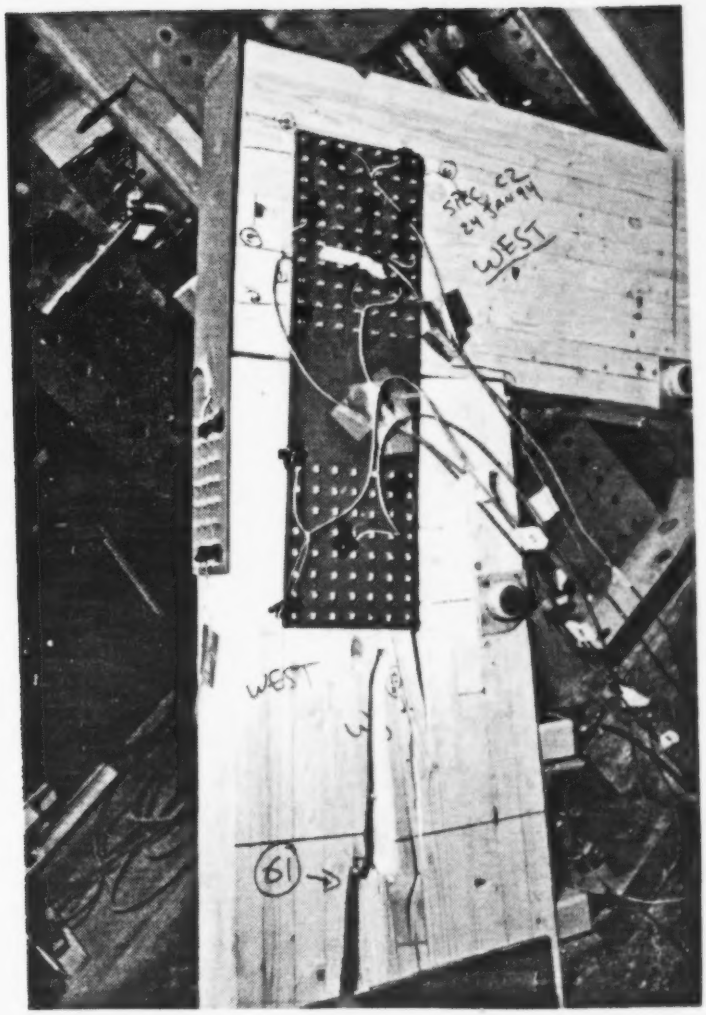

Figure 4.18 - Brittle Fracture through Member at Bracket Bolts (Specimen C2)

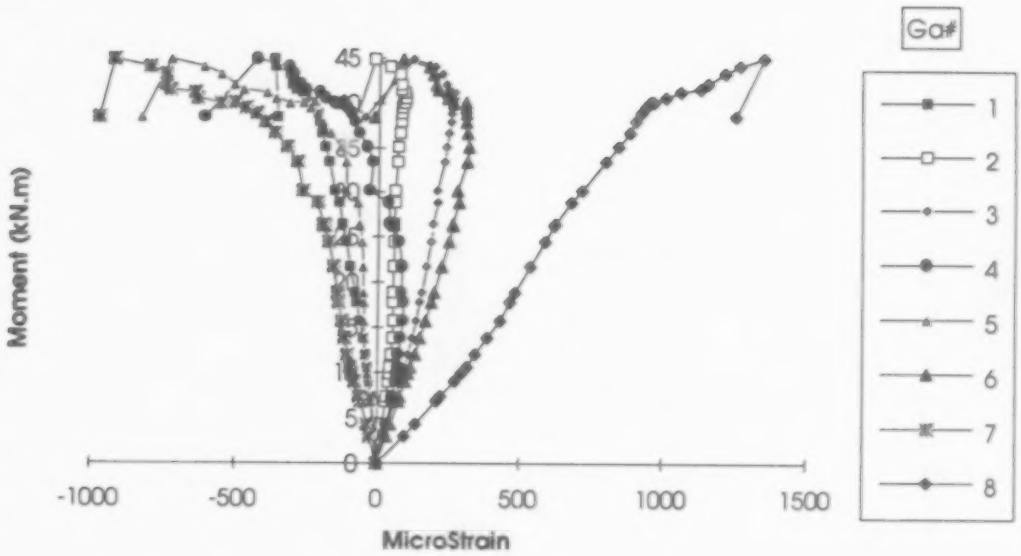

Figure 4.19 - Strain Gauge Readings for Top Part of Side Plate (Specimen C2,C3)

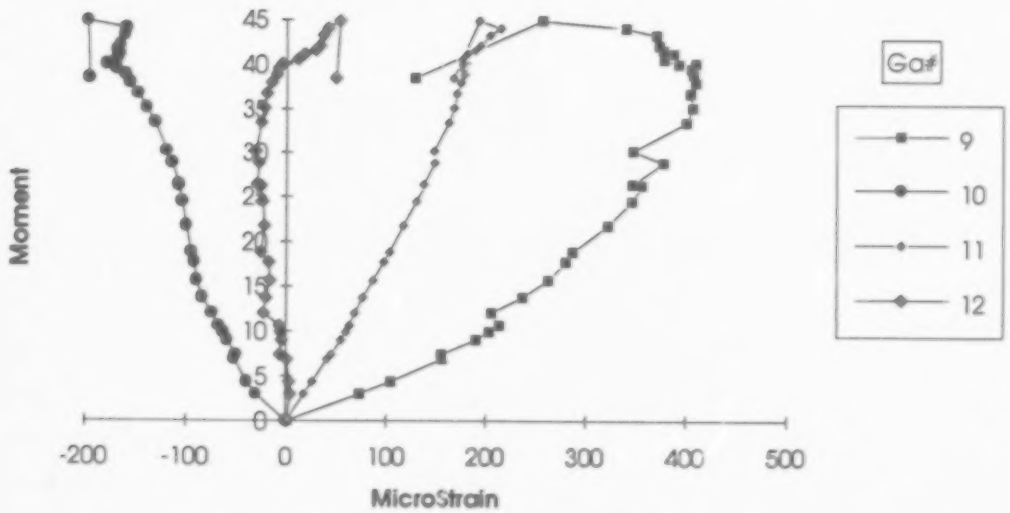

Figure 4.20 - Strain Gauge Readings for Bottom Part of Side Plate (Specimen C2,C3)

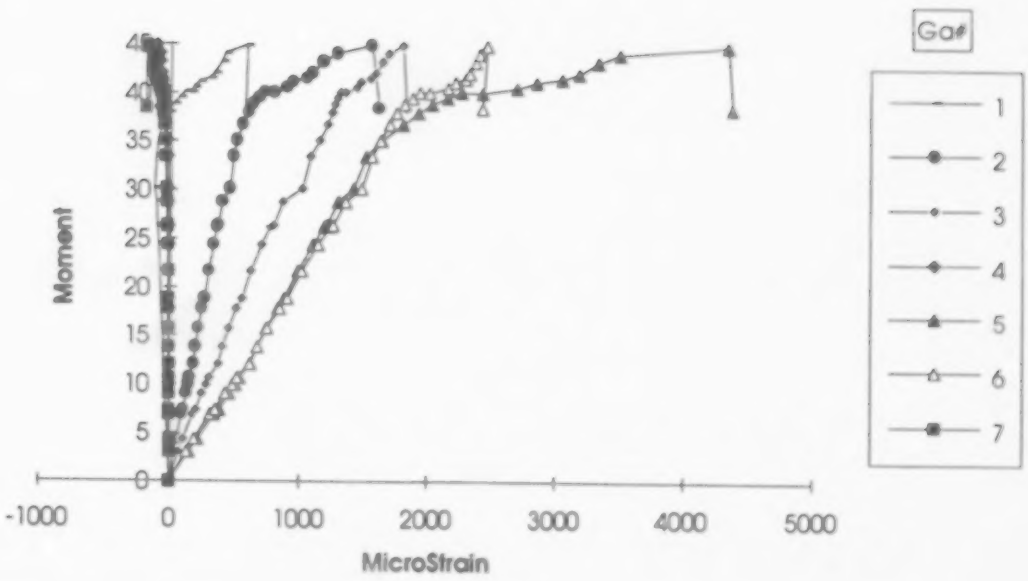

Figure 4.21 - Strain Gauge Readings for Top Bracket (Specimen C2,C3)

Figure 4.22 - Failure in Bearing Plate and Top Bracket (Specimen C4)

Figure 4.23 - Rivet Withdrawal and Wood Crack in Top Grain (Specimen C4)

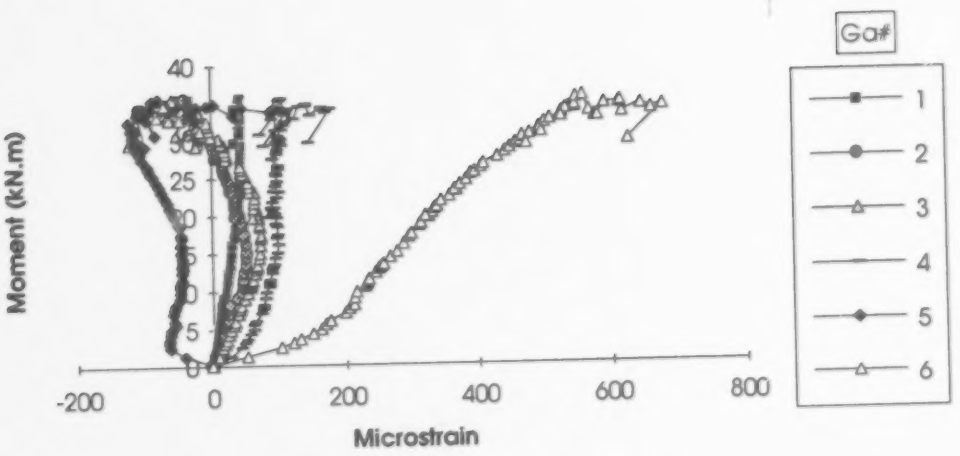

Figure 4.24 - Strain Gauge Readings for Top Part of Side Plate (Specimen C4)

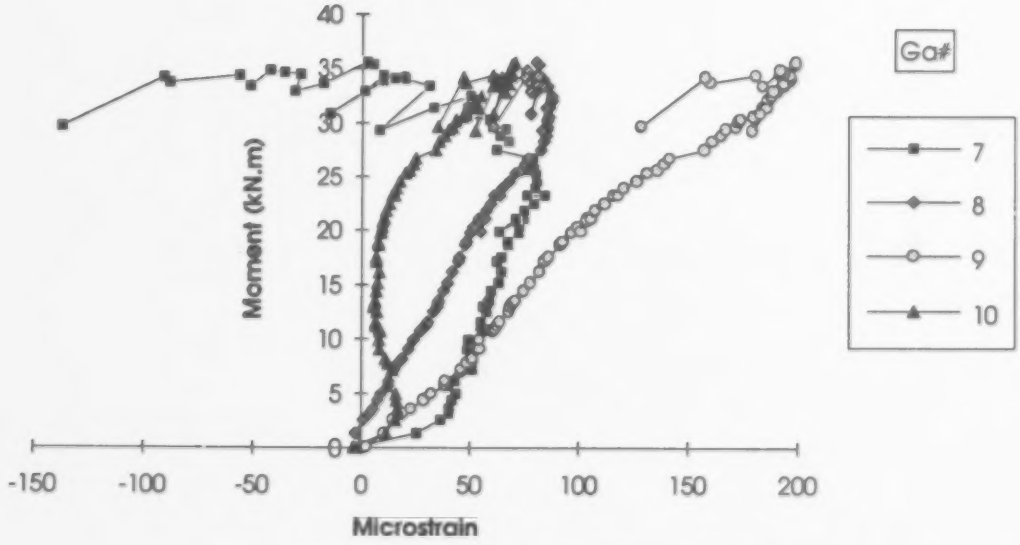

Figure 4.25- Strain Gauge Readings for Bottom Part of Side Plate (Specimen C4)

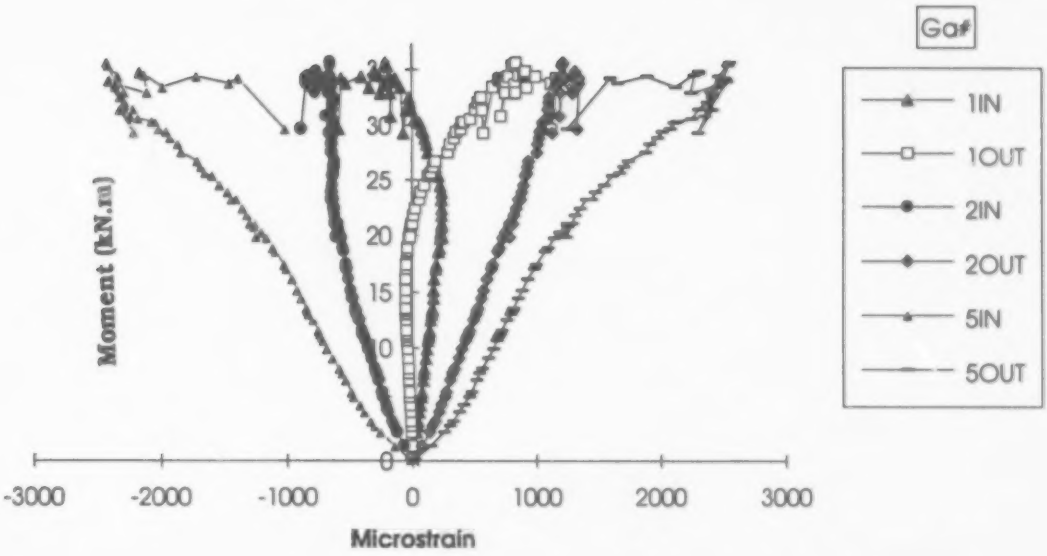

Figure 4.26 - Strain Gauge Readings for the Top Bracket (Specimen C4)

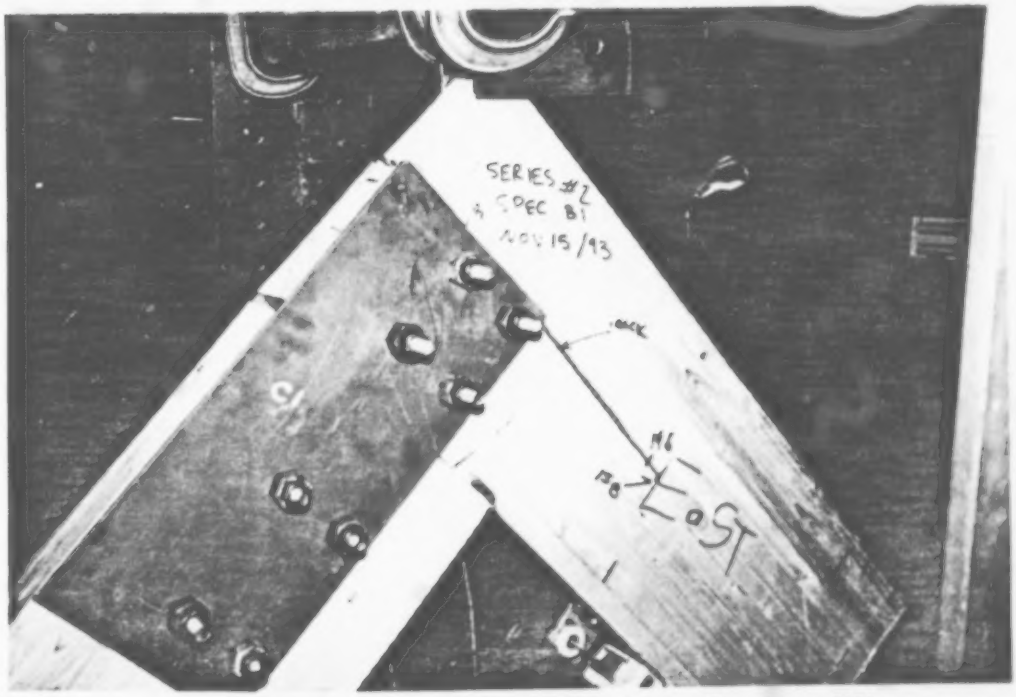

Figure 4.27 - Cracks in the Side Grain (Specimen B1)

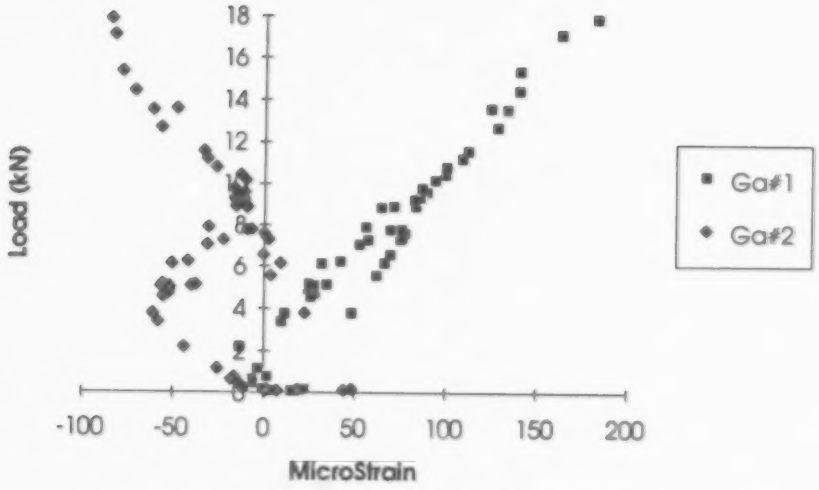

Figure 4.28 - Strain Readings Ga#1-Ga#2 (Specimen B1)

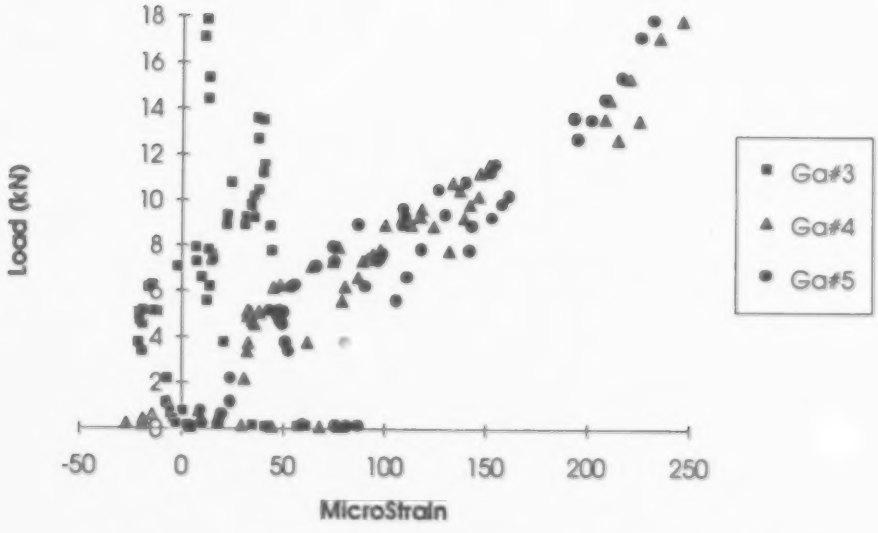

Figure 4.29 - Strain Readings Ga#3-Ga#5 (Specimen B1)

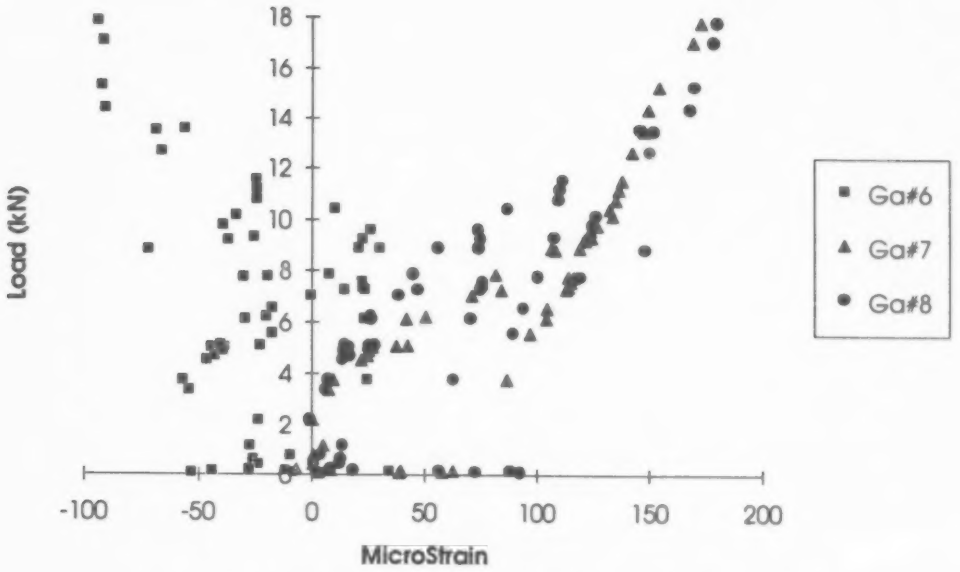

Figure 4.30 - Strain Readings Ga#6-Ga#8 (Specimen B1)

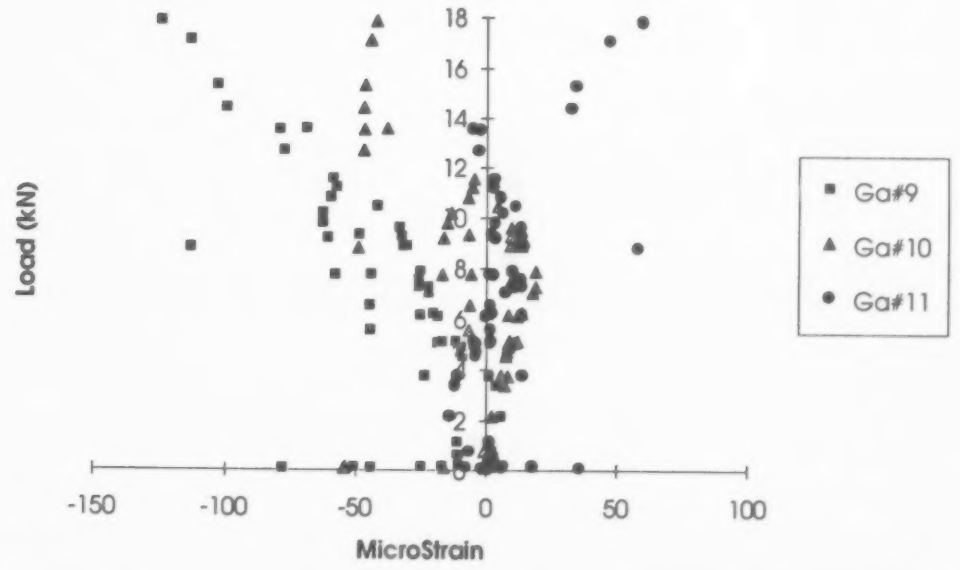

Figure 4.31 - Strain Readings Ga#9-Ga#11 (Specimen B1)

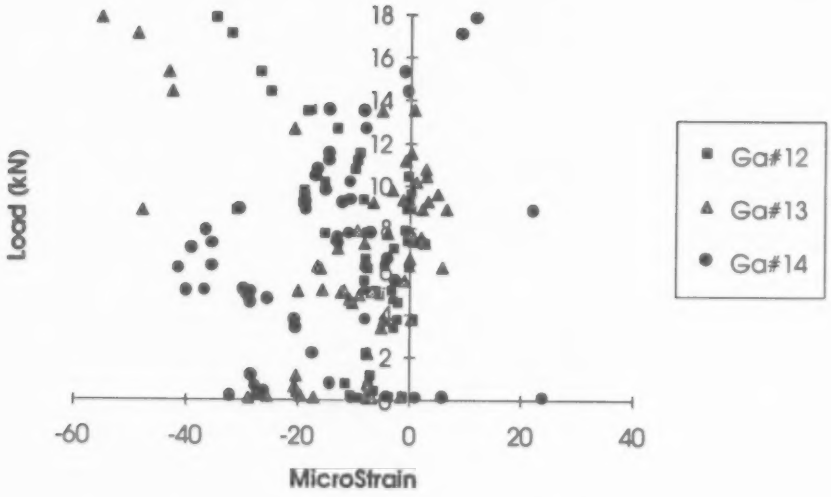

Figure 4.32 - Strain Readings Ga#12-Ga#14 (Specimen B1)

5.0 DISCUSSION OF THE TEST RESULTS

5.1 LOCATION OF THE INSTANTANEOUS CENTER (I.C.)

The need to accurately locate the I.C. arises when calculating the moment lever arm about which the moment is applied. Specimen B1 was tested to confirm that the I.C. of butt type joints is at the bottom corner of the joint. A simple rectangular bolted pattern butt joint was used for simplicity. The load applied is transferred from the bolts and shear plates in the one member to the steel cover plates then to the other member through the bolts again. Rosette gauges were mounted on the steel cover plate beneath every bolt to determine the direction of the principal strains in the steel plates, hence the direction of the principal force on every bolt could be determined. The principal force lever arms from the bolts are extended to coincide at the of the joint as in shown Figure 5.1.

A rosette strain gauge consists of three longitudinal strain gauges positioned with 45° between each as in Figure 5.2. The strain readings from the gauges mounted on the steel cover plate as shown in Figure 3.20, are presented in Chapter 4.

Referring to Figure 5.2, the shear strain γ_{XY} is calculated as in Eqn. 5.1

$$\gamma_{xy} = 2\varepsilon_x - (\varepsilon_x + \varepsilon_y) \qquad \textbf{(Eqn. 5.1)}$$

where ε_X and ε_Y are longitudinal strains.

The principal strains are then calculated as in Eqn. 5.2:

$$\varepsilon_x = \frac{\varepsilon_x + \varepsilon_y}{2} \pm [\frac{(\varepsilon_x + \varepsilon_y)^2}{2} + \gamma_{xy}^{\ 2}]^{0.5} \qquad \textbf{(Eqn. 5.2)}$$

Most importantly, the principal strain directions are determined as ϕ_P and $\phi_P + 90^\circ$ from the ε_x axis as in Eqn. 5.3:

$$\tan 2\phi_P = \frac{2\gamma_{xy}}{(\varepsilon_x - \varepsilon_y)} \qquad \textbf{(Eqn. 5.3)}$$

During the initial loading, the force lever arms coincided at a point on the interboundary line between the two connecting members 85 mm from the bottom corner of the joint (i.e. point a in Figure 5.1). This point shifted outwards quickly as the load progressed until it reached the bottom corner of the joint (i.e. point b in Figure 5.1) at a load of 7 kN.

The load was initially carried by the friction between the shear plates and the steel cover plates. After small loads, the friction was overcome and the load path transferred to the bolt bearing against the steel cover plates. Also, as soon as cracks developed, the load redistributed itself among the bolts. These phenomena are apparent in the individual strain graphs shown in Chapter 4.

5.2 DESIGN AND EVALUATION

5.2.1 Design Model and Calculation of Design Values

A design model for the calculation of the moment resistance values was chosen based on elastic analysis and principle of equilibrium. The design values did not consider the redistribution of forces among the rivets; only elastic analysis was performed. The material strengths specified in the CAN/CSA-O86.1-M89 (1989) and obtained from the material tests listed in Table 4.2 were used in calculating the design and predicted moment resistance, respectively. The design (excluding the safety factor) and predicted moment resistance values, compared with the ultimate moment resistance values are presented in Table 5.1. See Appendix A for sample calculations and comments.

The design values were calculated as follows:

1) An analysis was conducted based on the pattern of the rivets or bolts and the assumed I.C.(bottom corner for butt joint and pattern centroid for lap joint). The resultant force components (x and y) were, then, found based on Eqn. 2.1, as shown in Figure 2.3 .

2) The resistance of the 65 mm rivets and of the embedded 67 mm (2-5/8") shear plates with 19 mm (3/4") bolts were calculated in the perpendicular and parallel directions to the grain from the resistance values published in the CAN/CSA-O86.1-M89 (1989) or obtained from the material tests. The Hankinson Formula (Eqn. 5.4) was used to calculate N_r which is the resistance of the fastener loaded at an acute angle ϕ to the grain.

$$N_r = \frac{P_r Q_r}{P_r \sin^2 \phi + Q_r \cos^2 \phi} \qquad \textbf{(Eqn. 5.4)}$$

where P_r is the fastener resistance parallel to the grain.

Q_r is the fastener resistance perpendicular to the grain.

3) The load and resistance for each individual fastener parallel and perpendicular to the grain and at angle ϕ to the grain was determined based on points 1 and 2 using a spreadsheet as shown in Appendix A. The moment resistance of the joint was, hence, determined as the load-resistance ratio approached 1.0 for the most stressed fastener. The effect of the shear and axial loads on the mechanical fasteners and the joint was ignored because it was significantly less than the effect of the moment.

5.2.2 Evaluation of Specimen Performance

The results of the experiments show that the specimens failed at loads greater than the design values and the predicted values (except Specimen B1). The comparison of the ultimate moment reached in each specimen with the design values (M_u/M_d) and the predicted values (M_u/Mp) is listed in Table 5.1. Both the (M_u/M_d) and the (M_u/Mp) ratios ranged between 1.0 and 2.0 for all specimens with the exception of Specimen B1 ($M_u/Mp = 0.88$).

5.2.2.1 Phase 1

5.2.2.1.1 The Riveted Connections

For Specimens A1 to A3, no material tests have been conducted for rivet patterns greater than 8x4. However, since the various rivet patterns in the material tests gave resistance

values within 5% of the specified values in CAN/CSA-O86.1-M89 (1989), it was assumed that the strength of the 10x10, 10x7 and 7x10 rivet patterns would also be similar to the specified values. Hence, the predicted moment resistance values were equated to those of the design values.

The riveted connections failed at loads higher than the design and predicted values. Specimen A2 (10x10 rivet pattern) failed at a moment of 32.4 kN.m higher than the expected 26.6 kN.m. The expected failure moments for Specimen A1 and A3 were 14.4 kN.m and 21.6 kN.m, respectively, whereas their ultimate failure moments were 22.3 kN.m and 30.9 kN.m, respectively. The main cause for this discrepancy, is that the predicted values were based on the specified strengths published in the CAN/CSA-O86.1-M89 (1989) since there is no tested material strength data for rivet patterns greater than 8x4. The use of the specified strengths led to conservative design values different from the ultimate load capacities.

The mode of failure in the riveted connections is splitting on the side (along the grain) and in the end grain. This is due to the high stresses that occur at the furthest rivets from the I.C. in the rectangular rivet pattern in the top member. The cracks then start to spread through the member. During the testing of Specimen A2, the side cracks on the east side were noticed to be much shorter than the west side. The air gap between the two connecting members on the east side was initially smaller than that on the west side, hence as the test progressed, the smaller gap closed much sooner. This lead to earlier and higher compressive forces between the laminates through the member on the east side; hence, resisting the spread of the east side.

5.2.2.1.2 The Bolted Connections

Specimen A6 failed at an ultimate moment of 35.6 kN.m higher than the design and predicted values of 19.0 kN.m and 22.3 kN.m, respectively. This is a significant increase, caused partly by the fact that the existence of the steel side plates was not accounted for in the calculation of the design failure loads since their interactive behaviour with the shear plates is not well understood. However, they do increase the resistance of the bolted shear plates. The steel plates added more resistance than the wood sided plates since Specimen A5 (exact same connection but with wooden side plates) failed at a moment of 29.7 kN.m, still higher than the design and predicted values of 19.0 kN.m and 22.3 kN.m respectively but less than the moment of Specimen A6 (35.6 kN.m).

Specimen A4 failed at a moment of 17.6 kN higher than the design and predicted values of 14.4 kN.m and 16.2 kN.m, respectively. The addition of the steel side cover plates caused part of the difference similar to Specimen A6. Since the bolt pattern in Specimen A4 was a rectangle, high stresses were induced perpendicular to the grain at the most distant bolt from the I.C. when subjected to a moment, causing an early failure. The use of a circular bolted pattern in Specimens A5 and A6 appeared to be quite advantageous. It eliminated the high stress point by uniformly distributing the applied stresses among all bolts. This increased the ultimate moment resistant capacity of the joint. The failure in circular patterns occurs as splitting of the grain at the bolt closest to the end grain where the edge distance is least.

The use of shear plates in conjunction with bolts increases the bearing area in the wood, hence, providing a higher resistance value. This indicates that the use of high strength

bolts would not increase the resistance of the joint, since its failure was governed by wood failure.

Part of the discrepancy between the design and actual resistance values for the moment joints is attributed to the use of the published specified strengths in the CAN/CSA-O86.1-M89 (1989) which are usually conservative. The predicted values were higher than the design values but still lower than the ultimate moment. This is probably due to the redistribution of stresses among the shear plates in the moment joint.

5.2.2.2 Phase 2

Similar to phase 1, the specimens failed generally at moments higher than the design and predicted values. As in Table 5.1, Specimen C1 failed at an applied ultimate moment of 36.0 kN.m higher than the design and predicted value of 21.6 kN.m. The discrepancy is larger than that of Specimen A3 (ultimate moment of 30.9 kN.m) due to the existence of the bottom steel bracket which was not accounted for in the analysis. The bottom bracket was mounted on the inner side at the bottom corner of the joint with 8 relatively small screws (size #8x19 mm). Its shear resistance was considered to be negligible compared to glulam rivets. However, its existence between the two members during the loading process increased the stiffness of the moment joint and reduced crushing of the wood. The side grain and end grain cracks at the furthest column of rivets from the I.C. were the main failure criteria.

Specimens C2 and C3 had ultimate moment resistance of 45 kN.m higher than the design and predicted values of 40.0 kN.m and 41.0 kN.m, repectively. The resistance of the top rivet bracket was included in the analysis, but not the bottom bracket. Cracks in the side

grain did develop, however, failure was attributed to the local yielding at the apex in addition to the overall bending of the bracket. The bracket kept the end grain from splitting and cracks in the top member confined as the specimen was loaded, hence increased its strength. The top bracket strain gauges showed that the top bracket carried a significant portion of the load, up to 60% of the total applied moment.

Specimen C4 failed at a moment of 34 kN.m higher than the design and predicted values of 26.6 kN.m and 27.2 kN.m, repectively. The existence of the bearing plate between the two members was not accounted for. However, its contribution to the performance of the specimen is limited to a slight increase in the stiffness of the joint since it commenced to bend at an early stage during the loading. Its effectiveness in reducing the crushing of the wood between the two members was small. It bent as shown in Figure 4.22 and still allowed crushing but at a later stage.

In this specimen, the spacing between the rivets on the side plate was increased to increase the chance of rivet yield type of failure rather than wood splitting, hence increasing the ductility of the joint. At failure, there was no significant side cracks or cracks in the end grain. The strain gauges mounted on the top bracket indicated that it carried up to 85% of the total applied moment. Similar to Specimens C2 and C3, the failure was due to local yielding at the apex and the overall bending of the top bracket.

The magnitude of the stresses in the side plates was less than that in Specimen C1, again because of the existence of the top bracket. Specimen C4 had a top rivet bracket greater in thickness than that of Specimens C2 and C3, since it was predicted to carry a larger portion of the applied load. This encouraged the wood shear mode of failure in the top grain and the rivet withdrawal mode of failure at the same location.

Specimen B1 failed at a moment of 14.3 kN.m higher than both the design value of 10.6 kN and the predicted value of 12.2 kN.m. For the material tests, all shear plates were tested in members of 130 mm thickness only. However, for Specimen B1 (with a member thickness of 80 mm), a connector end distance factor of 0.75 (as in CSA/CAN-O86.1-M89 (1989)) was included to account for the smaller member thickness.

5.3 EFFECT OF RIVET DISTRIBUTION PATTERN

The strain gauges mounted on the side plates indicate the rivets at the furthest column from the I.C., especially the ones closest to the interboundary line between the two members such as Ga#8 in Figure 3.21, were the most critical tension stress in the surrounding steel plate. The steel plate surrounding the rivets in the columns closer to the I.C. was mainly in compression (Ga#1 and Ga#7 in Figure 3.21).

The interaction between the steel plate and the wood distributes the load in a non-uniform mode in tension joints (Cramer, 1968). Similarly in these tests, the steel plate interaction with the wood affected the load distribution among the rivets. Hence, the rivets in the top row in the top member carried the most significant loads in their respective columns causing them to bend the most.

If it was required to reduce the number of rivets on the side grain, then from the spreadsheet analysis based on Eqn. 5.4, it appears that by removing the close end column of rivets to the I.C., a stress increase of 10% takes place among the rest of the rivets. However, by removing the far end column, a stress increase of 25% occurs. If the two

rows of rivets closest to the I.C. were removed, an increase of 15% would take place as opposed to 43% if the last 2 rows were removed.

So removing the line of rivets with the lowest force component parallel to the grain (the row close to the I.C.) causes the lowest increase among all rivets and maintains more uniform stress distribution than if the furthest row (from I.C.) was removed. Hence, it is preferable not to remove the row of rivets with the highest force component parallel to the grain (furthest from I.C.).

5.4 GENERAL COMPARISON AND IMPLICATION OF THE TEST RESULTS

The moment rotation curves presented in Figures 4.5 and 4.6 demonstrate the difference in performance among the different tested specimens. However, any future recommendations based on this data will be based on the initial portions of the curve (mainly linear), that is the portions with relatively low rotation changes. Hence, the portion of the curves up to a rotation of 3° is presented in Figure 5.3. Furthermore, in order to evaluate the performance of the connections in a portal frame application, it is necessary to compare the performance of the moment connections with the strength and stiffness of the beam used to construct the tested specimens. This led to the employment of the beam-line concept as apparent in Figure 5.3.

The y-axis intersection of the beam-line represents a fixed-ended moment for a transversely loaded beam corresponding to a rotation equal to zero (in this case, it is the maximum bending moment that this 130 mm x 380 mm glulam beam can withstand). The x-axis intersection of the line represents the rotation of the end of a simply supported

beam under a concentrated moment at the other end, as shown schematically in Figure 5.3 corresponding to span lengths of L= 4.5 m and L= 9 m respectively.

The intersection of the moment vs. rotation curves with the beam-line indicates the amount of moment the connection can absorb. The rigidity ratio of the connection is the ratio between the amount of moment the connection can absorb and the fixed-ended moment. The notation of "Rotation Ratio" is used here to indicate the ratio between the amount of rotation the connection exhibits, (the value of the rotation corresponding to the moment that the connection can absorb) and the rotation of the end of the simply supported beam. The rotation ratio is inversely proportional with the stiffness of the connection. Hence, as the rotation ratio approaches unity, the connection approaches a simply supported edge boundary condition. Where as the rigidity ratio approaches unity, the connection approaches a fixed-ended boundary condition. The stiffness of such connection is the slope of the moment-rotation curve. Table 5.2 is based on Figure 5.3, and shows the rigidity ratios and rotation ratios of the different moment resistant joints for a span lengths of L= 4.5 m and L=9 m.

Table 5.2 shows the superiority of the riveted connections. Rigidity ratios as high as 39% and rotation ratios as low as 63% were achieved in Specimens C2 and C3. The rivet plate connections have a higher number of fasteners among which it can more uniformly distribute the load; hence, less highly stressed fasteners and higher joint strengths are obtained. This was apparent in Specimen A4 where there was only a total of 8 fasteners hence, the stress distribution per fastener was high leading to severe cracks at the ultimate load. The rivet joints also had a higher stiffness since the tolerance in the bolt holes allowed more rotation in the bolted joints. Specimens A2 and A3 performed very similar in terms of strength and stiffness even though Specimen A3 is 120 rivets less in total. In

addition, since in Specimen A3 there were less columns of rivets perpendicular to the grain (i.e. holding the grain together), more side grain cracks developed in lieu of one big sudden crack, hence it performed with much more ductility than Specimen A2. This underlines the importance of the rivet spacing, rivet distribution, and their effect on the performance of the joint. The distance from the I.C. to the furthest rivet in Specimen A1 is longer than that in Specimen A3. This led to a higher rivet stress perpendicular to the grain; hence, earlier failure in Specimen A1.

In series C, the existence of the bottom bracket increased the stiffness and strength slightly, but both were increased significantly with the addition of the top bracket. This bracket kept the end grain splits and cracks in the top member confined as the specimen was loaded; hence, increasing its strength. The ultimate load for Specimens C2 and C3 was achieved when the top steel bracket commenced yielding at the apex, after which, the specimen underwent large rotations. These two specimens presented the most strength and stiffness among all tested specimens. The number of splits along the side grain and end grain was significantly reduced by increasing the space between the rivets and reducing the number of rivets on the side plate as done in Specimen C4. However the strength and stiffness achieved in this specimen was less than that of Specimen C1, but the ductility shown by this specimen was the highest among all (ultimate rotation θ_u= 9.5°) (see Table 5.2 and Figure 5.3).

5.5 ADVANTAGE OF SEMI-RIGID JOINT APPLICATION

In series C of the tests, Specimens C2 and C3 achieved a moment resistance equal to 39% of the fixed end moment of the beam used in Table 5.2. Hence, when this joint is utilized

in a portal frame, it cannot be considered as a fully rigid joint, and to consider it as a fully pin joint would be too conservative and a waste of its potential as a resistant joint.

It is, therefore, beneficial to utilize such a joint and account for its use in a frame as a partially restrained joint or semi-rigid joint. These joints can be applied to improve strength design or stiffness for serviceability needs. The benefit is significant for reducing beam mid-span deflections leading to a reduction in materials and cost.

The use of partially restrained joints reduces the mid-span moments in pinned end connections and redistributes them to the ends as in Figure 5.4. If such restraint was used in design, one should check the satisfaction of the serviceability requirements.

One advantage is that for inertia-oriented loads such as earthquakes, the energy absorption of semi-rigid connections could keep excessive lateral drift of tall portal frames within reason. Nevertheless, on a philosophical level, it is apparent that neither pinned nor rigid connections are actually obtained in real structures. The need exists to approach reality. Even approximate estimates of frame flexibility are closer to truth than the assumed ideals of nil or full restraint in the connections (Chen et al., 1992).

Table 5.1 - Summary of Test Results

Spec.	Conn. Config.	Ult. Load P_u (kN)	Ult. Mom. M_u (kN.m)	Ult. Rot. Ang. θ_u (Deg)	Design Mom. Value M_d (kN.m)	Pred. Mom. Value Mp (kN.m)	M_u/M_d	M_u/Mp
A1	7x10	31	22.3	3.9	14.4	14.4	1.55	1.55
A2	10x10	45	32.4	3.55	26.6	26.6	1.22	1.22
A3	10x7	43	30.9	5.5	21.6	21.6	1.43	1.43
A4	4x2	24.5	17.6	6.2	14.4	16.2	1.22	1.08
A5	8circw	30	29.7	6.6	19.0	22.3	1.56	1.33
A6	8cirst	36	35.6	6.5	19.0	22.3	1.87	1.6
B1	4x2	18	14.3	3.7	10.6	12.2	1.35	1.17
C1	10x7b	50	36	6	21.6	21.6	1.67	1.04
C2	10x7bt	61	44	6	40	41.0	1.10	1.07
C3	10x7bt	45	45	7	40	41.0	1.13	1.1
C4	5x4tbr	47	34	9.5	26.6	27.2	1.28	1.25

Table 5.2 - Evaluation of Specimen Performance

		L = 4.5 m				L = 9 m			
Spec.	Confg.	Mom. (kN.m)	Rot. (Deg.)	Rig. Ratio	Rot. Ratio	Mom. (kN.m)	Rot. (Deg.)	Rig. Ratio	Rot. Ratio
A1	7x10	10.0	1.0	0.14	0.83	15.0	1.9	0.21	0.79
A2	10x10	15.0	0.9	0.21	0.75	23.0	1.7	0.33	0.71
A3	10x7	17.0	0.85	0.24	0.71	23.0	1.7	0.33	0.71
A4	4x2	4.0	1.15	0.06	0.96	7.0	2.15	0.10	0.90
A5	8circw	7.0	1.1	0.1	0.92	15.0	1.9	0.21	0.79
A6	8cirst	7.0	1.1	0.1	0.92	13.0	1.9	0.19	0.79
B1	4x2	5.0	1.15	0.07	0.96	9.0	2.1	0.13	0.88
C1	10x7	13.0	1.0	0.19	0.83	22.0	1.6	0.31	0.67
C2	10x7	17.0	0.85	0.24	0.71	27.0	1.5	0.39	0.63
C3	10x7	18.0	0.85	0.26	0.71	27.0	1.5	0.39	0.63
C4	5x4	14.0	0.95	0.20	0.80	21.0	1.6	0.30	0.67

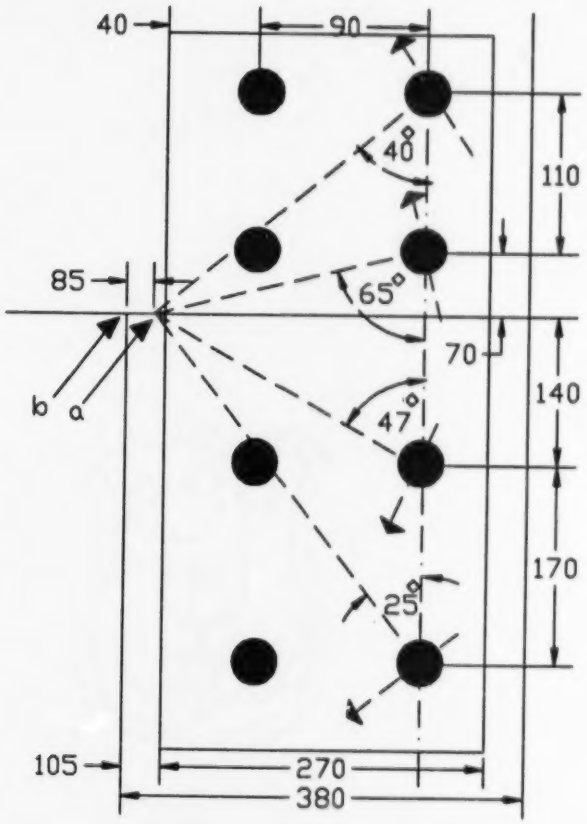

Figure 5.1 - Principal Force Directions on Bolts in Specimen B1

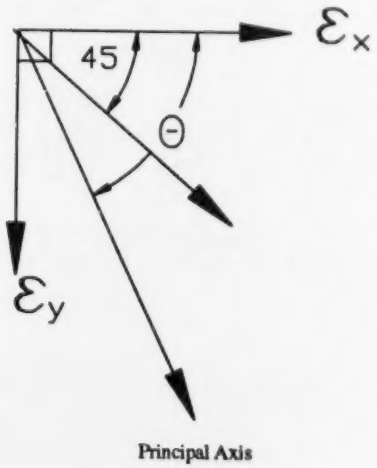

Figure 5.2 - Axes of Longitudinal Strain Gauges in a Rosette Gauge

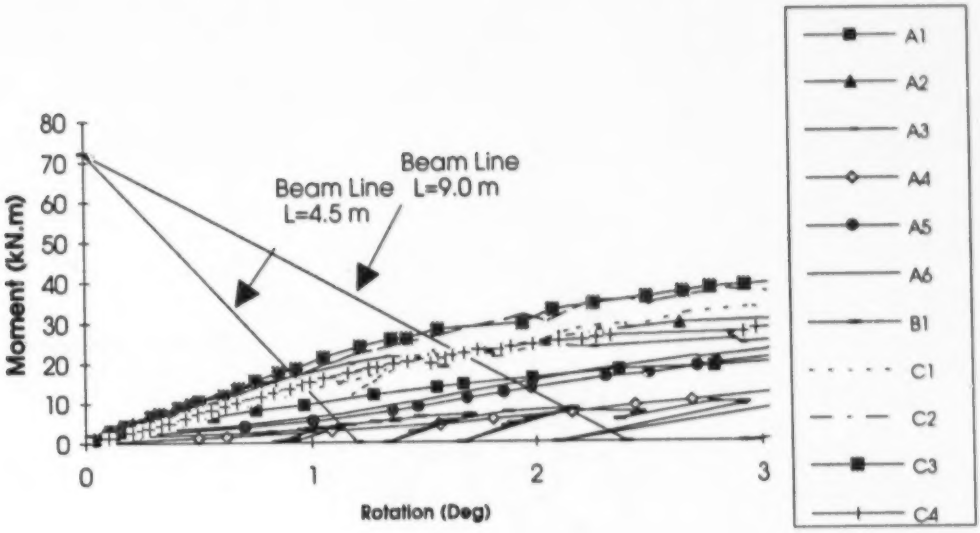

Figure 5.3 - Beam-Line Applied on Moment Rotation Curves

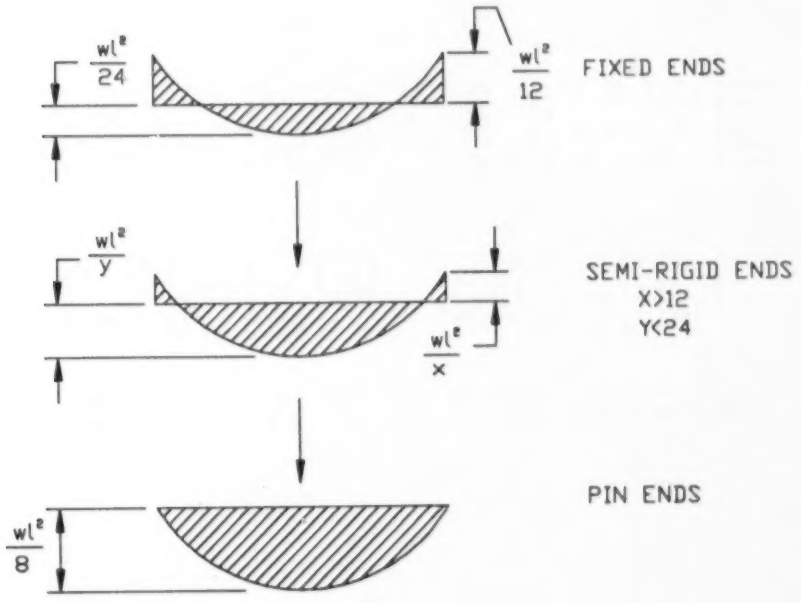

Figure 5.4 - Bending Moment Diagrams for Various Boundary Conditions

6.0 SUMMARY AND CONCLUSIONS

6.1 GENERAL

A preliminary study and experimental program has been conducted to develop a moment resistant joint in glued-laminated timber manufactured from Alberta spruce and pine. The first phase of the study investigated the performance of moment joints made with various types of fasteners. Further investigation and improvements to glulam rivet connections were conducted in the second phase of the program.

The test results in the first phase exhibit the superior performance (both strength and stiffness) of the glulam rivet side plate moment joints compared with the bolted type moment connections. The tolerance of the bolt holes allow slight bolt free movement; hence, reducing the stiffness of the joint. Specimen A2 and A3 (10x10 and 10x7) were very similar in their performance even though the number of rivets were reduced by 30% in Specimen A3.

In the second phase, the rosette strain gauges on Specimen B1 located the instantaneous center in the rectangular patterns of butt type of joints to be at the bottom corner of the joint (point (b) in Figure 5.1).

Improvements to glulam rivet joints such as the addition of a bottom steel bracket in Specimen C1 increased the strength and stiffness of the joint. However, a more significant improvement in the performance was achieved with a top cover rivet steel bracket (in addition to the bottom bracket) as in Specimens C2 and C3. The maximum rigidity achieved was 39% (of the bending strength of the beam). The contribution of the top steel

bracket in Specimen C3 reached values of 60% of the total moment resistance. In Specimen C4, exchanging the steel bottom bracket with a bearing plate between the two members did not eliminate the wood crushing between the two members, nor did it increase the stiffness of the joint. Using the bearing plate and reducing the number of rivets on the side plates by 70% caused the top cover bracket in this specimen to carry a higher portion of the total applied moment (up to a maximum of 85%).

All failures witnessed wood splitting in the end grain and on the sides at the most distant column of rivets from the I.C. and at the closest bolt to the outer corner edge in the circular bolted patterns, indicating the high stresses and the weak tensile strength of the timber perpendicular to the grain. The splitting of the wood was reduced significantly with the reduction of rivets on the side plates, and the increase of the spacing between the rivets in both directions. This enhances the rivet yielding mode of failure; however, in Specimens C2, C3 and C4, the top bracket confined the whole connection, hence the mode of failure was in local yielding in the apex and bending of the bracket.

The failures also occurred at loads higher than the design values and the predicted values. This took place since the conservative strengths of the materials specified in CAN/CSA-O86.1-M89 (1989) were used in the design values' calculation, and since the redistribution of forces among the fasteners was not accounted for in the predicted values' calculation (i.e. only an elastic analysis was performed).

6.2 RECOMMENDATIONS

In order to predict the design strength of a moment joint, the use of the torsional formula (Eqn. 2.1) and the specified strengths in CAN/CSA-O86.1-M89 (1989) is recommended.

The predicted design values found throughout this study were reasonable and conservative results; however, more investigation is required to asses the validity of this formula for other types of moment joints. Further research should include the examination of benefits obtained in the use of semi-rigid moment resistant connections in glued-laminated portal timber frames.

Further research to improve the performance of the glulam rivet moment connections is required. The maximum rigidity ratio achieved (39% of the bending strength of the beam) is still moderate. Some of this research should be directed towards the utilization of other fasteners and techniques to increase the strength and stiffness of the joint, such as the use of fibre reinforced plastic sheets glued to the end grain to strengthen the tensile strength of the timber perpendicular to the grain.

Other ideas to improve the performance of the joints include prestressing tendons with triangular wedges on each end which could be very effective in increasing the stiffness of the joints. The result of split ring use in moment joints was not examined in this study, but is recommended as part of future research for this project.

The glulam rivet pattern layout on the side plates is an important variable worth investigating, since the quantity, spacing and location of the rivets dictate the strength and mode of failure of the joint. The effect of the end and edge distances should also be re-examined.

In addition to the above, other variables that should be investigated in future research include the size effect of the members, the effect of the loading rate and load duration. The

study of cyclic loading on the moment joints is also important to achieve a comprehensive understanding of the joints' behaviour.

REFERENCES

ASTM,1988. "Structural Steel", A36/A36M-88c, American Society for Testing and Materials, Philadelphia, Pa.

ASTM,1990. "Standard Test Methods for Mechanical Fasteners in Wood", ASTM 01761-88. American Society for Testing and Materials, Philadelphia, Pa.

Aune P. and Patton-Mallory M., 1986. "Lateral Load Bearing Capacity of Nailed Joints Based on the Yield Theory: Experimental Verification", Research paper FPL 470, Madison, Wi, US Department of Agriculture, Forest Service, Forest Products Laboratory.

Batchelar M.L., June 1982. "Nailed Plywood Gusset Joints for Timber Portal Frames", Dept. Civil Engineering, University of Auckland N.Z..

Buchanan A., 1990. "Report on Portal Frame Knee Joints with Epoxied Steel Dowels", Report CP/4006 - University of Canterbury.

Buchanan A. and Lai J., 1993. "Glulam Rivets in Radiata Pine", Canadian Journal of Civil Engineering p. 340-350, (1994).

Canadian Standard Association, 1987. "Structural Quality Steels", CAN3-G40.21-M87.

Canadian Standard Association, 1989. "Engineering Design in Wood (Limit States Design)", CAN/CSA-O86.1-M89.

Chen W.F., Lorenz R. and Kato B., 1992. "Semi-Rigid Connection in Steel Frames", Council on Tall Buildings and Urban Habitat.

Cramer C., 1968. "Load Distribution in Multiple-Bolt Tension Joints", Journal of the Structural Division, Proceedings of the American Society of Civil Engineers, May.

Crews K., 1990. "Gottstein Report", Forest Research Institute, Rotorua, New Zealand.

Foschi R. O., 1974. "Load-Slip Characteristics of Nails", Wood Science Vol:7, No1.

Foschi R.O. and Longworth J., 1975 . "Analysis and Design of Griplam Nailed Connections". Journal of the Structural Division, American Society of Civil Engineering. 101(ST12):2537-2555.

Gardner G.P., 1989. "A Reinforced Glued Laminated Timber System", PTEC (Vol2)-Auckland.

Gehri E., 1982. "Fachwerktrager aus Buche und Fichte mit Stahlknotenplatten in Eingeschlitzten Holzern" ETH Zurich.

Johansen K. W., 1949. "Theory of Timber Connections", Int. Assoc. for Bridge and Struc. Engrg., 9, 249-262.

Karcabeyli E. and Fraser H., 1989. "Short-term Strength of Glulam Rivet Connections Made with Spruce and Douglas Fir Glulam, and Douglas Fir Solid Timber". Unpublished report, Forintek Canada Corp., Vancouver, BC.

Kivell B.T., Moss P. and Carr A., Dec. 1981. "Hysteretic Modelling of Moment-Resisting Nailed Timber Joints", Bull. of the N. Z. National Soc. for Earthquake Engineering, Vol. 14, No. 4.

Kivell B.T., Moss P. and Carr A., July 1982. "Cyclic Load Behaviour of Two Timber Portal Frames with Moment Resistant Nailed Joints", Transactions of the IPENZ, Civil Engineering Section. Vol. 9 No.2, pp.54.

Larsen H. J., 1973. "The Yield Load of Bolted and Nailed Joints". Proceedings, International Union of Forestry Research Organization Meeting-5 Congress.

Lheude E. P., 1985. "Tension Loads for Shear Plates and Split Rings in Timber Loaded Parallel to the Grain". Journal of the Institute of Wood Science. London. England.

Masse D.I., Salinas J.J. and Turnbull J.E., 1988. "Lateral Strength and Stiffness of Single and Multiple Bolts in Glue Laminated Timber Loaded Parallel to the Grain", Eng. and Stat. Research Center, Research Branch, Agriculture Canada, Ottawa.

McGowan W.M., 1966. "A Nailed Plate Connector for Glued-Laminated Timbers", Journal of Materials, Vol. 1, No. 3, p. 509.

Mitchell T.M., 1979. "Design of a Rigid Joint Incorporating Nailed Steel Side Plates". Section 7.6 of Timber Design and Detailing Manual, Ministry of Works and Development, Wellington.

Perkins R.H., Suddarth S.K. and Dale A.C., 1964. "Rotational Resistance of Three-Membered Nailed Joints Subjected to Bending Moment", U.S. Forestry and Conservation.

Riberholt H., 1986. "Glued Bolts in Glulam", Department of Structural Engineering, Technical University of Denmark.

Rodd P., 1973. "The Analysis of Timber Joints made with Circular Dowel Connections", PhD Thesis, University of Sussex.

Rodd, Hilson and Spriggs, 1989. "Resin Injected Mechanically Fastened Timber Joints", Pacific Timber Engineering Conference.

Smith I., Rodd P., Whale R.J. and Anderson C., 1987. "Characteristic Properties of Nailed and Bolted Joints under Short Term Lateral Loads". Parts 1-5, Journal of The Institute of Wood Science.

Syme D., 1987. "A Study Tour of Timber Engineering in Europe", Gottstein Report.

Walford G. B., 1988. "Analysis of Timber Portal Frame Gusset Joints". IPENZ

Wilkinson T. L., 1993. "Bolted Connection Design Values Based on European Yield Model", Journal of Structure Engineering, Vol. 119, No. 7.

APPENDIX A

SAMPLE CALCULATIONS' OF MOMENT CONNECTIONS' RESISTANCE

SAMPLE CALCULATIONS OF MOMENT CONNECTIONS' RESISTANCE

Calculation of Moment Resistance of Specimen A5/A6 Based on Material Tests

From the material tests, embedment strength of 67 mm (2-5/8") shear plate as in Table 4.2:

1- Parallel to grain P_r = 32 kN.
2- Perpendicular to grain Q_r = 17.5 kN.

From Figure 3.8 and 3.9, four embedded shear plates are at 45° to the grain direction. Hence using equation 5.4, strength of each plate :

So the moment is calculated as the contributed resistance of each plate about the centre of the pattern. There are 2 plates parallel and 2 plates perpendicular to the grain in addition to the 4 mentioned above.

$Mp = [(2 \times 17.5\ kN) + (2 \times 32\ kN) + (4 \times 22.6\ kN)] \times 120 \times 10^{-3}\ m$

= 22.3 kN.m. as in Table 4.3.

Calculation of Moment Resistance of Riveted Specimens Based on Specified Material Strengths and Material Tests

Strength of rivet joints tested parallel to grain based on rivet patterns 8x4 (Sp=25 mm) and 5x4 (Sp=40 mm), and strength of the 4x4 rivet pattern tested perpendicular to the grain were found to be very similar to those specified in CAN/CSA-O86.1-M89 (1989). Hence these values (strength per rivet) will be used in determining the strength of the moment connections. The specified strength values per rivet will be used in the rivet patterns that differ from the above mentioned rivet patterns. See Table 4.2.

Moment resistance of Specimen C4 is presented.

Note: Moment resistance of Specimen A4 and B1 is calculated similarily however, using the tested resistance values of the shear plates in both directions as presented above. In addition, shear plate resistance values used to calculate the moment resistance in Specimen B1, would include a connector end distance factor of 0.75.

Spreadsheet Analysis Program															
This sheet analyzes force distribution in moment resistant joints at the rivets or bolts.															
Specimen C4															
Upper Member															
Moment = Force x lever arm=			37.8	x		720	=	27216							
								kN.mm							
Rivet/	rx	ry	r^2	Tx	Ty	Tx/P	Ty/Q	T	ø (Deg)	ø-90 (Deg)	ø-90 (Rad)	N	T/N		
Bolt #															
1	170	75	34525	0.26	0.59	0.04	0.33	0.64	23.81	66.19	1.16	2.05	0.31		
2	210	75	49725	0.26	0.73	0.04	0.40	0.77	19.65	70.35	1.23	1.97	0.39		
3	250	75	68125	0.26	0.86	0.04	0.48	0.90	16.70	73.30	1.28	1.92	0.47	Rivets #1 thru #20	
4	290	75	89725	0.26	1.00	0.04	0.56	1.03	14.50	75.50	1.32	1.89	0.55	are the rivets on the	
5	170	115	42125	0.40	0.59	0.06	0.33	0.71	34.08	55.92	0.98	2.35	0.30	side plates	
6	210	115	57325	0.40	0.73	0.06	0.40	0.83	28.71	61.29	1.07	2.17	0.38	from the I.C.	
7	250	115	75725	0.40	0.86	0.06	0.48	0.95	24.70	65.30	1.14	2.07	0.46		
8	290	115	97325	0.40	1.00	0.06	0.56	1.08	21.63	68.37	1.19	2.00	0.54	P=rivet strength on	
9	170	155	52925	0.54	0.59	0.08	0.33	0.79	42.36	47.64	0.83	2.72	0.29	both sides parallel	
10	210	155	68125	0.54	0.73	0.08	0.40	0.90	36.43	53.57	0.93	2.44	0.37	to grain	
11	250	155	86525	0.54	0.86	0.08	0.48	1.02	31.80	58.20	1.02	2.27	0.45		
12	290	155	108125	0.54	1.00	0.08	0.56	1.14	28.12	61.88	1.08	2.16	0.53	Q=rivet strength on	
13	170	195	66925	0.67	0.59	0.10	0.33	0.89	48.92	41.08	0.72	3.11	0.29	both sides	
14	210	195	82125	0.67	0.73	0.10	0.40	0.99	42.88	47.12	0.82	2.74	0.36	perpendicular	
15	250	195	100525	0.67	0.86	0.10	0.48	1.09	37.95	52.05	0.91	2.50	0.44	to grain	
16	290	195	122125	0.67	1.00	0.10	0.56	1.21	33.92	56.08	0.98	2.34	0.52		
17	170	235	84125	0.81	0.59	0.12	0.33	1.00	54.12	35.88	0.63	3.51	0.29		
18	210	235	99325	0.81	0.73	0.12	0.40	1.09	48.22	41.78	0.73	3.07	0.35		
19	250	235	117725	0.81	0.86	0.12	0.48	1.18	43.23	46.77	0.82	2.76	0.43		
20	290	235	139325	0.81	1.00	0.12	0.56	1.29	39.02	50.98	0.89	2.55	0.51		
71	305	380	237425	1.31	1.05	0.44	1.05	1.68	51.25	38.75	0.68	1.68	1.00		
72	305	380	237425	1.31	1.05	0.44	1.05	1.68	51.25	38.75	0.68	1.68	1.00	Rivets #71 through	
73	305	380	237425	1.31	1.05	0.44	1.05	1.68	51.25	38.75	0.68	1.68	1.00	#102 are rivets on	
74	305	380	237425	1.31	1.05	0.44	1.05	1.68	51.25	38.75	0.68	1.68	1.00	the top bracket	
75	280	380	222800	1.31	0.97	0.44	0.97	1.63	53.62	36.38	0.64	1.76	0.93	from the I.C.	
76	280	380	222800	1.31	0.97	0.44	0.97	1.63	53.62	36.38	0.64	1.76	0.93		
77	280	380	222800	1.31	0.97	0.44	0.97	1.63	53.62	36.38	0.64	1.76	0.93	P= rivet strength	
78	280	380	222800	1.31	0.97	0.44	0.97	1.63	53.62	36.38	0.64	1.76	0.93	parallel to grain	
79	255	380	209425	1.31	0.88	0.44	0.88	1.58	56.14	33.86	0.59	1.85	0.85		
80	255	380	209425	1.31	0.88	0.44	0.88	1.58	56.14	33.86	0.59	1.85	0.85	Q=rivet strength	

81	255	380	209425	1.31	0.88	0.44	0.88	1.58	56.14	33.86	0.59	1.85	0.85	perpendicular	
82	255	380	209425	1.31	0.88	0.44	0.88	1.58	56.14	33.86	0.59	1.85	0.85	to grain	
83	230	380	197300	1.31	0.79	0.44	0.79	1.53	58.82	31.18	0.54	1.95	0.79		
84	230	380	197300	1.31	0.79	0.44	0.79	1.53	58.82	31.18	0.54	1.95	0.79		
85	230	380	197300	1.31	0.79	0.44	0.79	1.53	58.82	31.18	0.54	1.95	0.79		
86	230	380	197300	1.31	0.79	0.44	0.79	1.53	58.82	31.18	0.54	1.95	0.79		
87	205	380	186425	1.31	0.71	0.44	0.71	1.49	61.65	28.35	0.49	2.07	0.72		
88	205	380	186425	1.31	0.71	0.44	0.71	1.49	61.65	28.35	0.49	2.07	0.72		
89	205	380	186425	1.31	0.71	0.44	0.71	1.49	61.65	28.35	0.49	2.07	0.72		
90	205	380	186425	1.31	0.71	0.44	0.71	1.49	61.65	28.35	0.49	2.07	0.72		
91	180	380	176800	1.31	0.62	0.44	0.62	1.45	64.65	25.35	0.44	2.20	0.66		
92	180	380	176800	1.31	0.62	0.44	0.62	1.45	64.65	25.35	0.44	2.20	0.66		
93	180	380	176800	1.31	0.62	0.44	0.62	1.45	64.65	25.35	0.44	2.20	0.66		
94	180	380	176800	1.31	0.62	0.44	0.62	1.45	64.65	25.35	0.44	2.20	0.66		
95	155	380	168425	1.31	0.54	0.44	0.54	1.42	67.81	22.19	0.39	2.33	0.61		
96	155	380	168425	1.31	0.54	0.44	0.54	1.42	67.81	22.19	0.39	2.33	0.61		
97	155	380	168425	1.31	0.54	0.44	0.54	1.42	67.81	22.19	0.39	2.33	0.61		
98	155	380	168425	1.31	0.54	0.44	0.54	1.42	67.81	22.19	0.39	2.33	0.61		
99	130	380	161300	1.31	0.45	0.44	0.45	1.39	71.11	18.89	0.33	2.48	0.56		
100	130	380	161300	1.31	0.45	0.44	0.45	1.39	71.11	18.89	0.33	2.48	0.56		
101	130	380	161300	1.31	0.45	0.44	0.45	1.39	71.11	18.89	0.33	2.48	0.56		
102	130	380	161300	1.31	0.45	0.44	0.45	1.39	71.11	18.89	0.33	2.48	0.56		
Totals			7882100												
Lower member															
Rivet/	nx	ny	r^2	Tx	Ty	Tx/Q	Ty/P	T	ø (Deg)	ø-90 (Deg)	ø (Rad)	N	T/N		
Bolt #															
1	170	140	48500	0.54	0.65	0.30	0.09	0.84	39.47	50.53	0.69	3.23	0.26		
2	210	140	63700	0.54	0.80	0.30	0.11	0.96	33.69	56.31	0.59	3.71	0.26		
3	250	140	82100	0.54	0.96	0.30	0.14	1.10	29.25	60.75	0.51	4.14	0.26	Rivets #1 thru #16	
4	290	140	103700	0.54	1.11	0.30	0.16	1.23	25.77	64.23	0.45	4.53	0.27	are the rivets on the	
5	170	180	61300	0.69	0.65	0.38	0.09	0.95	46.64	43.36	0.81	2.77	0.34	side plates	
6	210	180	76500	0.69	0.80	0.38	0.11	1.06	40.60	49.40	0.71	3.15	0.34	from the I.C.	
7	250	180	94900	0.69	0.96	0.38	0.14	1.18	35.75	54.25	0.62	3.52	0.33		
8	290	180	116500	0.69	1.11	0.38	0.16	1.30	31.83	58.17	0.56	3.88	0.34	P=rivet strength on	
9	170	220	77300	0.84	0.65	0.47	0.09	1.06	52.31	37.69	0.91	2.49	0.43	both sides parallel	
10	210	220	92500	0.84	0.80	0.47	0.11	1.16	46.33	43.67	0.81	2.79	0.42	to grain	
11	250	220	110900	0.84	0.96	0.47	0.14	1.27	41.35	48.65	0.72	3.10	0.41		

12	290	220	132500	0.84	1.11	0.47	0.16	1.39	37.18	52.82	0.65	3.41	0.41	Q=rivet strength on
13	170	260	96500	0.99	0.65	0.55	0.09	1.19	56.82	33.18	0.99	2.32	0.51	both sides
14	210	260	111700	0.99	0.80	0.55	0.11	1.28	51.07	38.93	0.89	2.55	0.50	perpendicular
15	250	260	130100	0.99	0.96	0.55	0.14	1.38	46.12	43.88	0.81	2.80	0.49	to grain
16	290	260	151700	0.99	1.11	0.55	0.16	1.49	41.88	48.12	0.73	3.06	0.49	
71	380	75	150025	0.29	1.45	0.29	0.48	1.48	11.16	78.84	0.19	2.79	0.53	
72	380	75	150025	0.29	1.45	0.29	0.48	1.48	11.16	78.84	0.19	2.79	0.53	
73	380	75	150025	0.29	1.45	0.29	0.48	1.48	11.16	78.84	0.19	2.79	0.53	
74	380	75	150025	0.29	1.45	0.29	0.48	1.48	11.16	78.84	0.19	2.79	0.53	
75	380	100	154400	0.38	1.45	0.38	0.48	1.50	14.74	75.26	0.26	2.66	0.57	
76	380	100	154400	0.38	1.45	0.38	0.48	1.50	14.74	75.26	0.26	2.66	0.57	Rivets #71 through
77	380	100	154400	0.38	1.45	0.38	0.48	1.50	14.74	75.26	0.26	2.66	0.57	#102 are rivets on
78	380	100	154400	0.38	1.45	0.38	0.48	1.50	14.74	75.26	0.26	2.66	0.57	the top bracket
79	380	125	160025	0.48	1.45	0.48	0.48	1.53	18.21	71.79	0.32	2.51	0.61	from the I.C.
80	380	125	160025	0.48	1.45	0.48	0.48	1.53	18.21	71.79	0.32	2.51	0.61	
81	380	125	160025	0.48	1.45	0.48	0.48	1.53	18.21	71.79	0.32	2.51	0.61	P= rivet strength
82	380	125	160025	0.48	1.45	0.48	0.48	1.53	18.21	71.79	0.32	2.51	0.61	parallel to grain
83	380	150	166900	0.57	1.45	0.57	0.48	1.56	21.54	68.46	0.38	2.36	0.66	
84	380	150	166900	0.57	1.45	0.57	0.48	1.56	21.54	68.46	0.38	2.36	0.66	Q=rivet strength
85	380	150	166900	0.57	1.45	0.57	0.48	1.56	21.54	68.46	0.38	2.36	0.66	perpendicular
86	380	150	166900	0.57	1.45	0.57	0.48	1.56	21.54	68.46	0.38	2.36	0.66	to grain
87	380	175	175025	0.67	1.45	0.67	0.48	1.60	24.73	65.27	0.43	2.22	0.72	
88	380	175	175025	0.67	1.45	0.67	0.48	1.60	24.73	65.27	0.43	2.22	0.72	
89	380	175	175025	0.67	1.45	0.67	0.48	1.60	24.73	65.27	0.43	2.22	0.72	
90	380	175	175025	0.67	1.45	0.67	0.48	1.60	24.73	65.27	0.43	2.22	0.72	
91	380	200	184400	0.76	1.45	0.76	0.48	1.64	27.76	62.24	0.48	2.09	0.78	
92	380	200	184400	0.76	1.45	0.76	0.48	1.64	27.76	62.24	0.48	2.09	0.78	
93	380	200	184400	0.76	1.45	0.76	0.48	1.64	27.76	62.24	0.48	2.09	0.78	
94	380	200	184400	0.76	1.45	0.76	0.48	1.64	27.76	62.24	0.48	2.09	0.78	
95	380	225	195025	0.86	1.45	0.86	0.48	1.69	30.63	59.37	0.53	1.97	0.85	
96	380	225	195025	0.86	1.45	0.86	0.48	1.69	30.63	59.37	0.53	1.97	0.85	
97	380	225	195025	0.86	1.45	0.86	0.48	1.69	30.63	59.37	0.53	1.97	0.85	
98	380	225	195025	0.86	1.45	0.86	0.48	1.69	30.63	59.37	0.53	1.97	0.85	
99	380	250	206900	0.96	1.45	0.96	0.48	1.74	33.34	56.66	0.58	1.87	0.93	
100	380	250	206900	0.96	1.45	0.96	0.48	1.74	33.34	56.66	0.58	1.87	0.93	
101	380	250	206900	0.96	1.45	0.96	0.48	1.74	33.34	56.66	0.58	1.87	0.93	
102	380	250	206900	0.96	1.45	0.96	0.48	1.74	33.34	56.66	0.58	1.87	0.93	
Totals			7121200											